EFFECT OF PRE-OVULATORY FOLLICLE SIZE ON OOCYTE TRANSCRIPT ABUNDANCE IN BEEF COWS

A Thesis Presented to

the Faculty of the Graduate School

at the University of Missouri

In Partial Fulfillment

Of the Requirements for the Degree

Master of Science

---

by

SARAH ELIZABETH DICKINSON

Dr. Michael F. Smith, Thesis Advisor

MAY 2016

The undersigned, appointed by the Dean of the Graduate School, have examined the thesis entitled

EFFECT OF PRE-OVULATORY FOLLICLE SIZE ON OOCYTE TRANSCRIPT ABUNDANCE IN BEEF COWS

presented by Sarah Elizabeth Dickinson,

a candidate for the degree of Master of Science,

and hereby certify that, in their opinion, it is worthy of acceptance.

_____

Dr. Michael F. Smith

_____

Dr. Jonathan A. Green

_____

Dr. Thomas W. Geary

_____

Dr. Scott E. Poock

DEDICATION

This thesis is dedicated to my family, for their support and guidance throughout my life and their encouragement as I have embarked on this journey:

I am forever grateful to my parents, Bryan and Christine. They have been supporting and nurturing parents since my childhood. I think my mom had a small heart attack when I informed her, at age twelve, that I had decided I wanted to be "a cow person" when I grew up. That year I showed my first 4-H steer project and my family began a journey that has led me to this very point in my life. My mom and dad allowed me to learn and develop my own herd of Simmental cattle as I gained knowledge. I appreciate that they always challenged me to "do it myself" but were always willing to load up and travel across the country to attend a sale, show, or conference. Their willingness to step beyond our family's current boundaries in the beef cattle industry allowed me to develop the knowledge, skillset, and network that allowed me to nurture my love of beef cattle and my desire to teach others. They have supported my goals to achieve the utmost highest education possible, and have been supportive as I have followed the paths that have led me away from home and the farm. They have worked continuously to allow my cattle operation to continue to flourish in my absence, and are my number one support system.

ACKNOWLEDGEMENTS

Many individuals contributed tremendously to the completion of my Master's thesis, both to the completion of the research involved in this thesis and to my professional development into an individual who understands and will share the science of reproductive physiology in the future.

I would first like to thank Dr. Michael Smith for his guidance throughout my Master's program. I sought to work with Dr. Smith for my graduate studies because of my interest in his research on beef cattle reproduction following estrous synchronization. Without knowing, I also selected a thesis advisor who would become one of the most influential people in my life for his mentoring and teaching skills. Dr. Smith has pushed me to dig deeply into the science behind my project and reproduction in general. Through his guidance, I have journeyed beyond my comfort zone and feel that I have learned much more than I had ever expected. Dr. Smith has also helped me develop into a person who can relate my scientific knowledge to producers. He put time into my development in extension by allowing me opportunities to work with local producers for the estrous synchronization, AI, and pregnancy diagnosis of their herds. He has presented me with numerous opportunities to enhance my palpation and ultrasound skills, and has always provided a nurturing environment for my learning. I am forever grateful for my time spent with Dr. Smith, and I will always remember the opportunities he gave me to step up and lead during journal clubs or lab meetings, his ability to help me learn the "hard stuff" and push me to independence simultaneously, and the positive, responsible attitude he has engrained in me as we have navigated through my thesis. I am happy to say that upon

my graduation, I will have completed my Master's program without acquiring a bull stamp!

I appreciate Dr. Jonathan Green for his guidance as I have embarked into the land of molecular biology. He has been a great mentor who has pushed me to understand the biochemistry and molecular aspects of my project. He was always on hand to provide insight and encouragement to truly understand these advanced topics. He led me to remain inquisitive as we analyzed my data and to retain my ability to think for myself when analyzing my data or reading the literature. Dr. Green has also been the de-stressor of our team, as he has often provided insight and helped me keep from becoming overly obsessed about the challenges my project presented. I have enjoyed getting to work with Dr. Green and learning many different "cool" facts from him as we traveled for data collection this past fall.

Dr. Thomas Geary was the first member of my committee that I worked closely with. He offered me my first experiences as a graduate student by allowing me an internship at Fort Keogh in the summer of 2014. I hadn't officially started graduate school at the time, but we collected all of the oocytes for my project that summer. Tom had no qualms about giving me opportunities to organize my project and be in charge to the best of my ability. He has always encouraged me to take charge and has proved to be an influential mentor as he has taken time to discuss just about anything with me. I am very grateful for his guidance throughout my first summer, as well as his encouragement to be confident in my abilities as I returned to Montana last summer. Looking back, I believe we will always remember our struggles in locating and processing oocytes for this project. I'm proud to say we didn't lose half as many oocytes as we thought!

Dr. Scott Poock has also contributed greatly to my development and sanity throughout my Master's project. We are fellow Simmental breeders, and I appreciate Dr. Poock always being up for a discussion of Simmental genetics and cattle in general. Dr. Poock has been kind enough to show me his personal cowherd and has taken me with him to enhance my artificial insemination techniques with dairy cattle. In our travels, I saw a great example of how to relate to and care for others while providing them with insight. I've always taken pride in my preciseness and efficiency when inseminating cattle, and I always thought I was rather time efficient. Then I bred cows with Dr. Poock!

I also owe thanks to the graduate students and faculty of the Animal Science Research Center. I have thoroughly enjoyed walking these halls with each of you for the past two years. Many of you have provided me with much more insight and encouragement than you will ever imagine. I have specifically enjoyed building close friendships with a number of you, and hope you know that you have taught me that I am capable of moving to a completely unknown city, interacting with, and making friends with complete strangers. I wish each of you the best as you move toward the future. I also thank the 2014 Fort Keogh interns for their friendship and encouragement during my first summer away from home. You guys will be in my memory forever and I appreciate your marks on my life.

TABLE OF CONTENTS

LIST OF TABLES

Table **Page**

LIST OF FIGURES

Figure **Page**

LIST OF APPENDIX TABLES

Table **Page**

LIST OF APPENDIX FIGURES

Figure **Page**

LIST OF ABBREVIATIONS

µg	micrograms
µl	microliters
µm	micrometers
AI	artificial insemination
ANOVA	analysis of variance
ATP	adenosine triphosphate
BCS	body condition score
BCV	biological coefficient of variation
C	Celsius
cAMP	cyclic adenosine monophosphate
cDNA	complementary deoxyribonucleic acid
CIDR	controlled internal drug release (progesterone)
CL	corpus luteum, corpora lutea
COC	cumulus-oocyte complex
CPM	counts per million
DNA	deoxyribonucleic acid
FC	fold change
FDR	false discovery rate
FSH	follicle stimulating hormone
FTAI	fixed-time artificial insemination
g	grams

GnRH	gonadotropin releasing hormone
GV	germinal vesicle
GVB	germinal vesicle breakdown
hr	hour
IGF	insulin-like growth factor
IVF	in vitro fertilization
IVM	in vitro maturation
kg	kilograms
LH	luteinizing hormone
mg	milligrams
MI	metaphase one
MII	metaphase two
ml	milliliters
mm	millimeters
mRNA	messenger ribonucleic acid
MZT	maternal zygotic transition
NCBI	National Center for Biotechnology Information
ng	nanograms
PGF	prostaglandin $F_{2\alpha}$
RNA	ribonucleic acid
RPKM	reads per kilobase per million
RT-PCR	real-time polymerase chain reaction
UPP	ubiquitin-proteasome pathway

LIST OF OFFICIAL GENE SYMBOLS AND NAMES

Official Gene Symbol	Gene Name
ADORA1	adenosine A1 receptor
AGXT2	alanine--glyoxylate aminotransferase 2
ALKBH7	alkB homolog 7
ANKRD35	ankyrin repeat domain 35
ANKRD45	ankyrin repeat domain 45
ASB16	ankyrin repeat and SOCS box containing 16
ATP6	ATP synthase F0 subunit 6 (mitochondrion)
ATP6V0D1	ATPase, H+ transporting, lysosomal 38kDa, V0 subunit d1
ATXN1L	ataxin-1-like
BEX2	brain expressed X-linked 2
BRINP3	family with sequence similarity 5, member C
C16H1orf159	chromosome 16 open reading frame
C19H17orf62	chromosome 19 open reading frame
C1QA	complement component 1, q subcomponent, A chain
C22H3orf62	chromosome 22 open reading frame
C6H4orf19	chromosome 6 open reading frame
C7H19ORF43	chromosome 7 open reading frame
C8H9orf152	chromosome 8 open reading frame
C9H12orf49	chromosome 9 open reading frame
CAPS	calcyphosine
CBR3	carbonyl reductase 3

CBX6	chromobox 6
CCDC178	coiled-coil domain containing 178
CD247	CD247 molecule
CDC25A	cell division cycle 25A
CLEC4F	c-type lectin domain family 4, member F
CMIP	c-Maf inducing protein
COLEC12	collectin subfamily member 12
COX1	cytochrome c oxidase subunit I (mitochondrion)
COX3	cytochrome c oxidase subunit III (mitochondrion)
COX6A1	cytochrome c oxidase subunit VIa polypeptide 1
CRMP1	collapsin response mediator protein 1
DAB2	disabled homolog 2, mitogen-responsive phosphoprotein
DAB2	dab, mitogen-responsive phosphoprotein, homolog 2
DCP1B	decapping mRNA 1B
DCXR	L-xylulose reductase-like
DFNB31	deafness, autosomal recessive 31
DSN1	DSN1 homolog, MIS12 kinetochore complex component
EDA	ectodysplasin A
EDF1	endothelial differentiation-related factor 1
EIF2B5	hypothetical LOC783760
ENTPD1	ectonucleoside triphosphate diphosphohydrolase 1
EPDR1	ependymin related protein 1
EVI2B	ecotropic viral integration site 2B

EXOC7	exocyst complex component 7
FAM213B	family with sequence similarity 213 member B
FAM89A	family with sequence similarity 89 member A
FBXO21	F-box protein 21
FGF11	fibroblast growth factor 11
FLYWCH1	FLYWCH-type zinc finger 1
FRMPD1	FERM and PDZ domain containing 1
FUT11	fucosyltransferase 11
GADD45GIP1	GADD45G interacting protein 1
GIGYF2	GRB10 interacting GYF protein 2
GLTPD1	glycolipid transfer protein domain containing 1
GPHA2	glycoprotein hormone alpha 2
GPNMB	glycoprotein (transmembrane)
GSTM3	glutathione S-transferase mu 3
HAX1	HCLS1 associated protein X-1
HDDC3	HD domain containing 3
HS3ST1	heparan sulfate-glucosamine 3-sulfotransferase 1
HUNK	hormonally up-regulated Neu-associated kinase
IFIH1	interferon induced with helicase C domain 1
IRF2BP1	interferon regulatory factor 2 binding protein 1
KAT2B	K(lysine) acetyltransferase 2B
KIF26B	kinesin family member 26B
LOC101906828	transmembrane protein 202-like

LOC521568	ATP-binding cassette, sub-family C, member 4-like
LOC530348	chondroitin sulfate proteoglycan 4-like
LSM2	LSM2 homolog, U6 small nuclear RNA associated
MAK	male germ cell associated kinase
MAP4K1	mitogen-activated protein kinase kinase kinase kinase 1
MAP7D1	arginine/proline rich coiled-coil 1-like
MAP7D2	MAP7 domain containing 2
MBLAC1	metallo-beta-lactamase domain containing 1
MED18	mediator complex subunit 18
MED9	mediator complex subunit 9
MFAP3	microfibrillar-associated protein 3
MRPL48	mitochondrial ribosomal protein L48
MSANTD2	similar to C11orf61 protein
MTHFSD	methenyltetrahydrofolate synthetase domain containing
MTMR11	myotubularin related protein 11
MYPOP	myb-related transcription factor, partner of profilin
ND1	NADH dehydrogenase subunit 1 (mitochondrion)
ND5	NADH dehydrogenase subunit 5 (mitochondrion)
NDUFA13	NADH dehydrogenase 1 alpha subcomplex, 13
NOL12	nucleolar protein 12
NOL4L	chromosome 13 open reading frame
NSUN5	NOP2/Sun domain family, member 5
NXPH4	neurexophilin 4

OAS1Y	2',5'-oligoadenylate synthetase 1, 40/46kDa
PCDHGA11	protocadherin gamma subfamily A, 11
PKN1	protein kinase N1
PLIN3	perilipin 3
PRKCG	protein kinase C gamma
PSMB9	proteasome subunit beta 9
PTN	pleiotrophin
R3HCC1L	hypothetical LOC616788
RALYL	RALY RNA binding protein-like
RASSF1	ras association domain family member 1
RETSAT	retinol saturase
RTN4R	reticulon 4 receptor
SEMA5B	sema domain seven thrombospondin repeat(semaphorin)5B
SEPT10	septin 10
SHROOM1	shroom family member 1
SIRT6	sirtuin 6
SLC22A17	solute carrier family 22, member 17
SLC25A42	solute carrier family 25, member 42
SLC2A10	solute carrier family 2(facilitated glucose transporter), 10
SPATS2L	spermatogenesis associated, serine-rich 2-like
SRRM4	serine/arginine repetitive matrix 4
SYNCRIP	synaptotagmin binding, cytoplasmic RNA interacting protein

SYNM	synemin, intermediate filament protein
TAF1D	TATA-box binding protein associated factor, RNA polymerase I
TBX4	T-box 4
TCN1	transcobalamin 1
TGFB1I1	transforming growth factor beta 1 induced transcript 1
TGOLN2	trans-Golgi network integral membrane protein 2-like
TM7SF2	transmembrane 7 superfamily member 2
TMEM136	transmembrane protein 136
TMEM229A	transmembrane protein 229A
TMEM69	transmembrane protein 69
TTBK2	TTBK2 protein-like
TTC6	tetratricopeptide repeat domain 6
UBE2B	ubiquitin conjugating enzyme E2B
UBE2D4	ubiquitin-conjugating enzyme E2D 4
UBE3C	ubiquitin protein ligase E3C
UNC119	unc-119 lipid binding chaperone
USP29	ubiquitin carboxyl-terminal hydrolase 29-like
VEPH1	ventricular zone expressed PH domain containing 1
VSTM5	V-set and transmembrane domain containing 5
WDR77	WD repeat domain 77
YIPF1	protein YIPF1-like
ZFP62	zinc finger protein 62

ZHX1	zinc fingers and homeoboxes 1
ZNF341	zinc finger protein 341
ZNF496	zinc finger protein 496

ABSTRACT

Inadequate oocyte competence is a potential explanation for reduced pregnancy rates and(or) increased late embryonic mortality when small dominant follicles are induced to ovulate prematurely with gonadotropin releasing hormone (GnRH) in beef cows. Previous studies have shown that follicle size at GnRH- induced ovulation may affect oocyte competence, as higher fertilization rates and higher embryo quality were reported after induction of ovulation in large (≥12.5mm) compared to small (<12.5mm) follicles. The objective of the current study was to determine if the size and physiological status of the pre-ovulatory follicle affects the oocyte transcriptome. To synchronize ovulation in suckled beef cows (n=250), GnRH1 was administered on day -9, prostaglandin F2α on day -2, GnRH2 (to initiate the ovulatory process) on day 0, and dominant follicles were trans-vaginally aspirated on day 1 before follicular rupture. On day 0, cows were assigned to one of the following follicle classifications: Small (<11.7mm; no estrus expression), Large (>12.5 mm; no estrus expression), and Spontaneous (11.6-13.9 mm; estrus expression and endogenous gonadotropin surge). Cumulus-oocyte complexes were collected after trans-vaginal aspiration, and oocytes were fully denuded of surrounding cumulus cells. RNA was later extracted from pools of 4 oocytes (n= 6 oocyte pools from both small and large follicles; n=5 oocyte pools from the spontaneous (control) group) and submitted for sequencing on an Illumina HiSeq 2000 (single reads, 100 bases per read) to generate an average of 8,363,823 raw reads per pool that were aligned to a Bos Taurus transcriptome from NCBI, with additional annotations, and the bovine genome (Cow_3.1_btau_4.6.1_Y_ncbi). After alignment to the bovine transcriptome or genome, differential transcript abundance between oocyte

pools from large and small follicle classifications, small and spontaneous follicle classifications, and large and spontaneous follicle classifications was determined by the edgeR-robust program with a false discovery rate (FDR) P-value of <0.10 to denote differences in transcript abundance. When the differentially abundant transcripts from the genome and transcriptome analysis were combined, 19 annotated transcripts were more abundant in small follicle oocyte pools compared to large follicle oocytes, and 35 transcripts were more abundant in large follicle oocyte pools. When small follicle oocyte pools were compared to spontaneous follicle oocyte pools, 17 annotated transcripts were higher in abundance in small follicle oocyte pools; whereas, 33 genes were higher in abundance in spontaneous follicle oocyte pools. Comparison of large and spontaneous follicle oocyte pools revealed that 15 annotated transcripts were higher in abundance in large follicle oocyte pools and 31 were higher in abundance in spontaneous follicle oocyte pools. When the differentially abundant transcripts were submitted to clustering and pathway analysis, no biological pathways were identified. However, a proportion of the differentially abundant transcripts between follicle classifications could be classified into three main biological categories: 1) Transcription or cell cycle regulation, 2) Ubiquitin/proteasome pathway, and 3) Mitochondrial function. The preceding biological pathways are known to have a role in acquisition of oocyte competence. Transcripts associated with the ubiquitin/proteasome pathway and mitochondrial function were higher in abundance in oocytes from follicles that were presumably more physiologically mature. In summary, a greater abundance of transcripts associated with the ubiquitin/proteasome pathway and mitochondrial function in oocytes from large and

spontaneous follicles compared oocytes from the small follicle category imply that oocytes from the small follicles may be less competent.

CHAPTER I

INTRODUCTION

The early calving cow is a profit driver of the cow calf operation. In progressive beef production schemes, the cowherd is managed as a unit and is thus exposed to breeding within a pre-determined breeding season. This leads to calving dates limited to a set period of time and the ability to wean all calves on the same date, regardless of exact date of birth. Cows that calve earlier in the breeding season are more profitable than their later calving herd mates, as they hold large advantages in both calf age and a longer postpartum period before the subsequent breeding season. Despite the effect of genetics, sex of calf, and nutrition on weaning weight, calf age is the number one factor determining weaning weight (Larson and Funston, 2009). Early born calves are heavier at weaning, primarily because of their age advantage. Furthermore, early calving cows have a longer period from calving to breeding, allowing them more time to return to estrus. This leads to a high probability that the early calving cow will continue to calve early, continue to wean a heavier calf, and have greater longevity in the herd compared to later calving cows.

One method to increase the number of early calving females is the implementation of an estrous synchronization program in combination with fixed-time artificial insemination (FTAI) at the start of the breeding season. Ovulation of the entire herd is synchronized such that all females are inseminated at one time regardless of estrous expression, and thus given the opportunity to conceive, on day 1 of the breeding season. Another advantage of FTAI, is the induction of a fertile ovulation in anestrous females, if a progestin-based protocol is used. Administration of a progesterone releasing vaginal

implant (Controlled Internal Drug Release; CIDR) can mimic the short luteal phase that often precedes return to cyclicity in anestrous females, as reviewed by Day (2004). A fertile estrus occurs following CIDR removal in a proportion of anestrous cows, allowing them to conceive earlier in the breeding season.

Injection times and treatments vary among estrous synchronization protocols. However, in all FTAI protocols two main objectives are accomplished- management of the luteal and follicular phase of the estrous cycle. First, administration of a progestin (i.e. CIDR) causes elevated circulating concentrations of progesterone sufficient to block estrous expression until CIDR removal. An injection of prostaglandin $F_{2\alpha}$ (PGF) at CIDR removal induces corpus luteum regression. This reduction of progesterone allows for females to develop a pre-ovulatory follicle capable of ovulating in response to an endogenous or induced pre-ovulatory gonadotropin surge. Secondly, an injection of gonadotropin releasing hormone (GnRH) at CIDR insertion induces ovulation of a dominant follicle in 66% of postpartum beef cows (Geary et al., 2000), followed by the initiation of a new follicular wave. This leads to the synchronization of follicular waves, which allows for the synchronization of ovulation following CIDR removal and PGF injection. A proportion of females will express estrus spontaneously prior to FTAI. However, a number of females will not exhibit estrus by the time of insemination. Therefore, a second injection of GnRH is given at breeding to induce a pre-ovulatory gonadotropin surge in females that have not yet exhibited estrus. This allows for the insemination of all females at a set time. It is noteworthy that animals that exhibit estrus and spontaneously ovulate experience higher pregnancy rates following insemination

than do those animals which undergo GnRH-induced ovulation (Larson et al., 2006; Perry et al., 2005).

When ovulation is induced, the size or physiological maturity of the pre ovulatory follicle influenced pregnancy rate in cattle (Lamb et al., 2001; Vasconcelos et al., 2001; Perry et al., 2005). Postpartum beef cows induced to ovulate small dominant follicles (<11.3mm) experienced lower pregnancy rates than did those induced to ovulate large (>11.3mm) dominant follicles. Interestingly, ovulatory follicle size did not affect pregnancy attainment when animals exhibited estrus and underwent spontaneous ovulation (Perry et al., 2005). This led to the hypothesis that the physiological maturity, rather than the size, of a pre-ovulatory follicle affects the establishment and maintenance of pregnancy (Perry et al., 2005; Atkins et al., 2013). Small (immature) dominant follicles have been shown to have negative effects on pregnancy due to an inadequate uterine environment, as animals induced to ovulate small follicles were observed to have lowered serum concentrations of estradiol at the time of ovulation and lowered concentrations of progesterone following ovulation. Both of the above conditions reduced pregnancy rates in beef cattle and support the hypothesis that that lowered pregnancy rates following GnRH-induced ovulation of a small dominant follicle may be due to a compromised maternal environment (Atkins et al., 2013; Jinks et al., 2013). There is also evidence that the GnRH-induced ovulation of small follicles resulted in inadequate oocyte competence. Atkins et al. (2013) reported that fertilization rate and the probability of recovering a transferable embryo increased as ovulatory follicle size increased. However, in the preceding study embryos were collected on day 7 after AI; therefore, an early effect of the maternal environment cannot be ruled out.

Oocyte competence is known to greatly impact the developing embryo in the cow. A competent oocyte can be defined as having the ability to resume meiosis, cleave after fertilization, develop to the blastocyst stage, and induce and bring to term a successful pregnancy (Sirard et al., 2006). To reach developmental competence, the oocyte must undergo meiotic, cytoplasmic, and molecular maturation. During molecular maturation, the oocyte experiences a rapid increase in RNA transcription beginning at the secondary follicle stage of development (Fair et al., 1997). Transcription continues until germinal vesicle breakdown, which occurs after an endogenous or induced gonadotropin surge. Transcription and storage of important maternal RNA is necessary to allow the oocyte to continue through maturation and the formation of a viable embryo until embryonic genome activation, which is at the 8 cell stage in cattle (Sirard, 2012).

In previous studies, certain genes were identified to be associated with higher levels of oocyte competence. Oocyte expression of Follistatin (FST), Inhibin Beta A (INHA), and Inhibin Beta B (INHB)was increased in higher quality bovine oocytes in a study that utilized oocytes originating from mature beef females (high quality) or pre-pubertal heifers (low quality) (Patel et al., 2007). Furthermore, decreased expression of Cathepsins B, S, and Z in surrounding cumulus cells indicated greater oocyte competence as seen in a study that measured both time to first cleavage and cleavage rates for as a marker of oocyte competence (Bettegowda et al., 2008). Finally, our laboratory has collected preliminary data, from a relatively small number of cows, in which cumulus cell mRNA abundance of Cathepsin B was decreased in large dominant follicles collected 48 hr after PGF injection (CO-Synch protocol). These data support the hypothesis that oocytes from large dominant follicles are more competent.

While the data from the studies mentioned above suggest there are negative effects of the GnRH-induced ovulation of small dominant follicles on oocyte competence (Atkins et al., 2013) and identify genes (FST, INHA, INHB, Cathepsins B,S,Z) associated with oocyte competence in non-ovulatory follicles (Patel et al., 2007; Bettegowda et al., 2008), no studies have been performed in which the competence of oocytes derived from pre-ovulatory follicles has been measured without the influence of the maternal environment. Therefore, the specific aim of this project was to compare the transcriptomes of oocytes originating from small (<11.7mm, GnRH-induced gonadotropin surge, no estrous expression), large (>12.5mm, GnRH-induced gonadotropin surge, no estrous expression), and spontaneous (11.6-13.9 mm; estrus expressed) dominant follicles. Analysis of differential transcript abundance revealed differentially abundant transcripts between oocytes originating from the preceding follicle classifications, with transcripts related to the mitochondria and ubiquitin/proteasome pathways being more abundant in oocyte pools originating from follicles that were presumably more mature.

CHAPTER II

REVIEW OF LITERATURE

2.1 Introduction

Fixed-time artificial insemination (FTAI) allows beef producers to synchronize estrus and ovulation such that a large proportion of females conceive on day one of the breeding season. Fixed-time AI protocols for beef cattle frequently involve the following sequence: 1) an injection of gonadotropin releasing hormone (GnRH) to induce a pre-ovulatory gonadotropin surge and subsequent ovulation resulting in synchronization of a new follicular wave, 2) the injection of prostaglandin $F_{2\alpha}$ (PGF) for the induction of corpus luteum regression, and 3) GnRH-induced ovulation of a dominant follicle resulting in ovulation approximately 28 to 32 hours after GnRH injection (Patterson et al., 2003). For FTAI protocols, the timing of insemination is scheduled to result in an overlap between the period of oocyte viability following ovulation and availability of capacitated sperm in the ampulla of the oviduct. However, at the time of FTAI there is a mixed population of heifers or cows - those that have expressed estrus and those that have not. Animals that have not expressed estrus by FTAI require an injection of GnRH to induce a gonadotropin surge and subsequent follicular rupture such that all animals can be inseminated at the same time. Females that exhibit estrus prior to insemination normally have a spontaneous gonadotropin surge and experience higher pregnancy rates compared to those that fail to exhibit estrus (Perry et al., 2005; Larson et al., 2006).

Pre-ovulatory follicle size affects pregnancy rates in females that rely on GnRH-induced ovulation. Perry et al. (2005) observed that cows induced to ovulate large (>11.3mm) follicles experienced higher pregnancy rates and lower rates of late

embryonic mortality compared to cows induced to ovulate smaller follicles. However, pregnancy rate was independent of follicle size in animals that spontaneously exhibited estrus, leading to the hypothesis that follicle size is in indicator of follicle maturity in those animals which do not express estrus and have an endogenous gonadotropin surge.

The overall hypothesis is that the decrease in pregnancy rate and late embryonic/fetal survival (days 28 to 70 post breeding) is due to a combination of decreased oocyte competence and (or) an inadequate preparation of the maternal environment for pregnancy establishment. Therefore, Atkins et al. (2013) performed a reciprocal embryo transfer experiment to distinguish between effects of the follicular microenvironment on oocyte competence versus the maternal environment. Single GnRH-induced ovulations were synchronized in recipient and donor postpartum beef cows. Animals were classified into large (≥12.5mm) and small follicle (<12.5mm) groups at GnRH-induced ovulation, and none of the animals were detected in estrus. Donor animals were inseminated, and embryos or unfertilized oocytes were recovered seven days later. Viable embryos from donors with large follicles were transferred to recipients with large follicles to serve as a positive control, and to recipients that were induced to ovulate a small follicle to examine effects of the uterine environment. Likewise, embryos from donors in which small follicles were induced to ovulate were transferred to recipients that ovulated small follicles (negative control) or to recipients that ovulated a large follicle to reveal effects of GnRH-induced ovulation on oocyte competence. Evidence of a compromised uterine environment and inadequate oocyte competence in females induced to ovulate a small compared to a large ovulatory follicle was reported. Evidence for inadequate oocyte competency included reduced fertilization rate and

embryo quality when donor animals were induced to ovulate a small follicle. However, more research was required to eliminate the effect of the post-ovulation maternal environment on oocyte and subsequent embryo quality. Thus an experiment was performed to explore differences in the transcriptome of oocytes and cumulus cells from small or large follicles in beef cows approximately 20 hours after a GnRH-induced gonadotropin surge and control oocytes and cumulus cells from follicles which were exposed to an endogenous gonadotropin surge. This literature review will focus on the following areas: 1) Formation of oocytes and follicles, 2) Growth and maturation (i.e. meiotic, cytoplasmic, and molecular maturation) of the oocyte and the contributions of the surrounding cumulus cells to oocyte maturation, and 3) Influence of the follicular microenvironment on acquisition of oocyte competence.

2.2 Oocyte Competence

The oocyte is essential in the establishment of a successful pregnancy and the continuation of future generations. For pregnancy to be established and result in the birth of live offspring, the oocyte must obtain developmental competence before ovulation and subsequent fertilization. Sirard et al. (2006) described oocyte competence as the ability of the oocyte to resume meiosis, cleave upon fertilization, develop to the blastocyst stage, and induce and bring to term a pregnancy in good health. Oocytes that have acquired a degree of meiotic competence spontaneously resume meiosis when they are removed from their surrounding follicular cells or after they are exposed to a pre-ovulatory gonadotropin surge. However, this does not insure developmental competence. The ability of an oocyte to resume meiosis can be visualized through the breakdown of the germinal vesicle and the expulsion of a polar body. It is noteworthy that most oocytes

that have resumed meiosis are capable of interacting with a spermatozoa to form a zygote (Sirard, 2001). Bovine oocytes that have resumed meiosis are also thought to intrinsically have the ability to cleave following fertilization, as parthenogenetically activated oocytes have been shown to cleave even without a fertilizing spermatozoa (Bhak et al., 2006). However, the ability of a fertilized oocyte to reach the blastocyst stage is far more dependent on the maturity of the oocyte and the follicle from which it originated.

Maternally stored RNAs, proteins, and transcription factors are necessary for the activation of the embryonic genome which allows for development past the maternal zygotic transition (MZT) to the blastocyst stage (Sirard, 2012). Interestingly, when oocytes are matured in vivo, greater than 2/3 of fertilized oocytes develop to the blastocyst stage compared to only 1/3 of their in vitro matured and fertilized counterparts. Such data suggest that oocytes gradually acquire the capacity to reach the blastocyst stage as they produce and store RNA during follicular development up to germinal vesicle breakdown. In addition to the lower blastocyst rates discussed above, lower pregnancy rates are observed from oocytes matured in vitro versus those matured in vivo (Peterson and Lee, 2003), and a greater degree of late embryonic mortality is observed in bovine pregnancies resulting from the induced ovulation of small versus large follicles (Perry et al., 2005). Such differences may be due, in part, to inadequate oocyte competence.

2.3 Oocyte and follicular development

The formation of oocytes takes place before birth in most female mammals such that by the time of birth, the ovaries contain a finite number of oocytes encased in

follicles that may remain in a quiescent state for many months or years before initial recruitment of folliculogenesis occurs.

Primordial germ cell migration and development of primordial follicles

Ovarian formation begins when primordial germ cells, from the yolk sac, migrate through the hind gut to the genital ridge, where they will colonize the developing ovary and begin the process of developing into the individual's store of oocytes (van den Hurk and Zhao, 2005). Presence of primordial germ cells in the genital ridge is established from days 27-30 of fetal development in cattle (Wrobel and Süß, 1998). As reviewed by Picton et al. (1998), primordial germ cells lose their motility once established in the gonad and are referred to as oogonia. The oogonia undergo numerous mitotic divisions before their entrance into meiosis, at which point they become primary oocytes.

In ruminants, there are three hypotheses regarding the origin of the somatic cells which surround the individual's stockpile of oogonia as pre-granulosa cells. Possible sources of the pre-granulosa cells include mesonephric cells derived from the proximal third of the mesonephros, cells migrating from the blastema, and mesothelial cells derived from the surface epithelium of the ovary (Juengel et al., 2002; Juengel and Smith, 2014). Clusters of pre-granulosa cells surrounding groups of oogonia form and are surrounded by a basal lamina which serves as a barrier between the developing follicles and the surrounding ovarian stroma. These walled off clusters form the ovigerous cords which open at the surface epithelium. Hence, mesothelial cells from the surface epithelium of the ovary are believed to be the primary source of pre-granulosa cells in sheep as they can continue to migrate into the ovigerous cords after the

compartmentalization that separates the oogonia from other possible somatic cells sources (Juengel et al., 2002; Juengel and Smith, 2014).

At the time of ovigerous cord formation, a high level of mitosis is seen in both oogonia and pre-granulosa cells. High rates of transcription in the oogonia are associated with this stage of rapid proliferation. However, by day 80 of fetal development in cattle the oogonia have begun to enter meiosis and will have entered prophase, marking a rapid decline in transcriptional activity (Fair, 2003; van den Hurk and Zhao, 2005). Interestingly, the timing of the onset of meiosis appears to be regulated by the location of germ cells within the ovigerous cords. Oogonia located deep in the ovarian cortex enter meiosis before their more externally located counterparts. After entering meiosis, the germ cells are referred to as oocytes. Such oocytes will continue meiosis before entering diplotene arrest at around day 170 of gestation (Fair, 2003). Transcription increases as oocytes enter the diplotene stage of meiosis, and transcriptional activity continues throughout diplotene arrest. Transcription is elevated following primordial follicle activation and remains active throughout subsequent oocyte growth. Diplotene arrest is continued until the oocyte is either removed from the surrounding follicular cells or exposed to a luteinizing hormone (LH) surge, both of which lead to a cascade of events culminating in germinal vesicle breakdown (GVB), polar body expulsion, and the resumption of meiosis (van den Hurk and Zhao, 2005). Newly formed oocytes are extremely sensitive to apoptosis while progressing through the first prophase of meiosis; therefore, a large number of oocytes will die before reaching their first meiotic arrest. A 95% loss of oocytes during early meiosis has been observed in bovine females (van den Hurk and Zhao, 2005).

A basal lamina forms the boundary of the ovigerous cords to separate forming follicles from the rest of the ovary until follicle assembly is complete. At this time, the ovigerous cords break down and allow for the dispersion of clusters of developing follicles that will continue to separate from each other until individual primordial follicles are formed, each individually encased in a basal lamina (Juengel et al., 2002; Juengel and Smith, 2014). Primordial follicles are formed in cattle by day 90 of gestation (Fair, 2003). Oocytes encased in primordial follicles are characterized by the lack of a zona pellucida and by the single layer of flattened, non-dividing pregranulosa cells that surround them. The intimate association between the plasma membranes of the primary oocyte and surrounding pregranulosa cells provides the basis for subsequent formation of transzonal processes (discussed later). At this point, the oocyte is not growing and is developmentally incompetent. Upon activation of the primordial follicle, the granulosa cells transform from a squamous to cuboidal morphology and begin proliferation (Fair, 2003). This is the initiation of folliculogenesis.

Primary, secondary, and tertiary stages of follicular development

The oocyte has a key role in the progression of follicles past the primary stage of development (Eppig, 2001). In the subsequent stages of development, the oocyte gradually increases in size and synthesizes and stores molecules of mRNA, protein, lipid, and sugar while remaining under meiotic arrest (Marteil et al., 2009). While the oocyte is growing, it is thought to be meiotically incompetent, and is not yet able to undergo GVB and continue through meiosis. The secondary follicle stage symbolizes many advancements in follicular development and oocyte maturity. The zona pellucida begins to form at the secondary follicle stage, and cortical granules are formed within the

oocyte's cytoplasm. Furthermore, oocyte RNA synthesis is first significantly detected at the secondary follicle stage (Fair et al., 1997). A second layer of granulosa cells also appear in the secondary follicle stage.

The formation of a fluid filled antrum marks the transition into the tertiary follicle stage. Ovarian follicles experience many morphological changes as they enter the tertiary stage of follicular development. The somatic cells experience continued proliferation and differentiate into theca externa and interna, the basement membrane, granulosa cells, and the cumulus cells which directly surround the oocyte (reviewed by Erickson and Shimasaki, 2000; Gilchrist et al, 2004). In farm animals, meiotic competence and ovum size are thought to increase with the increasing size of the antral follicle (Arlotto et al., 1996).

Progression of follicles recruited through the estrous cycle

A transient rise in follicle stimulating hormone (FSH) leads to the recruitment of a small cohort of ovarian follicles, which are dependent on FSH for continued growth. The group of follicles grow in size and collectively synthesize estradiol and inhibin, which in turn negatively regulate the animal's FSH secretion. At this time, all but one follicle undergo atresia due to the rapid decline of available FSH. One follicle is selected for continued growth due to increased sensitivity to the gonadotropins gained from higher levels of free insulin-like growth factor (IGF), and its acquisition of LH receptors which lead to a switch in dependency from FSH to LH (Lucy, 2007). The dominant follicle and its enclosed oocyte continue growth and development for a period of days before ovulation. In vivo, the final maturation of the ovulatory follicle is initiated by the pre-ovulatory LH surge (Lonergan et al., 2003). Here a progression of changes occur in the

follicle wall that lead to ovulation, luteinization of the thecal and granulosa cells, and cumulus cell expansion. The oocyte has now attained meiotic competence, and exposure to the pre-ovulatory LH surge leads to GVB and the conclusion of maternal mRNA transcription. Chromosomes now separate from each other with one set extruded as the first polar body. The set of chromosomes remaining in the oocyte nucleus line up to begin the second metaphase. In cattle, there is a second meiotic arrest at this point, metaphase two (MII), which continues until fertilization allows for meiotic resumption and the extrusion of a second polar body. The male and female pronuclei join, and the resulting zygote begins a series of mitotic divisions that lead to further stages of development. The early embryo will rely on maternally stored RNA for continued development until the time of the maternal-zygotic transition. Embryonic genome activation and the ability of the embryo to begin RNA transcription is thought to be a pivotal event that may be affected by oocyte competence level. Oocytes gain competence throughout oogenesis, and it is known that oocytes acquire competence as they progress towards the final stage of follicular development. Specific phenomena that result in oocyte competence will be described in following sections and will emphasize cattle unless stated otherwise.

2.4 Oocyte Maturation

Oocyte maturation can be discussed as three interlinked events which allow the oocyte to gain the ability to be fertilized, cleave, and provide instruction for early embryonic development until the activation of the embryonic genome. Meiotic or nuclear maturation refers to the ability of the oocyte to condense its chromatin and progress to MII. Cytoplasmic maturation involves ultrastructural changes that ready the oocyte for successful fertilization and subsequent development. Before germinal vesicle breakdown,

the oocyte must synthesize and store RNA transcripts to be used in early embryonic development. The process of RNA transcription and storage is referred to as molecular maturation.

Developmental competence is acquired throughout oocyte and follicular growth as the oocyte progresses through meiotic, cytoplasmic, and molecular maturation. During the period of oocyte growth, the bovine oocyte grows from an intra-zonal diameter of less than 30 µm in the primordial follicle to sizes exceeding 120 µm in tertiary follicles (Hyttel et al., 1997). Oocyte competence can be examined by evaluating the rate at which fertilized oocytes reach the blastocyst stage. Otoi et al. (1997) reported the percentage of fertilized oocytes that reached the blastocyst stage increased significantly when oocytes with an intrazonal diameter of 115-120 µm were compared to those with a diameter of 100-115µm. Blastocyst rates were increased further in oocytes that had a diameter of 120-125µm.

Further evidence has demonstrated that the ability to reach the blastocyst stage is enhanced in oocytes derived from follicles greater than 6mm compared to those from follicles 2-6mm in size. Hendricksen et al. (2000) reviewed oocyte competence and reported higher developmental competence in oocytes derived from follicles greater than 6-8mm compared to those encased in follicles less than 6mm in size. A further rise in oocyte competence was also noted in oocytes encased in follicles greater than 13mm in size, which supports the hypothesis that oocytes continue to gain developmental competence throughout follicular development.

Meiotic Maturation

In fetal life, DNA synthesis doubles the chromatin content in the oocyte. Here the chromosomes are partially condensed and undergo rearrangement by homologous recombination to increase genetic diversity in subsequent generations. The chromatin then enters the dictyate or diplotene stage and is arrested in a state of intermediate chromatin condensation which allows for the transcription of mRNA that can be stored within the oocyte for weeks due to polyadenylation of the 3' untranslated region (Sirard, 2001). Oocytes remain in diplotene arrest until they are either removed from their surrounding follicular cells or are exposed to the pre-ovulatory gonadotropin surge. The ability to be released from meiotic diplotene arrest, have fully condensed chromatin, expel a polar body, and progress to metaphase II is acquired by the oocyte through the process of meiotic or nuclear maturation.

The acquisition of the ability to resume meiosis in the oocyte begins as the oocyte enters its growth stage. It is commonly accepted that actively growing oocytes are meiotically incompetent, and acquisition of meiotic competence is a progression that takes place as the oocyte grows (Sirard, 2001). The first step toward acquiring meiotic competence occurs when the oocyte gains the ability to condense its chromatin. This is followed by the formation of the metaphase I (MI) plate and a functional spindle. The MII plate is then formed and is followed by expulsion of a polar body. The final event in meiotic maturation occurs when the oocyte's chromatin is arrested at the MII spindle (Sirard, 2001). At an intrazonal diameter of 100 µm, the oocyte acquires the ability to resume meiosis, but the level of competence required to reach MII is not reached until an oocyte diameter of 110 µm. Therefore, full meiotic competence is said to occur when an

oocyte attains a diameter of 110 µm, which is contained in a 3 mm bovine follicle (Hyttel et al., 1997). Data supporting that meiotic competence is progressively acquired with increasing follicle and oocyte size was reported by Otoi et al. (1997). Researchers examined oocytes encased in 1-7mm follicles and found that the percentage of oocytes that underwent GVB increased significantly in oocytes with an intra-zonal diameter of 110µm compared to those with a diameter of 100µm. When the ability to reach the MII stage was evaluated, oocytes with a diameter of 100µm-115µm had a similar ability to reach MII, but the percentage of oocytes reaching MII increased as oocyte diameter went from 115-120µm. The ability to reach MII increased again when oocytes with a diameter of 120-125µm were examined.

Cytoplasmic Maturation

Arlotto et al. (1996) found that a greater percentage of bovine oocytes with an intrazonal diameter of greater than 115µm reached the blastocyst stage than did oocytes with a diameter of 105-114µm, despite an equal acquisition of meiotic maturation past the 110µm size. It can then be deduced that while oocytes from smaller follicles (>3mm) have reached nuclear maturation competency and the capacity to develop into an embryo, they remain cytoplasmically immature and require stages of pre-maturation or oocyte capacitation to reach full developmental competence.

Changes within the ultrastructure of the oocyte have been observed as the oocyte progresses from the germinal vesicle (GV) stage to MII. Even earlier changes in the oocyte's ultrastructure occurred when the follicle entered the secondary follicle stage. At this time, the zona pellucida and cortical granules were synthesized (Sirard, 2001). Few changes in the oocyte ultrastructure were observed from this point until the follicle

reached a size of 8-9 mm (Hendrickson et al., 2000). As the follicle grows to full ovulatory size, changes in the mitochondria, ribosomes, endoplasmic reticulum, Golgi complex, and cortical granules occur as the oocyte transitions from the GV to MII stage (Ferreira et al., 2009). The preceding reorganization is presumably regulated by cytoskeletal microfilaments and microtubules located in the cytoplasm. A brief description of changes in organelles within the bovine oocyte are described below.

Mitochondria: Adequate numbers of properly functioning mitochondria are essential for acquisition of oocyte competence (reviewed by Bavister and Squirrell, 2000). More specifically, mitochondrial production of ATP via oxidative phosphorylation is required for fertilization, meiotic maturation, and preimplantation embryo development. The number of mitochondria in oocytes increases throughout oocyte maturation (reviewed by Ferrierra et al, 2009; Bavister and Squirrel, 2000). Upon exposure to a pre-ovulatory gonadotropin surge, the mitochondria move from the peripheral regions of the oocyte to more internal areas surrounding the nucleolus (Ferreira et al., 2009; Bavister and Squirrell, 2000). The increased number and internalized location of the mitochondria are related to increased oocyte competency, as lower numbers or peripherally located mitochondria lead to less ATP availability to the nuclear compartments of the cell. The importance of increased mitochondrial numbers during cytoplasmic maturation is further highlighted, as mitochondria in embryos are derived solely from maternal mitochondria. Mitochondria present at the time of fertilization are divided among blastomeres during embryonic cleavage with no new mitochondria produced until the time of implantation in the mouse (reviewed by Dumollard et al., 2009). Interestingly, a specific phenotype of mitochondria, hooded

mitochondria, with a finger-like projection extending from the distal end of the mitochondrion were observed in bovine oocytes collected from both dominant and smaller follicles present on the ovaries of cows that were slaughtered at the time of estrus (Senger and Saacke, 1970). However, the functional significance of hooded mitochondria is unknown.

Endoplasmic reticulum, cortical granules, and Golgi complex: The endoplasmic reticulum is essential to proper protein folding, lipid metabolism, nuclear compartmentalization, membrane synthesis, and intracellular synthesis by the calcium ion gradient it provides. There is increased sensitivity to calcium ion signaling as the oocyte matures to allow for the release of cortical granules. Exclusively found in oocytes, cortical granules are essential to the cortical reaction, in which their exocytosis is key to preventing polyspermy (Ferreira et al., 2009). Beginning at the secondary follicle stage, cortical granules are synthesized by the Golgi complex (Ferreira et al., 2009). In GV oocytes cortical granules are located evenly throughout the cytoplasm, but as oocytes reach MII the cortical granules migrate to the peripheral edges of the cytoplasm where they await a fertilizing sperm to activate the cortical reaction. After a sperm penetrates the zona pellucida, calcium is released from the endoplasmic reticulum. This rise in calcium leads to the release of the oocyte's cortical granules to its outer surface. The Golgi complex is essential to the production of cortical granules and the zona pellucida. As the oocyte enters its growth stage, Golgi membranes possess increased numbers of swollen, stacked lamellae with numerous vacuoles, granules, and vesicles necessary for the processing of the secretory products mentioned above (Wassarman and Albertini, 1994).

Ribosomes: The oocyte requires translation of RNA into protein for continued development. Adequate numbers of ribosomes must be present within the maturing oocyte to allow for proper protein formation. A review by Ferreira et al. (2009) describes the translational activity and abundance of ribosomes throughout oocyte maturation. Higher numbers of ribosomes, accompanied by a 3 fold increase in protein translation is observed in MI oocytes compared to MII oocytes that had undergone GVB.

Cytoskeleton: Cytoskeletal filaments are essential to oocyte viability, as they are responsible for the segregation of the chromosomes during mitotic and meiotic progression, cell division during cytokinesis, and the movement of organelles and other molecules within the cell (Ferreira et al., 2009).

Molecular Maturation

The third, and least well understood, aspect of oocyte maturation, molecular maturation, refers to the transcription and storage of the mRNA blueprint (i.e. transcriptome) from which the oocyte and subsequent embryo will synthesize proteins. This section will focus on how the oocyte acquires its transcriptome and the influence of surrounding follicular cells on the oocyte transcriptome. The accumulation of specific transcripts is required for the acquisition of meiotic and developmental competence in the oocyte (Hyttel et al., 1997). In bovine, transcripts produced and stored by the oocyte are essential for subsequent oocyte maturation and early embryonic development up to activation of the embryonic genome (reviewed by Sirard et al., 2006). Both the quantity and integrity of the transcriptome affects oocyte competence, as adequate numbers of high quality maternal mRNA transcripts are necessary for the oocyte to develop into a viable embryo and successful pregnancy.

Maternal mRNAs are rapidly transcribed and stored during the oocyte growth stage, and transcriptional activity continues, at a lower rate, until condensation of the chromosomes following germinal vesicle breakdown (see below). From the time of the preovulatory gonadotropin surge to activation of the bovine embryonic genome (8 to 16 cell stage), maternal transcripts are translated into proteins necessary for early embryonic development; consequently, an inadequate transcriptome may be present due to a premature stop of transcription (e.g. GnRH-induced gonadotropin surge) and(or) inadequate transfer of mRNA from the cumulus cells.

Transcriptional activity in bovine oocytes was observed to begin at the secondary follicle stage (Fair et al., 1997). The transcriptional activity of resting primordial, activated primordial, primary, secondary, and tertiary follicles was determined by ^{3}H-uridine incorporation. No oocytes from resting primordial follicles and few oocytes from activated primordial follicles or primary follicles exhibited ^{3}H-uridine incorporation, but the majority of oocytes from secondary and tertiary follicles displayed evidence of transcription.

Furthermore, transcriptional activity is more robust in oocytes encased in small follicles (<1-2mm) compared to those derived from larger antral follicles (>2mm) (Fair et al., 1995). Oocytes were collected from follicles that were <1mm, 1-2mm, 2-3mm, 3-4mm, and >4mm in diameter. Measurement of the oocyte's intra-zonal diameter revealed oocytes of the following diameters (<100µm, 100-110µm, 110-120µm, and >120µm) were encased within each follicle size classification. However, a majority of oocytes <100µm in diameter originated from <1mm follicles, oocytes 100-110µm in diameter predominantly originated from <2 mm follicles, oocytes from 110-120µm in diameter

originated from >2mm follicles, and oocytes >120µm were encased in >3mm follicles. When transcriptional activity was monitored by ^{3}H-uridine incorporation, transcription was observed in 85% and 61% of oocytes <100µm and 100-110µm in diameter respectively. There was a significant decline in ^{3}H-uridine incorporation in oocytes as intra-zonal diameter reached 110µm, as only 20% and 17% of oocytes 110-120µm and >120µm exhibited ^{3}H-uridine incorporation, signifying transcription.

Mamo et al. (2011) further explored the transcriptional activity of bovine oocytes by analyzing the transcriptome of immature (GV) and in-vitro matured (MII) oocytes. In this study, 2117 transcripts were differentially abundant between GV and MII oocyte classifications, with 1528 transcripts that were higher in abundance in GV oocytes and 589 that were higher in abundance in MII oocytes. These results support that transcription continues as oocyte maturation progresses past the early stages of rapid oocyte growth (described earlier). Furthermore, treatment of maturing oocytes with the transcriptional inhibitor α-amanitin reduced quantities of specific transcripts that were higher in abundance in MII oocytes. MII oocytes that were cultured in the presence of α-amanitin possessed lower amounts of specific transcripts than oocytes matured 24 hours in the absence of α-amanitin, and oocytes matured with α-amanitin showed an expression profile similar to the immature GV oocytes previously analyzed. The accumulation of the transcripts observed to be higher in abundance in MII oocytes was studied by collecting oocytes at 0 (GV), 3, 6, 12, and 24 (MII) hours of in vitro maturation (IVM). It is noteworthy that during in-vitro maturation GVB usually occurs within 4-8 hours. One group of genes analyzed had decreased abundance after 3 hours of maturation, followed by a gradual rise in abundance until hour 12 or 24 of IVM. Other transcript groups

revealed no difference in abundance after 3 hours of IVM, but had a rapid increase in abundance until 12 or 24 hours of IVM. This study supports the concept that the majority of transcriptional activity takes place while the oocyte is in a stage of rapid growth, but also reveals transcriptional activity in fully grown GV oocytes as they complete the final stages of maturation to reach MII.

Mourot et al. (2006) investigated differences in the mRNA content of oocytes matured in-vivo or in-vitro to determine possible transcript differences that may explain the differences in viability associated with in-vivo versus in-vitro maturation methods. The transcriptome of oocytes collected by ovariectomy 6 hours after the LH surge was compared to that of oocytes collected from slaughterhouse ovaries and matured in-vitro for 6 hours to determine possible differences in transcript abundance. A set of genes were identified to be differentially abundant between oocytes of the above maturation categories. The abundance of selected genes was then analyzed in oocytes collected from <3, 3-5, 5-8, and >8 mm follicles. Of the candidate genes analyzed by real-time polymerase chain reaction (PCR), one subset of genes showed no difference in abundance between follicle size classifications, a second subset of genes showed higher mRNA levels in oocytes from the >8mm follicles compared to oocytes from all other follicles, and a final category of genes had different levels of RNA abundance in oocytes of each follicle category with either rapid or slow increases in abundance seen as follicle size increased. This study revealed small differences in the transcriptome of oocytes of high (in-vivo matured) and low (in-vitro matured) competence, and that a subset of these genes are accumulated in oocytes of progressively larger follicles.

Storage of mRNA transcripts

Messenger RNA transcripts are stored in the oocyte's cytoplasm through the incorporation and extension of a 3' poly(A) tail (Brevini-Gandolfi et al., 1999). Availability of transcripts for interaction with the polyribosome, and subsequent transcription, is allowed by the shortening of the poly(A) tail. The polyadenylation status of transcripts is known to be of importance for embryonic developmental success. Thus, Brevini-Gandolfi and colleagues (1999) studied the polyadenylation of transcripts from oocytes pre-determined to have high or low developmental competence throughout the maturational process. Nearly all transcripts studied from both oocyte classifications had shorter poly(A) tails at the MII stage compared to the GV stage, however it is noteworthy that the deadenylation of transcripts does not always correlate to their immediate translation. Furthermore, oocytes of low developmental competence had lower levels of polyadenylation than oocytes with high developmental competence at both the GV and MII stage revealing possible differences in the integrity of important transcripts that may lead to the observed differences on oocyte competence.

Surrounding cumulus cell contributions to oocyte RNA accumulation

Bi-directional communication between the oocyte and surrounding cumulus cells includes both paracrine and gap junctional communication (reviewed by Eppig, 2001). Although much of the research on the oocyte transcriptome has focused on transcription and mRNA storage within the oocyte, the surrounding cumulus cells also transcribe and transport mRNA to the oocyte (Macaulay et al., 2014, Macaulay et al., 2016). The innermost layer of cumulus cells, the corona radiata, possess cellular projections (i.e. transzonal projections) that penetrate the zona pellucida and directly contact the

oolemma. The initial contact between the plasma membrane of a preganulosa/granulosa cell and the oolemma occurs at the primordial/primary follicle stage, before the formation of the zona pellucida. The zona pellucida forms around the transzonal projections allowing for the continued direct contact of the two cell types. Although it is well known that small molecules (e.g. cAMP) can be delivered from cumulus cells to the oocyte, via transzonal processes, transport of mRNA to the oocyte has recently been reported (Macaulay et al, 2014). In 2016, Macaulay and others demonstrated active transport of molecules (e.g. mRNA) from the cumulus cells, through the transzonal projections, into the oocyte. Furthermore, they showed an increased concentration of cumulus cell transcripts in regions of the oocyte that were close to intact cumulus cells and a lower concentration in areas of the oocyte where the surrounding cumulus cells were denuded. Evidence that mRNA within cumulus cells was transferred to and translated within the oocyte was based on the observation that a percentage of the transcripts that increased in the oocyte from the GV to MII stage were present within transzonal processes (suggesting their transport from the cumulus cells) and present on both GV and MII oocyte polyribosomes (suggesting the timely translation of such transcripts into protein). Cumulus cells have the ability to transfer mRNA to the oocyte until the gonadotropin surge initiates cumulus expansion and disruption of the integrity and RNA transferring capabilities of the transzonal projections.

2.5 Follicular influence on oocyte competence

The bovine oocyte and surrounding follicular cells are intimately associated from early development (i.e. primordial follicle) and participate in bi-directional

communication. Oocyte growth and mitosis of follicular cells occurs in parallel until the follicle reaches a diameter of 3mm, after which oocyte growth is basically complete (120-130µm diameter); whereas, follicular growth continues until it attains ovulatory size, often equal to or greater than 15mm (Fair, 2003.) Sirard (2012) reviewed the effect of follicular size and apparent health of the oocyte's surrounding follicular cells on acquisition of oocyte developmental competence. His lab reported higher developmental competence in oocytes incased in follicles in which there was evidence of apoptosis within some of the outermost cumulus cells. Apoptosis begins with the outermost follicular cells types and continues inward until the follicle and encased oocyte die (Sirard, 2012). Atresia of subordinate follicles begins after one selected follicle achieves dominance and inhibits circulating concentrations of FSH, upon which the subordinate follicles are dependent.

To determine the viability of oocytes from bovine follicles on differing days of a follicular wave, Machatkova et al. (2000) monitored the rate of progression to the blastocyst stage after in-vitro maturation and fertilization of oocytes aspirated from all antral follicles on day 3, 4, or 5 of the first follicular wave. Higher blastocyst rates were observed when oocytes were aspirated on day 5, coinciding with establishment of follicular dominance, as compared to day 3, when circulating concentrations of FSH were elevated.

As the oocyte progresses from the GV to the MII stage, the organization of its chromatin becomes more condensed and can be classified as GV0, GV1, GV2, and GV3 (Lodde et al., 2008). More specifically, the degree of chromatin condensation is described as follows: 1) GV0 - virtually no condensation of the chromatin, 2) GV1 - a very small

degree of condensation, 3) GV2 - clumps of chromatin condensation noted throughout the nucleoplasm, and GV3 - full chromatin condensation in the nucleus (Lodde et al., 2008). Progression to the GV3 stage was associated with the final increase in oocyte size, increased meiotic competence, cytoplasmic maturation, and competence for embryonic development. H^3-Uridine incorporation further demonstrated that transcriptional activity was repressed as oocytes progressed from the GV0 to GV3 state. Transcription was observed in GV0 oocytes, with a marked reduction of transcription found in GV1 and GV2 oocytes, and a complete halt to transcriptional activity found by the GV3 stage of development. Sirard (2012) interpreted that transcription within the oocyte was turned off as follicles approached ovulation, or when one follicle gained dominance and subordinate follicles began showing signs of atresia. It was furthermore determined that oocyte developmental competence was increased once transcriptional activity was shut down.

FSH is commonly used for superovulation in cattle, with administration of FSH occurring before the selection of a dominant follicle and continuing throughout the development of a follicular wave. Consequently, multiple follicles are selected to continue growing and subsequently ovulating. A positive effect on oocyte competence has been shown when oocytes were recovered after a 48 hour period of FSH withdrawal ("FSH coasting"; Blondin et al., 1997; Blondin et al., 2002). Higher rates of embryonic development after an FSH coasting period was attributed to the physiological effect of the follicle on oocyte maturation. As discussed above, oocytes progressed towards the GV3 phase of maturity following a decline in FSH during the first follicular wave. The practice of FSH coasting may create a similar situation in which there may be reduced

transcriptional activity and higher developmental competence in oocytes derived from FSH starved follicles.

2.6 Summary

Oocytes must reach developmental competence to allow for the establishment of a viable pregnancy. Differences in oocyte competence, both in-vivo and in-vitro, have been observed in oocytes originating from different follicular environments (Fair et al., 1995; Blondin et al., 1997; Machatkova et al,2000; Blondin et al, 2002). More specifically, different degrees of developmental competency can be attributed to differences in the meiotic, cytoplasmic, and molecular maturation of oocytes encased in follicles that vary in physiological status (reviewed by Sirard et al., 2006). Oocytes must acquire the ability to resume meiosis, expel a polar body, and continue meiotic progression to the MI stage to allow for successful fertilization. Proper accumulation and redistribution of specific organelles is imperative for RNA transcription, protein assembly, and cellular processes that are essential to maintaining the genomic integrity of the oocyte (ie. polar body expulsion, polyspermy block, decondensation of fertilizing sperm nucleus, and syngamy). Adequate quantity and quality of mRNA transcripts must be present in the mature oocyte to provide a transcript pool from which the MII oocyte and early embryo can produce essential proteins. Furthermore, the pool of stored RNA must contain adequate numbers of transcripts essential for early embryonic cleavages and the activation of the embryonic genome. Therefore, acquisition of oocyte competence is essential to the establishment of pregnancy.

CHAPTER III

EFFECT OF PRE-OVULATORY FOLLICLE SIZE ON OOCYTE TRANSCRIPT ABUNDANCE IN BEEF COWS

3.1 Abstract

Inadequate oocyte competence is a potential explanation for reduced pregnancy rates and(or) increased late embryonic mortality when small dominant follicles are induced to ovulate prematurely with gonadotropin releasing hormone (GnRH) in beef cows. Previous studies have shown that follicle size at GnRH- induced ovulation may affect oocyte competence, as higher fertilization rates and higher embryo quality were reported after induction of ovulation in large (≥12.5mm) compared to small (<12.5mm) follicles. The objective of the current study was to determine if the size and physiological status of the pre-ovulatory follicle affects the oocyte transcriptome. To synchronize ovulation in suckled beef cows (n=250), GnRH1 was administered on day -9, prostaglandin F2α on day -2, GnRH2 (to initiate the ovulatory process) on day 0, and dominant follicles were trans-vaginally aspirated on day 1 before follicular rupture. On day 0, cows were assigned to one of the following follicle classifications: Small (<11.7mm; no estrus expression), Large (>12.5 mm; no estrus expression), and Spontaneous (11.6-13.9 mm; estrus expression and endogenous gonadotropin surge). Cumulus-oocyte complexes were collected after trans-vaginal aspiration, and oocytes were fully denuded of surrounding cumulus cells. RNA was later extracted from pools of 4 oocytes (n= 6 oocyte pools from both small and large follicles; n=5 oocyte pools from the spontaneous (control) group) and submitted for sequencing on an Illumina HiSeq 2000 (single reads, 100 bases per read) to generate an average of 8,363,823 raw reads per pool that were aligned to a Bos Taurus transcriptome from NCBI, with additional

annotations, and the bovine genome (Cow_3.1_btau_4.6.1_Y_ncbi). After alignment to the bovine transcriptome or genome, differential transcript abundance between oocyte pools from large and small follicle classifications, small and spontaneous follicle classifications, and large and spontaneous follicle classifications was determined by the edgeR-robust program with a false discovery rate (FDR) P-value of <0.10 to denote differences in transcript abundance. When the differentially abundant transcripts from the genome and transcriptome analysis were combined, 19 annotated transcripts were more abundant in small follicle oocyte pools compared to large follicle oocytes, and 35 transcripts were more abundant in large follicle oocyte pools. When small follicle oocyte pools were compared to spontaneous follicle oocyte pools, 17 annotated transcripts were higher in abundance in small follicle oocyte pools; whereas, 33 genes were higher in abundance in spontaneous follicle oocyte pools. Comparison of large and spontaneous follicle oocyte pools revealed that 15 annotated transcripts were higher in abundance in large follicle oocyte pools and 31 were higher in abundance in spontaneous follicle oocyte pools. A proportion of the differentially abundant transcripts between follicle classifications could be classified into three main biological categories: 1) Transcription or cell cycle regulation, 2) Ubiquitin/proteasome pathway, and 3) Mitochondrial function. The preceding biological pathways are known to have a role in acquisition of oocyte competence. Transcripts associated with the ubiquitin/proteasome pathway and mitochondrial function were higher in abundance in oocytes from follicles that were presumably more physiologically mature. In summary, a greater abundance of transcripts associated with the ubiquitin/proteasome pathway and mitochondrial function in oocytes

from large and spontaneous follicles compared to oocytes from the small follicle category imply that oocytes from the small follicles may be less competent.

3.2 Introduction

The physiological maturity of a bovine follicle may affect the establishment and maintenance of pregnancy by influencing oocyte competence and the maternal environment (Atkins et al., 2013; Jinks et al., 2013). In postpartum beef cows, GnRH-induced ovulation of small dominant follicles resulted in reduced pregnancy rates and an increased incidence of late embryonic mortality (Perry et al., 2005). Atkins et al. (2013) performed a reciprocal embryo transfer study to differentiate between the contribution of follicular determinants of oocyte competence versus the maternal environment on the establishment and maintenance of pregnancy in cattle. Although there is compelling evidence to support the hypothesis that the lowered pregnancy rate following GnRH-induced ovulation of a small dominant follicle is due to a compromised maternal environment (Atkins et al., 2013; Jinks et al., 2013), there is evidence that oocyte competence may also be a contributing factor. For example, fertilization rate and embryo quality at embryo recovery on day 7 post insemination were decreased following GnRH-induced ovulation of small compared to large dominant bovine follicles (Atkins et al., 2013). However, a potential confounding influence of the donor cow's oviductal/uterine environment from the time of fertilization until embryo collection could not be ruled out.

In cattle, oocytes enclosed in follicles ≥3 mm in diameter have acquired the ability to undergo nuclear maturation (i.e resumption of meiosis; Hyttel et al., 1997); however, acquisition of oocyte competence continues until germinal vesicle breakdown is initiated by the preovulatory gonadotropin surge (Hendricksen et al., 2000). Beginning at

the secondary follicle stage and continuing throughout growth of the oocyte, transcripts of mRNA are synthesized and stored in the oocyte and early embryo until activation of the embryonic genome (Fair et al., 1995). Though much of transcription ceases with the completion of rapid oocyte growth, oocyte transcription continues at a low level until germinal vesicle breakdown (Fair et al., 1995, Arlotto et al., 1996; Mourot et al., 2006; Mamo et al., 2011). Furthermore, the surrounding cumulus cells contribute to the oocyte transcriptome through the transfer of mRNA to the oocyte through trans-zonal processes that span the zona pellucida and form direct connections between the cumulus cells and the oolema (Macaulay et al., 2015). Trans-zonal connections remain intact during folliculogenesis until the pre-ovulatory gonadotropin surge, at which time they are disrupted. Therefore, a GnRH-induced gonadotropin surge in a cow with a physiologically immature follicle may induce a premature stop to oocyte transcription and (or) transfer of mRNAs from the cumulus cells to the oocyte via intercellular vesicle-mediated transfer and thereby reduce the competence of an oocyte. Therefore, an experiment was conducted to test the hypothesis that the physiological status of an ovulatory follicle has an effect on the bovine oocyte transcriptome.

3.3 Materials and methods

All protocols and procedures were approved by the Fort Keogh Livestock and Range Research Laboratory Animal Care and Use Committee (IACUC approval number 022014-2).

Animal handling

A timeline for synchronization of ovulation, blood collection, mapping of follicles and corpora lutea, and transvaginal aspiration is depicted in Figure 3.1. Suckled

postpartum beef cows (predominantly Hereford-Angus crossbred cows; n=250), ages 4-13 (mean=6 yr), were pre-synchronized using a 5-day CIDR protocol: administration of 100 µg GnRH (i.m.; 100µg; Factrel®; Zoetis Inc., Kalamazoo, MI) and insertion of a CIDR (intravaginal insert; 1.38g progesterone; Eazi-Breed® CIDR®; Zoetis Inc., Kalamazoo, MI) on day -15 followed by PGF2α (i.m.; 25 mg; Lutalyse®, Zoetis Inc., Kalamazoo, MI) and CIDR removal on day -10. Cows were divided into five replicates for transvaginal aspiration, with 50 cows per replicate.

Cows received a single injection of GnRH (GnRH1; i.m.;100µg; Factrel®; Zoetis Inc., Kalamazoo, MI) between days 10 and 14 after CIDR removal and PGF injection (pre-synchronization), which will be referred to as day 0, followed by PGF2α (PGF; i.m.; 25 mg; Lutalyse®; Zoetis Inc., Kalamazoo, MI) on day 7. A second injection of GnRH (GnRH2; i.m.; 100µg; Factrel®; Zoetis Inc., Kalamazoo, MI) was administered on day 9 to induce a pre-ovulatory gonadotropin surge in cows that had not expressed estrus. On day 10, approximately 23 hours after GnRH2 injection (mean=23 hr; range= 17-31hr), transvaginal aspiration of the largest follicle on either ovary was performed by one of two experienced technicians to collect follicular fluid and cumulus-oocyte complexes as described below.

Ovaries of all cows were examined by an experienced technician using trans-rectal ultrasonography (Aloka 3500 with 7.5 MHz probe) on days 7, 9, and 10. Any corpora lutea (CL) present and all follicles greater than 7 mm were recorded and follicle size was defined as the average of the greatest diameter and the diameter perpendicular to it. On day 0, cows received an estrous detection patch (Estrotect; Rockway Inc.; Spring Valley, WI) that was monitored on day 7 and replaced if scratched.

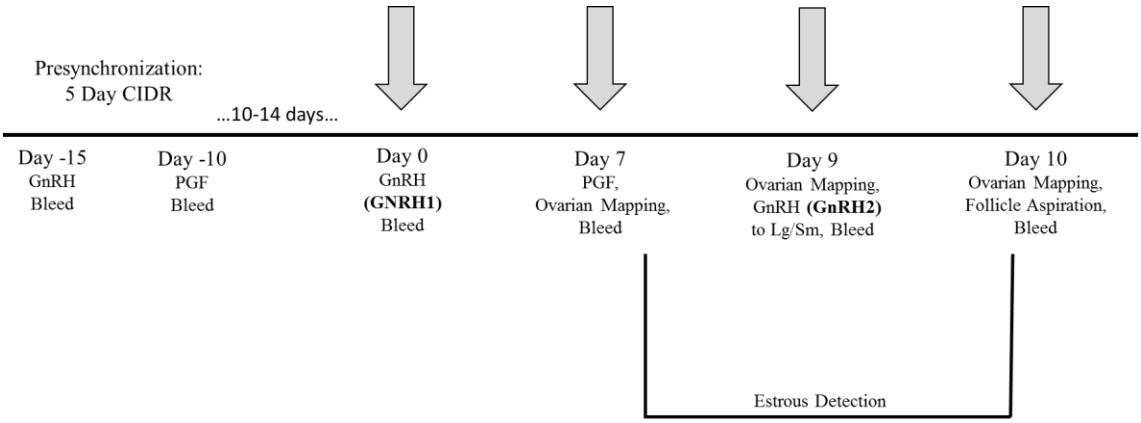

Figure 3.1. Animal handling procedures and the protocol for synchronization of ovulation. Follicle classification groups were assigned based on ovulatory follicle size at GnRH2 (day 9), administration of GnRH2 injection, and expression of estrus and were defined as follows: Small (<11.7mm; no estrus expression), Large (>12.5 mm; no estrus expression), and Control (11.6-13.9 mm; spontaneous estrus expression and endogenous gonadotropin surge). CIDR= Controlled Internal Drug Release, GnRH=Gonadotropin Releasing Hormone, PGF=Prostaglandin $F_{2\alpha}$, Bleed= blood collection for quantification of serum progesterone or estradiol, Ovarian Mapping=ultrasound examination or ovarian structures and measurement of follicles, Estrous Detection=visual detection of estrus 3 times daily.

Visual assessment of estrous expression combined with the usage of estrous detection patches was performed three times daily beginning on day 7 and continued until follicle aspiration on day 10. Estrus was determined when cows stood to be mounted or had a fully activated patch. Body weights (Mean ± SEM= 554 ± 55 kg) and body condition score (BCS; scale of 1-9 in which 1=emaciated and 9=obese; Mean ± SEM= 4.7 ± 0.5) were collected.

Animals were assigned to the following follicle classifications based on largest follicle size on day 9, estrous expression, and GnRH2 treatment: 1) **Small** (< 11.7 mm follicle, no estrous expression, and received GnRH2 injection), 2) **Large** (>12.5 mm follicle, no estrous expression, and received GnRH2), and 3) **Spontaneous** (11.6-13.9mm follicle, estrus expressed, and no GnRH2 injection).

Transvaginal aspiration of cumulus-oocyte complexes (COCs)

All cows received a spinal block via injection of approximately 5ml of 2% lidocaine into the spinal cord at the first intercoccygeal space of the tailhead. Next, the perineal area of each cow was cleaned of all contaminants. An ultrasound guided aspiration gun containing an 18 gauge needle and a series of tubing to allow for ovum pickup and follicular flushing was positioned in the anterior vagina. Both ovaries were located and examined by ultrasonography before the ovary containing the largest follicle was positioned onto the ultrasound probe such that the largest follicle was secured near the part of the probe that housed the aspiration needle. The needle was gently pushed through the vaginal wall before being guided through the ovarian cortex and into the antrum of the selected follicle. Follicular fluid was withdrawn into a clean 12 ml syringe. The syringe was replaced, and PVA-TL HEPES (see Appendix A) was flushed into the

collapsed follicle before being withdrawn into the second syringe. The follicle was flushed 3-4 times with all flushed media being collected. The needle was then withdrawn into the probe, and removed from the cow. The probe was washed with a dilute chlorohexidine solution and sprayed with 70% ethanol between each cow.

COC recovery and processing

Syringes containing the follicular fluid and subsequent follicular flushes were divided into 4-welled Petri plates and searched to find the cumulus-oocyte complex (COC). Once the COC was located, it was collected with 500 µl of surrounding media and placed into a 2ml RNAse free Eppendorf tube to be vortexed for 40 seconds. The COC and associated media were removed and placed into a smaller search plate filled with PVA-TL HEPES. The oocyte was separated from the surrounding cumulus cells by cutting away outlying cumulus cells with a clean pair of needles followed by further disruption by pipetting the COC up and down with a Cooke pipet (170 micron tip) to denude the oocyte from most surrounding cells. The oocyte was subsequently placed into a small plate with PVA-TL HEPES containing 1000 units of hyaluronidase per ml. The oocyte was further pipetted to completely denude it of all surrounding cumulus cells. Fully denuded oocytes were placed into 9 µl of lysis buffer (RNAqueous® MicroKit; Ambion®; Foster City, CA) and snap frozen (liquid nitrogen) in 1.5 ml RNAse free collection tubes. Lysed oocytes were stored at -80º C until extraction of RNA.

Follicular fluid processing

After the COC was located, follicular fluid was divided between two 2ml RNAse free Eppendorf tubes. Tubes were micro-centrifuged (2000 x g at room temperature) for 2

minutes to pellet any cellular debris before follicular fluid was pipetted into two 1.5 ml RNAse free collection tubes and snap frozen in liquid nitrogen.

RNA extraction, reverse transcription, and amplification

A preliminary experiment was conducted to determine the minimum number of oocytes that could be pooled and obtain adequate amounts of RNA for deep sequencing. Total RNA was extracted from pools of four oocytes (n=17 pools) using the AllPrep® DNA/RNA Micro Kit (Qiagen, Germantown, MD) with on column DNAse digestion following manufacturer's instructions. The mean concentration of RNA present in each pool was estimated to be 0.48 ng/µl (total volume 14 µl) based on spectrometry of practice samples (oocyte pools n=4) utilizing the NanoDrop 1000 Spectrophotometer (Thermo Fisher Scientific, Wilmington, DE).

Each pool was designed to be as uniform as possible; therefore, the criteria for establishing each pool included the following: 1) Estrous expression or follicle diameter at GnRH2, 2) cow age, and 3) time from follicle aspiration to placement of the oocyte into lysis buffer.

After RNA was extracted, samples were subjected to reverse transcription and amplification utilizing the Ovation® RNA-Seq System V2 (NuGen Technologies, Inc., San Carlos, CA) following manufacturer's instructions. This approach allows for amplification to begin at both the 3' end and randomly throughout the sample, allowing for reads to be evenly distributed throughout the amplified complementary DNA (cDNA) sample. Therefore, cDNAs from both polyadenylated and non-polyadenylated mRNA transcripts were amplified.

Approximately 2.38ng of RNA (5µl) per pool of oocytes (n=17 pools) was used as input material for the reverse transcription and amplification process. Further refinement of amplified material was performed with the MinElute® Reaction Cleanup Kit (Qiagen, Germantown, MD) and eluted in 22 µl of Buffer EB. Complementary DNA content was determined to be an average of 208.48 ng/µl (127-282.3 ng/µl) (total volume 22 µl) in amplified oocyte pools. Oocyte pool 13 was removed from the analysis at this point due to an abnormally low cDNA concentration (22.7 ng/µl).

Illumina Sequencing

A total of 2000 ng of the amplified cDNA from each oocyte pool was diluted with RNAse free water to reach a concentration of 80ng/µl, after which 25 µl (2000 ng) of each diluted sample was sent to the University of Missouri DNA Core Lab for deep sequencing. Complementary DNA libraries were prepared for sequencing using the TruSeq DNA PCR-Free Library Preparation Kit (Illumina, Inc., San Diego, CA), and DNA was sheared into 350 base pair fragments. Barcodes of 6 nucleotides were assigned to each oocyte pool to allow for individual pool identification after sequencing. Sequencing was performed on an Illumina HiSeq 2000 (Illumina, Inc, San Diego, CA), with amplification of sequences occurring in a single direction for 100 base pairs to produce an output of roughly 1500 gigabases per lane, with a single lane utilized for all oocyte pools.

Sequence Trimming and Alignment

Processing of raw read data and alignment to a refseq Bos Taurus transcriptome from NCBI, with additional annotations and a Bos Taurus genome, (Cow_3.1_btau_4.6.1_Y_ncbi) was performed with NextGENe® (Soft Genetics, LLC;

State College, PA). Sequences were removed of their adaptors and evaluated to determine the confidence in which nucleotides were assigned during sequencing. To be retained for alignment to the transcriptome or genome and further analysis, reads were required to have a median quality score of at least 30 (99.9% probability that each nucleotide was identified correctly), maximum number of uncalled (unassigned) bases=2, minimum read length=50, and reads were trimmed where greater than or equal to 2 bases had a quality score of less than or equal to 26. The NextGENe user's manual (NextGENe-2.4.1-UG001; page 94) explains the above parameters in greater detail. Remaining sequences were aligned to the Bos Taurus genome and transcriptome. Upon alignment, a spreadsheet of raw read counts and of reads normalized for reads per kilobase per million (RPKM) was generated for each sample.

Statistical analysis of oocyte pools

Analysis of Variance (ANOVA) was utilized to determine any significant differences in cow age, weight, BCS, days post-partum, interval from PGF to GnRH2, interval from GnRH2 to follicle aspiration, and interval from follicle aspiration to oocyte snap freezing between follicle size classifications, as well as to confirm difference in follicle size at GnRH2 between classifications.

Determination of differentially abundant transcripts

The chronological steps for data analysis are depicted in Figure 3.2. Raw read counts were submitted to the edgeR (Robinson et al., 2010) software program, and an edgeR Robust test (GLM approach) was utilized to determine if there were differences in abundance of transcripts between the following follicle size classification groups: 1) small follicle oocyte pools compared to large follicle oocyte pools, 2) small follicle

oocyte pools compared to spontaneous follicle oocyte pools, and 3) large follicle oocyte pools compared to spontaneous follicle oocyte pools. Transcripts were considered to be differentially abundant between treatments when the false discovery rate (FDR) P-value was less than or equal to 0.10. The rational for using a FDR of ≤ 0.10 is that the goal of this study was to identify a short list of differentially abundant transcripts that can be further examined by quantitative PCR.

Gene Exploration

Transcripts determined to be differentially abundant within follicle size comparisons were first uploaded into DAVID Bioinformatics Resources (http://david.abcc.ncifcrf.gov/tools.jsp) (Dennis et al., 2003) to analyze overabundance of transcripts related to specific biological clusters or pathways. No significant clusters or pathways were identified for this study. Therefore, gene function and related pathways were devised through an intensive review of literature.

3.4 Results

Follicle aspiration and treatment classification

A total of 127 COCs were recovered (51%) from 250 cows following follicle aspiration. Results from follicle aspiration and oocyte recovery are further summarized in Table A.2. Of the 127 COCs there were 87 oocytes that were allotted to the following groups: 1) Small (30 oocytes), 2) Large (36 oocytes), and Spontaneous (21 oocytes). There were 28 oocytes recovered from cows that were detected in estrus after receiving a GnRH2 injection (Spontaneous + GnRH; Table A.2); however, these oocytes were not utilized in the current study. In addition, twelve intact COCs were collected and snap frozen, but were not utilized in the current study.

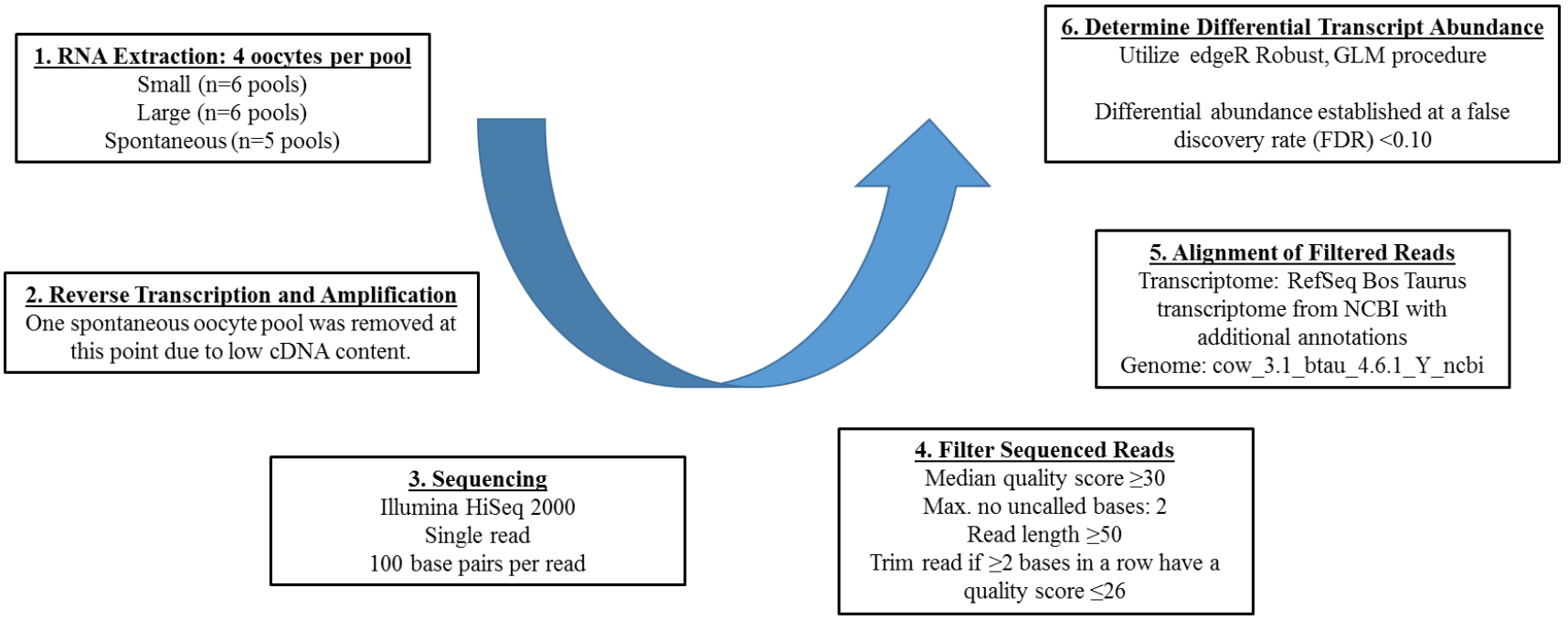

Figure 3.2. The chronological steps employed to generate and analyze the data for this project included the following: 1) Extracted RNA from pools of four oocytes from each follicle classification: small follicle (Small; <11.7mm; no estrus expression), large follicle (Large; >12.5 mm; no estrus expression) or a control group (Spontaneous; follicle diameter = 11.6-13.9 mm) in which cows expressed estrus but did not receive a GnRH2 injection), 2) Generated and amplified cDNA for each pool, 3) Generated nucleotide sequence data, 4) Filtered the data based on established criteria (e.g. Quality score), 5) Aligned the reads to the bovine transcriptome and genome, and 6) Analyzed the data for differential transcript abundance. A false discovery rate (FDR) of <0.10) was chosen since the purpose of this study was to identify genes that would be investigated further by RT-PCR.

Mean follicle diameter ±SEM (range) at GnRH2 injection differed among the Small, Large, and Spontaneous follicle classifications (10.4 ± 0.1^{a} mm [8.5 - 11.7 mm]; 13.6 ± 0.1^{b} mm [12.7 - 15.3 mm], and 12.2 ± 0.2^{c} mm [11.7 - 14.0 mm], respectively; Table 3.1; $^{abc}P<0.0001$); however, there was no difference in cow age (P>0.69), weight (P>0.54), body condition score (P>0.83), days postpartum (P>0.70); time from PGF to GnRH2 injection (P>0.89), time from GnRH2 injection to follicle aspiration (P>0.14) in small and large follicle classification groups, and time from follicle aspiration to freezing of the oocyte (P>0.57) in all groups (Table 3.1).

Analysis of reads generated from RNA-seq

A summary of read counts that aligned to the Bos Taurus transcriptome and genome is depicted in tables B.1 and B.2. Deep sequencing of cDNA libraries from oocyte pools yielded an average of 8,363,823 raw reads per pool. A mean of 88% (7,368,616 reads per pool) of the raw read counts met the criteria for alignment to the bovine transcriptome (Bos Taurus transcriptome from NCBI with additional annotations) and genome (Cow_3.1_btau_4.6.1_Y_ncbi). A mean of 4,523,842 read counts (61% of total) were successfully mapped to the Bos Taurus transcriptome). A mean of 4,865,319 read counts (66% of total) were successfully mapped to the Bos Taurus genome. The percentage of ambigious reads (sequences that mapped to greater than one specific location) that mapped to the transcriptome varied from 9.0 to 9.8%, but was 0% for the genome because ambiguous alignment was not allowed when reads were aligned to the genome; therefore, only the first mapped area for each read was recorded.

Table 3.1. Parameters describing the oocyte pools for small, large, or spontaneous follicle classifications.

Parameter	Small Follicle Classification	Large Follicle Classification	Spontaneous Follicle Classification
Follicle Size at GnRH2[a]	10.4^{x} ± 0.1 mm (8.5 - 11.7 mm)	13.6^{y} ± 0.1 mm (12.7 - 15.3 mm)	12.2^{z} ± 0.2 mm (11.7 - 14.0 mm)
Cow Age[b]	6.5 ± 0.4 yr (4-12 yr)	6.3 ± 0.4 yr (4-9 yr)	6.9 ± 0.5 yr (4-13 yr)
Cow Weight[c]	548 ± 11 kg (454-674 kg)	564 ± 11 kg (452-668 kg)	548 ±14 kg (468-646 kg)
Cow BCS[d]	4.8 ± 0.1 (4-5)	4.8 ± 0.1 (4-6)	4.7 ± 0.1 (4-5)
Cow Days Postpartum[e]	88±1.7 days (65-96 days)	86±1.7 days (58-98 days)	86±2.0 days (76-95 days)
Time from PGF to GnRH2 or Estrus[f]	51 ± 1.5 hr (43-56 hr)	51 ± 1.5 hr (43-56 hr)	73±2.24 hr (56-128 hr)
Time from GnRH2 to Follicle Aspiration[g]	24 ± 0.8 hr (18-31 hr)	22 ± 0.8 hr (17-30 hr)	NA
Time from Follicle Aspiration to Snap Freezing of the Oocyte[h]	22 ± 1.6 min (11-45 min)	24 ± 1.6 min (11-34 min)	25 ± 2.0 min (12-45 min)

[a] Size of the pre-ovulatory follicle on day 9 at GnRH2 injection; Mean ± SEM (range)
[b] Cow age ; Mean ± SEM (range)
[c] Body weight ; Mean ± SEM (range)
[d] Body condition score (BCS) ; Mean ± SEM (range)
[e] Days postpartum ; Mean ± SEM (range)
[f] Time from injection of PGF to injection of GnRH2 in cows within the small or large follicle size classifications and from PGF to estrus in the spontaneous follicle classification; Mean ± SEM (range)
[g] Time from injection of GnRH2 to follicle aspiration in cows within the small or large follicle size classifications; Mean ± SEM (range); NA=not applicable
[h] Time from follicle aspiration to snap freezing of the oocyte; Mean ± SEM (range)
[xyz] P- means having different superscripts differ ($P < 0.0001$)

Validation of sequencing results

The raw read counts were normalized to RPKM, and the fifteen most abundant transcripts for each follicle size classification were identified (Table B.3.) Regardless of follicle classification, the most abundant transcripts corresponded to transcripts that are known to be highly abundant in MII oocytes. Furthermore, the abundance of polyadenylated bovine transcripts (RPKM), previously reported by Reyes et al. (2016), were compared to RPKM abundance of transcripts from the current study (Table B.4.) Similar trends in abundance were seen, and the correlation between transcript abundance for the two studies was 0.93, which supports the assumption that cDNA amplification in the current study did not significantly skew transcript abundance.

Correlation of transcript abundance among and within classifications

Simple correlation coefficients were calculated among and between oocyte pools of small, large, and spontaneous follicle classifications as an initial attempt to examine the variation within and between follicle classifications. Higher correlations (R=0.90-0.99) were observed both within and among follicle classifications when all genes with a RPKM abundance >1 were analyzed (Table B.5.) As RPKM abundance decreased to include only those genes between 1 and 100 RPKM (Table B.6) and 50-100 RPKM (Table B.7) the correlation coefficients decreased. These data indicate that as transcript abundance decreased the amount of variation within and between follicle classifications increased. The preceding relationship was confirmed by calculating the biological coefficient of variation (BCV) for the different comparisons between follicle classifications. The BCV measures the (unknown) true amount of variation of a gene between replicates. It represents the coefficient of variation that would exist between

replicates if sequencing depth was increased indefinitely (McCarthy et al., 2012). Raw read counts were analyzed with the edgeR software program and the BCV was calculated for the following comparisons: 1) small versus large follicle oocyte pools aligned to the transcriptome (BCV=0.76; Figure B.1) and genome (BCV=0.90; Figure B.2), 2) small versus spontaneous follicle oocyte pools when aligned to the transcriptome (BCV=0.79; Figure B.3) and genome (BCV=0.92; Figure B.4), and 3) large versus spontaneous follicle oocyte pools when aligned to the transcriptome (BCV=0.74; Figure B.5) and genome (BCV=0.89; Figure B.6.) A trend was seen for a lower BCV associated with genes that had a higher transcript abundance as measured in counts per million (CPM).

Plots were made to display the fold change difference in transcript abundance in oocyte pools of different follicle size classifications as CPM increased. A strong trend was observed among all comparisons in which the highest fold change difference between follicle classifications was observed in transcripts of lower CPM (Figures B.7-B.12). For the current study, the greatest degree of differential transcript abundance between follicle size classifications occurred in more lowly abundant transcripts. Little variation in transcript abundance was observed between highly abundant genes in the current study.

Differential transcript abundance as determined by edgeR-Robust

Oocyte pools from small versus large pre-ovulatory follicles

After alignment to the Bos Taurus transcriptome, 24 transcripts were differentially abundant (FDR<0.10) between small follicle oocyte pools and large follicle oocyte pools, of which 10 were higher in abundance in small follicle oocyte pools and 14 were elevated in large follicle oocyte pools. A volcano plot is shown in Figure 3.3 that

depicts differentially abundant transcripts and shows the fold change difference between follicle size classifications. Table 3.2 displays differentially abundant genes that were higher abundance for small or large follicle oocyte classifications.

When analysis of differential transcript abundance was based off alignment to the bovine genome, 106 transcripts were determined to be differentially abundant (Figure 3.4.), of which 41 were derived from annotated regions of the genome. Of the annotated transcripts, 15 were higher in abundance in small follicle oocyte pools and 26 were elevated in large follicle oocyte pools. Annotated genes of differential abundance between oocyte pools from small and large follicle classifications are depicted in Table 3.3.

When differentially abundant transcripts between oocytes derived from small or large follicles were explored, three major transcript classifications occurred, 1) cell cycle/transcription, 2) mitochondrial function, and 3) ubiquitin/proteasome pathway. In regards to cell cycle progression and transcription, 6 transcripts (GADD45GIP1, ZXH1, DSN1, KAT2B, FBX021, MED9) were higher in small follicle oocytes and 5 transcripts (HUNK, BEX2, MAK, ZFP62, ZFP341) were higher in large follicle oocytes. Transcripts related to mitochondrial function (MRPL48, AGXT2, SLC25A42) and those involved in the ubiquitin/proteasome pathway (USP29, UBE2B) were solely upregulated in large follicle oocytes. Additionally, PRKCG (protein kinase C, gamma) was elevated in large follicle oocytes.

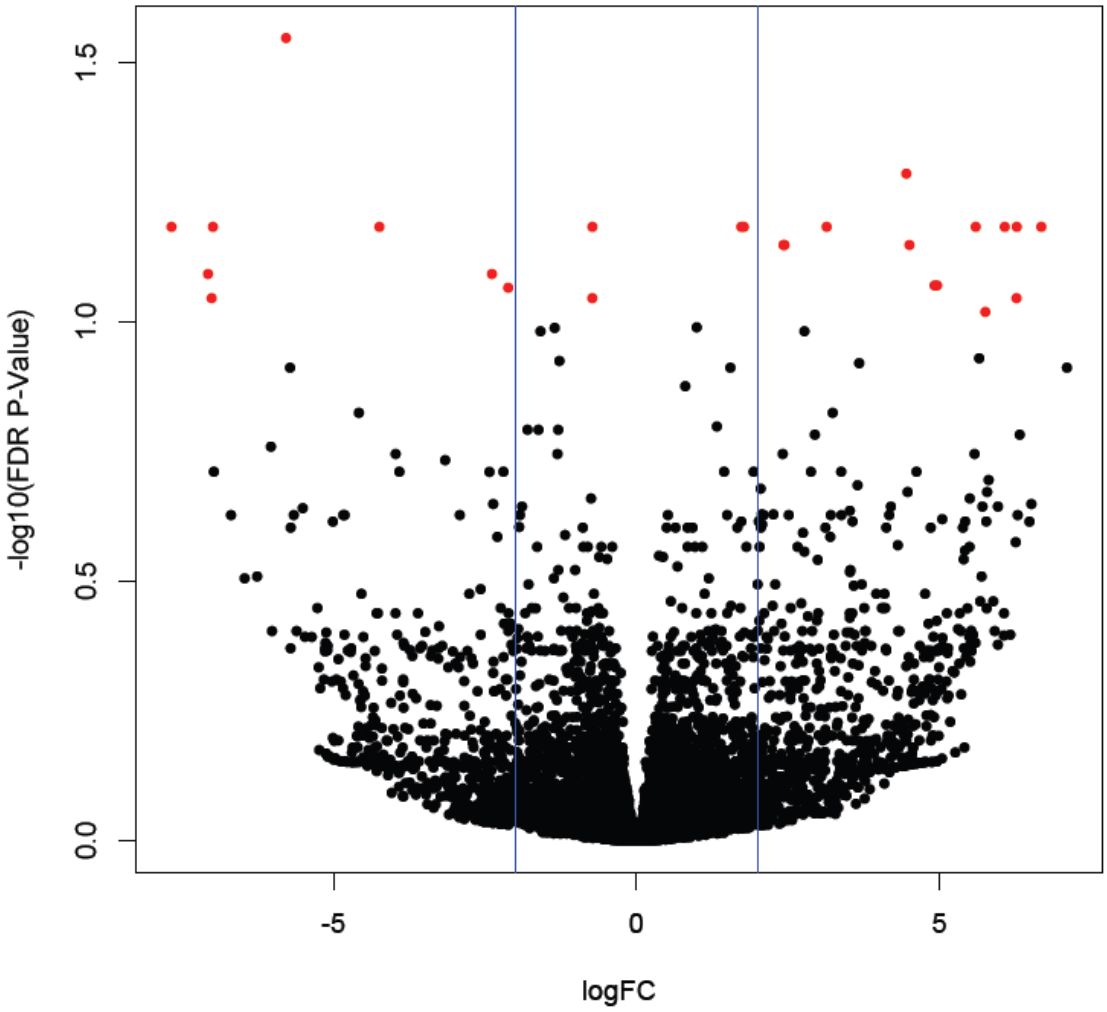

Figure 3.3. Volcano plot depicting differences in transcript abundance between small follicle oocyte pools and large follicle oocyte pools when mapped to a RefSeq Bos Taurus transcriptome from NCBI with additional annotations. X-axis denotes the $\log_2$ of the ratio between the normalized edgeR Robust read count values for small and large follicle oocyte pools (-5= 32 fold higher in small follicle oocyte pools; 0=equal transcript abundance between follicle classifications; 5= 32 fold lower in small follicle oocyte pools). Y-axis denotes $-\log_{10}$(FDR P-Value) where 1.3 equals FDR=0.05 and 1 equals FDR=0.10. Each dot represents one transcript. Red dots denote transcripts significantly different between small and large follicle oocyte pools at a false discovery rate (FDR) of <0.10

Table 3.2. Differentially abundant transcripts between oocyte pools derived from small and large pre-ovulatory follicles (Transcriptome)[a].

Transcripts Higher in Small Follicle Oocyte Pools compared to Large Follicle Oocyte Pools:

Accession Number	Gene ID	Function of Protein Encoded	Log FC[b]	P Value[c]	FDR[d]
NM_001035030.2	MTMR11	pseudophosphatase	-5.78	1.9e-06	0.028
XM_002691367.1	RETSAT	oxidoreductase ativity	-0.73	2.1-05	0.065
NM_001104973.1	C6H4orf19	chromosome 6 open reading frame	-7.67	3.1e-05	0.065
XM_002698914.1	FUT11	fucosyltransferase activity	-6.99	4.6e-05	0.065
NM_001193166.1	GPHA2	increases cAMP production	-4.24	5.7e-05	0.065
NM_001080224.1	GADD45GIP1	cell cycle regulation	-2.39	9.4e-05	0.081
XM_002692488.1	SLC2A10	glucose transporter	-7.07	9.8e-05	0.081
NM_001110095.1	ZHX1	transcriptional regulation	-2.12	1.2e-04	0.086
NM_001206964.1	VSTM5[y]	predicted membrane protein	-7.01	1.4e-04	0.090
NM_001100323.1	DSN1	kinetochore assembly	-0.73	1.4e-04	0.090

Transcripts Higher in Large Follicle Oocyte Pools compared to Small Follicle Oocyte Pools:

Accession Number	Gene ID	Function or Protein Encoded	Log FC[b]	P Value[c]	FDR[d]
XM_002684590.1	HUNK	cell cycle regulation	4.45	7.0e-06	0.052
NM_001077087.1	BEX2	transcriptional regulation	6.68	1.8e-05	0.065
XM_015466143.1	NOL4L[z]	nucleolar protein 4-like	1.77	3.0e-05	0.065
NM_001040598.1	FAM213B	oxidoreductase activity; prostaglandin-F synthase	5.60	3.9e-05	0.065
XM_002697592.1	MAK	cell cycle regulation	6.28	4.3e-05	0.065
NM_001046563.1	MRPL48	mitochondrial protein synthesis	3.14	4.3e-05	0.065
NM_001075212.1	MBLAC1	hydrolysis of βlactams	6.08	4.9e-05	0.065
NM_001075821.1	AGXT2	mitochondrial aminotransferase	4.51	7.1e-05	0.071
NM_001046557.1	NOL12	poly(A) RNA binding; rRNA binding	2.44	7.6e-05	0.071
NM_001166519.1	MFAP3	component of the elastin-associated microfibrils	2.43	7.7e-05	0.071
NM_001166502.1	PRKCG	regulation of nuclear activity and cortical granule exocytosis, oocyte maturation and activation	4.92	1.1e-04	0.085

Transcripts Higher in Large Follicle Oocyte Pools compared to Small Follicle Oocyte Pools cont.:

Accession Number	Gene ID	Function or Protein Encoded	Log FC[b]	P Value[c]	FDR[d]
XM_002684961.1	VEPH1	ventricular zone expressed PH domain containing 1	4.96	1.1e-04	0.085
NM_001193105.1	TCN1	Vitamin B12 binding protein	6.27	1.5e-04	0.090
NM_001034250.1	EXOC7	vesicular trafficking	5.76	1.6e-04	0.096

[a] Data represent transcripts aligned to a Ref Seq Bos Taurus transcriptome with additional annotations and found to be differentially abundant by the edgeR Robust GLM test (FDR <0.10).

[b] Log_2 of the ratio between the normalized edgeR read count values for small and large follicle oocyte pools (-5= 32 fold higher in small follicle oocyte pools; 0=equal transcript abundance between follicle classifications; 5= 32 fold higher in large follicle oocyte pools.)

[c] Unadjusted P-Value for the difference in transcript abundance between oocyte pools derived from small and large follicle classifications.

[d] False discovery rate (FDR) P-Value (adjusted for multiple comparisons) for the difference in transcript abundance between oocyte pools derived from small and large follicle classifications.

[y] Transcript listed is the updated form (from NCBI) of the transcript identified from the transcriptome to be differentially abundant.

[z] Transcript listed is an updated form of the transcript identified from the transcriptome to be differentially abundant (BLAST analysis of originally identified transcript matched this transcript with >99% accuracy.

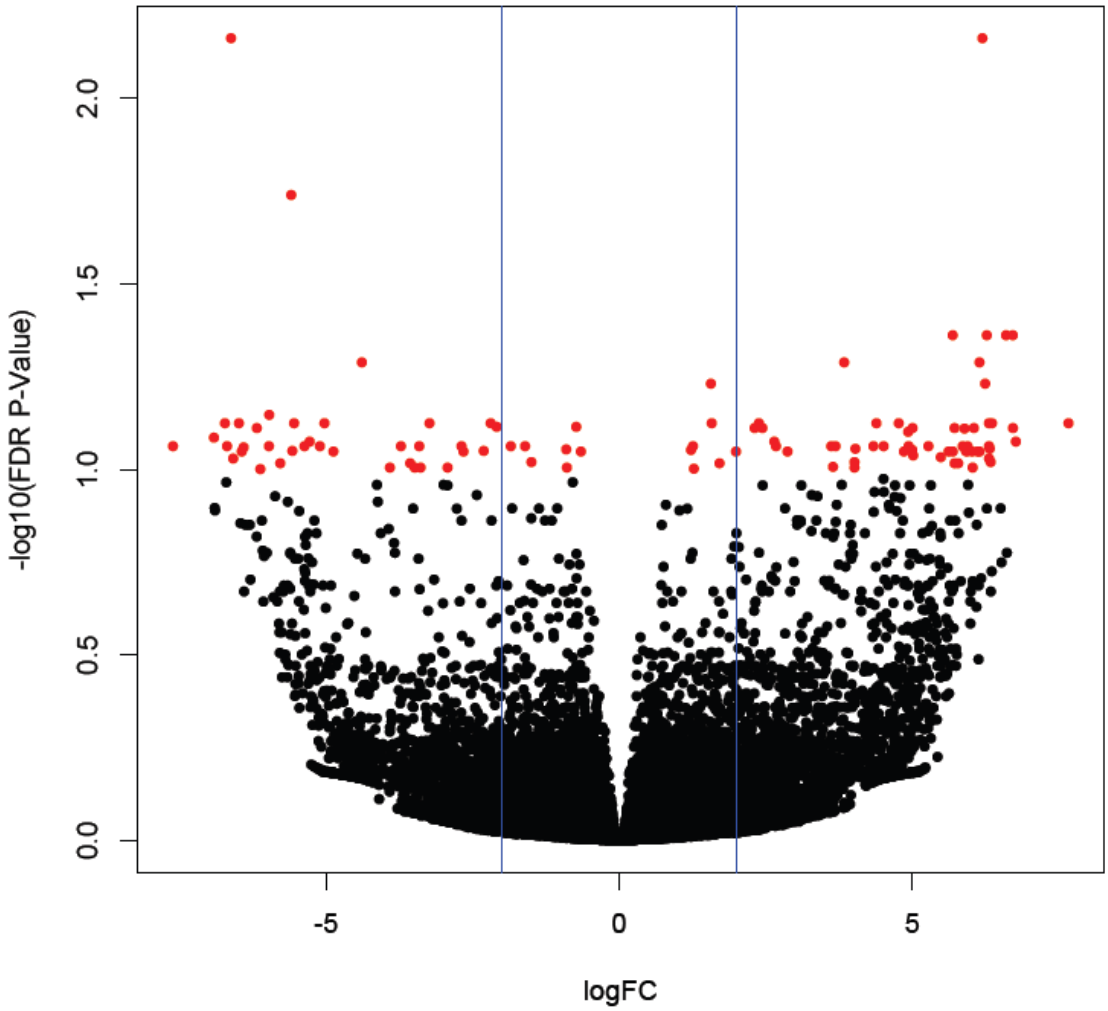

Figure 3.4. Volcano plot depicting differences in transcript abundance between small follicle oocyte pools and large follicle oocyte pools when mapped to the bovine genome (Cow_3.1_btau_4.6.1_Y_ncbi). X-axis denotes the $\log_2$ of the ratio between the normalized edgeR Robust read count values for small and large follicle oocyte pools (-5= 32 fold higher in small follicle oocyte pools; 0=equal transcript abundance between follicle classifications; 5= 32 fold lower in small follicle oocyte pools). Y-axis denotes $\log_{10}$(FDR P-Value) where 1.3 equals FDR=0.05 and 1 equals FDR=0.10. Each dot represents one transcript. Red dots denote transcripts significantly different between small and large follicle oocyte pools at a false discovery rate (FDR) of <0.10.

Table 3.3. Differentially abundant transcripts between oocyte pools derived from small and large pre-ovulatory follicles (Genome)[a].

Transcripts Higher in Small Follicle Oocyte Pools compared to Large Follicle Oocyte Pools:

Accession Number	Gene ID	Function or Protein Encoded	Log FC[b]	P Value[c]	FDR[d]
NM_001104973.1	C6H4orf19	chromosome 6 open reading frame	-6.62	4.7e-07	0.007
XM_005227191.1	GPHA2	increases cAMP production	-4.39	1.6e-05	0.051
NM_001206964.1	VSTM5	membrane protein	-6.73	4.0e-05	0.075
NM_001110095.1	ZHX1	transcription regulation	-2.20	6.7e-05	0.075
XM_002691368.5	TGOLN2	membrane trafficking to the golgi-complex	-0.74	7.2e-05	0.077
NM_001192439.1	SLC2A10	glucose transporter	-6.92	1.1e-04	0.082
XM_002684716.3	KAT2B	transcription regulation	-2.69	1.6e-04	0.087
XM_002687567.3	NXPH4	possible signaling molecule; resembles neuropeptides	-5.58	2.1e-04	0.089
NM_001080224.2	GADD45GIP1	cell cycle regulation	-2.31	2.1e-04	0.089
XM_005209314.1	SHROOM1	microtubule/actin cytoskeleton assembly	-6.44	2.5e-04	0.089
XM_005217929.1	FBXO21	maintenance of second meiotic arrest	-0.66	2.60e-04	0.089
XM_005209523.1	PCDHGA11	cell adhesion-signaling	-6.59	2.8e-04	0.093
NM_001080916.2	MED9	transcription regulation	-3.57	3.1e-04	0.096
NM_001101877.1	GIGYF2	tyrosine kinase receptor signaling regulation	-0.89	3.5e-04	0.099
XM_002689721.2	FRMPD1	stabilizes membrane-bound GPSM1	-3.39	3.5e-04	0.099

Transcripts Higher in Large Follicle Oocyte Pools compared to Small Follicle Oocyte Pools:

Accession Number	Gene ID	Function or Protein Encoded	Log FC[b]	P Value[c]	FDR[d]
NM_001076424.1	CAPS	calcium-binding protein	5.69	8.7e-06	0.043
NM_001077087.1	BEX2	transcription regulation	6.60	1.0e-05	0.043
NM_001075212.1	MBLAC1	hydrolysis of β-lactams	6.14	1.5e-05	0.051
XM_003587364.3	USP29	ubiquitin C-terminal hydrolase	6.24	2.2e-05	0.059
XM_005209650.1	MFAP3	component of the elastin-associated microfibrils	2.38	4.6e-05	0.075
XM_015466143.1	NOL4L[z]	nucleolar protein 4-like	1.58	4.7e-05	0.075
XM_002689031.2	ZFP62	C2H2 zinc finger protein	6.31	5.4e-05	0.075
XM_002696714.3	TTC6	tetratricopeptide repeat domain 6	5.00	7.8e-05	0.077
NM_001040598.1	FAM213B	oxidoreductase activity; prostaglandin-F synthase	5.89	9.5e-05	0.078
NM_001101257.1	FAM89A	family with sequence similarity 89, member A	2.64	1.1e-04	0.084
XM_005208424.1	SLC25A42	transport across the inner mitochondrial membrane	3.69	1.5e-04	0.087

Transcripts Higher in Large Follicle Oocyte Pools compared to Small Follicle Oocyte Pools cont.:

Accession Number	Gene ID	Function or Protein Encoded	Log FC[b]	P Value[c]	FDR[d]
NM_001101188.1	ASB16	suppressor of cytokine signalling	2.67	1.6e-04	0.087
NM_001101843.1	COLEC12	cell surface glycoprotein scavenger receptor	1.26	1.6e-04	0.087
XM_005208970.1	PLIN3	lipid droplet trafficking	5.94	1.8e-04	0.087
XM_005228384.1	MAP7D2	microtubule cytoskeleton organization	5.00	2.0e-04	0.089
NM_001037459.2	UBE2B	ubiquitin conjugating enzyme E2;DNA damage repair	1.22	2.1e-04	0.089
XM_005218315.1	RTN4R	activation of Rho; reorganization of actin cytoskeleton	5.69	2.4e-04	0.089
NM_001076122.1	HS3ST1	heparan sulfate glucosaminyl 3-O-sulfotransferase	6.11	2.5e-04	0.089
NM_001099166.2	EVI2B	single-pass type I membrane protein	6.15	2.5e-04	0.089
NM_001191453.1	SYNM	target PKA to intermediate filaments	1.99	2.5-04	0.089
XM_005217054.1	C16H1orf159	chromosome 16 open reading frame	5.93	2.6e-04	0.089
XM_002694095.3	ANKRD45	ankyrin repeat domain-containing protein 45	5.01	2.7e-04	0.092
XM_005208181.1	CRMP1	microtubule-associated protein	4.01	3.0e-04	0.095
NM_001192576.1	ZNF341	C2H2 zinc finger protein	1.71	3.0e-04	0.096
XM_005210575.1	DFNB31	actin cystoskeletal assembly	5.72	3.2e-04	0.096
XM_005211381.1	SLC22A17	cell surface receptor; role in iron homeostasis	6.03	3.4e-04	0.099

[a] Data represent transcripts aligned to a bovine genome (Cow_3.1_btau_4.6.1_Y_ncbi)and found to be differentially abundant by the edgeR Robust GLM test (FDR <0.10). Only protein coding transcripts from annotated regions of the genome are included in Table 3.3.

[b] Log_2 of the ratio between the normalized edgeR read count values for small or large follicle oocyte pools (-5= 32 fold higher in small follicle oocyte pools; 0=equal transcript abundance between follicle classifications; 5= 32 fold higher in large follicle oocyte pools.)

[c] Unadjusted P-Value for the difference in transcript abundance between oocyte pools derived from small and large follicle classifications.

[d] False discovery rate (FDR) P-Value (adjusted for multiple comparisons) for the difference in transcript abundance between oocyte pools derived from small and large follicle classifications.

[z] Transcript listed is an updated form of the transcript identified from the transcriptome to be differentially abundant (BLAST analysis of originally identified transcript matched this transcript with >99% accuracy.

Oocyte pools from small versus spontaneous pre-ovulatory follicles

When differential abundance was determined after alignment to the bovine transcriptome, 15 transcripts were differentially abundant between small and spontaneous follicle oocyte pools (Figure 3.5). Table 3.4 displays the 4 transcripts that were more abundant in small follicle oocyte pools and the 11 transcripts that were elevated in spontaneous follicle oocyte pools.

After alignment to the bovine genome, 88 transcripts were determined to be differentially abundant between small and spontaneous follicle oocyte pools (Figure 3.6). Of the 43 transcripts that were from annotated regions of the genome, 15 were higher in abundance in small follicle oocyte pools and 28 were elevated in spontaneous follicle oocyte pools (Table 3.5.)

Transcripts related to transcriptional and cell cycle regulation were also amongst differentially abundant genes between oocyte pools from small or spontaneous follicles, with relatively equal numbers of transcripts higher in small (ZNF391, TBX4, ZNF496) and spontaneous (CBZ2, CDC25A) follicle oocytes. The transcript PSMB9, which is involved in the ubiquitin/proteasome pathway, and PKN1, from the protein kinase C super family, were higher in spontaneous follicle oocytes. One nuclear gene that encoded mitochondrial protein (COX6A1) was elevated in spontaneous follicle oocyte pools. Interestingly, 4 transcripts from the mitochondrial genome (COX1, ND1,ND5, COX3) were higher in abundance in small follicle oocytes; however, the difference in transcript abundance of these genes between small and spontaneous follicle oocytes pools did not reach a two-fold change difference.

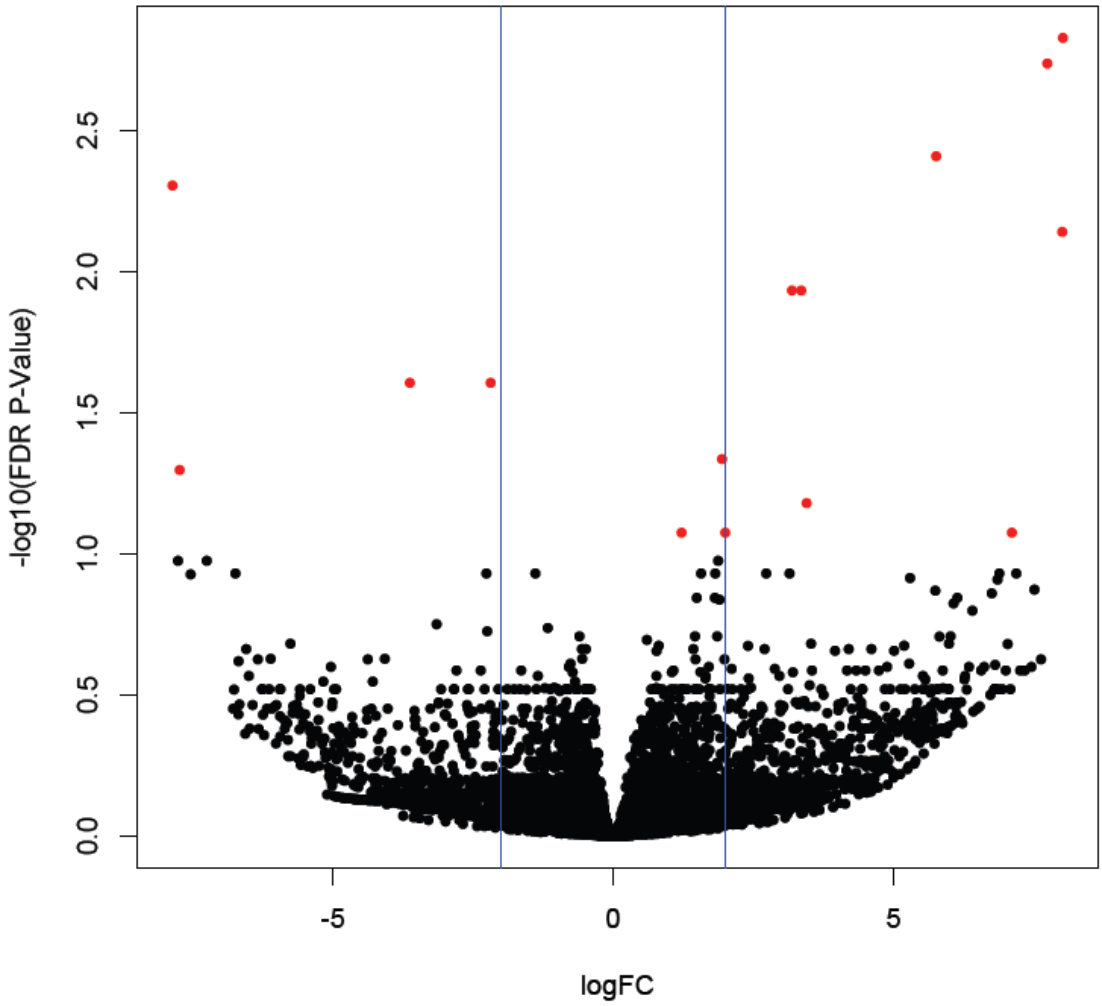

Figure 3.5. Volcano plot depicting differences in transcript abundance between small follicle oocyte pools and spontaneous follicle oocyte pools when mapped to a RefSeq Bos Taurus transcriptome from NCBI with additional annotations. X-axis denotes the $\log_2$ of the ratio between the normalized edgeR Robust read count values for small and spontaneous follicle oocyte pools (-5= 32 fold higher in small follicle oocyte pools; 0=equal transcript abundance between follicle classifications; 5= 32 fold lower in small follicle oocyte pools). Y-axis denotes $\log_{10}$(FDR P-Value) where 1.3 equals FDR=0.05 and 1 equals FDR=0.10. Each dot represents one transcript. Red dots denote transcripts significantly different between small and spontaneous follicle oocyte pools at a false discovery rate (FDR) of <0.10.

Table 3.4. Differentially abundant transcripts between oocyte pools derived from small and spontaneous pre-ovulatory follicles (Transcriptome)[a].

Transcripts Higher in Small Follicle Oocyte Pools compared to Spontaneous Follicle Oocyte Pools:

Accession Number	Gene ID	Function or Protein Encoded	Log FC[b]	P Value[c]	FDR[d]
NM_001035030.2	MTMR11	pseudophosphatase	-7.86	1.4e-06	0.005
XM_002690812.1	TTBK2	serine/threonine kinase; phosphorylates tubulin	-2.19	1.5e-05	0.025
NM_001193246.1	DAB2	mitogen activated phosphoprotein	-3.63	1.5e-05	0.025
XM_864370.6	MSANTD2	Myb/SANT-like DNA-binding domain-containing protein 2	-7.74	3.8e-05	0.050

Transcripts Higher in Spontaneous Follicle Oocyte Pools compared to Small Follicle Oocyte Pools:

Accession Number	Gene ID	Function or Protein Encoded	Log FC[b]	P Value[c]	FDR[d]
NM_001034388.1	PSMB9	essential subunit of 20S proteosome	8.02	1.0e-07	0.001
NM_001102288.1	EPDR1	transmembrane protein; possible role in cell adhesion	7.74	2.5e-07	0.002
NM_001103094.1	CBX6	transcriptional repressor	5.76	8.0e-07	0.004
XM_001787844.5	R3HCC1L	nucleotide binding; expressed in placenta	8.01	2.5e-06	0.007
NM_001083371.1	C7H19orf43	chromosome 7 open reading frame	3.19	5.2e-06	0.012
NM_001102303.1	NSUN5	possible methyltransferase	3.35	5.6e-06	0.012
NM_001077831.1	COX6A1	terminal enzyme of mitochondrial respiratory chain	1.94	3.2e-05	0.046
XM_001251995.5	EIF2B5	guanine nucleotide exchange; exchange GDP for GTP	3.45	5.4e-05	0.066
NM_001014945.1	C1QA	C1Q coats materials to be endocytosed by fibronectin	7.11	7.7e-05	0.084
NM_001034645.1	UNC119	enriched in photoreceptors of retina	1.22	8.5e-05	0.084
NM_174505.2	ATP6V0D1	vacuolar ATPase	2.00	8.6e-05	0084

[a] Data represent transcripts aligned to a Ref Seq Bos Taurus transcriptome with additional annotations and found to be differentially abundant by the edgeR Robust GLM test (FDR <0.10).

[b] Log_2 of the ratio between the normalized edgeR read count values for small or spontaneous follicle oocyte pools (-5= 32 fold higher in small follicle oocyte pools; 0=equal transcript abundance between follicle classifications; 5= 32 fold higher in spontaneous follicle oocyte pools.)

[c] Unadjusted P-Value for the difference in transcript abundance between oocyte pools derived from small and spontaneous follicle classifications.

[d] False discovery rate (FDR) P-Value (adjusted for multiple comparisons) for the difference in transcript abundance between oocyte pools derived from small and spontaneous follicle classifications.

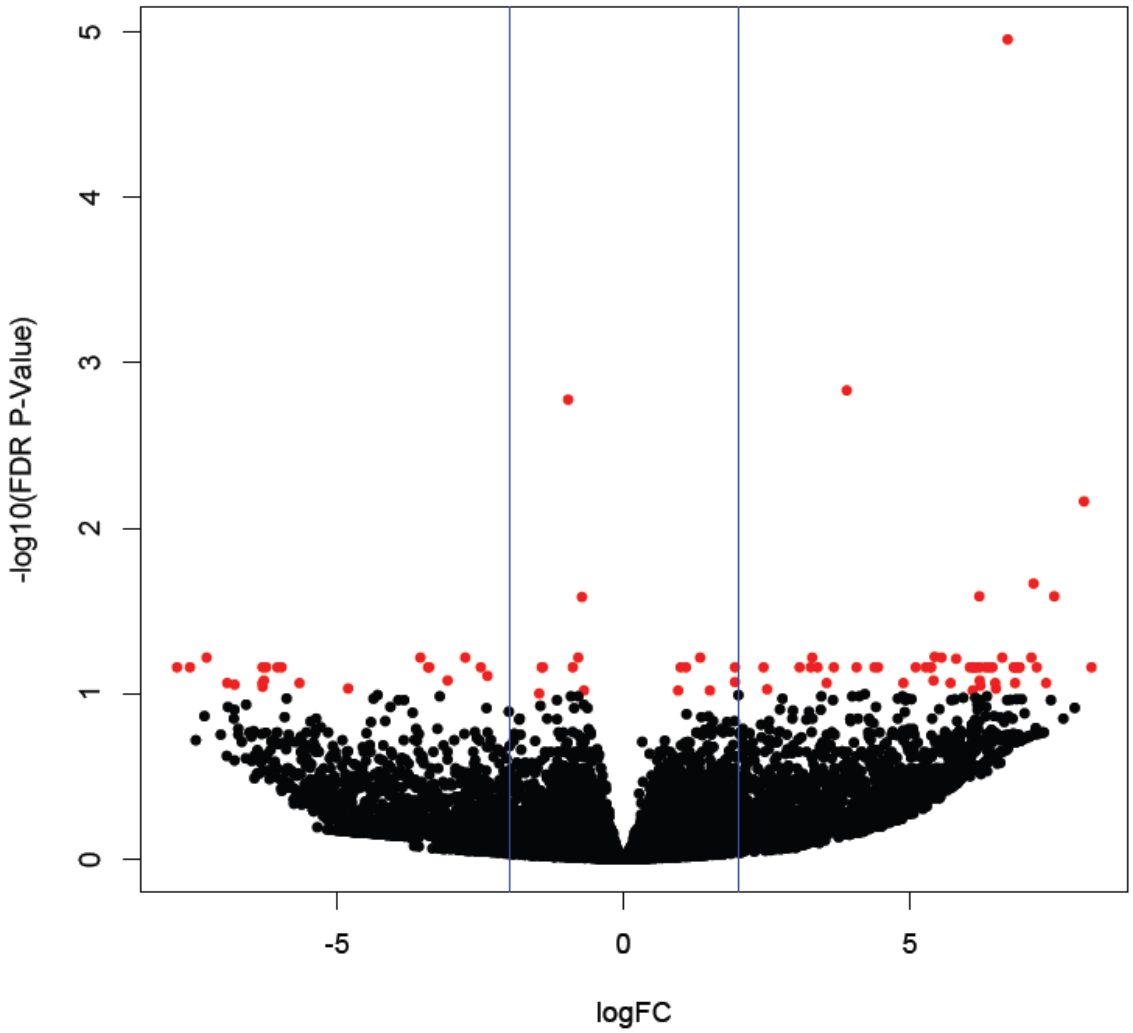

Figure 3.6. Volcano plot depicting differences in transcript abundance between small follicle oocyte pools and spontaneous follicle oocyte pools when mapped to the bovine genome (Cow_3.1_btau_4.6.1_Y_ncbi.) X-axis denotes the $\log_2$ of the ratio between the normalized edgeR Robust read count values for small and spontaneous follicle oocyte pools (-5= 32 fold higher in small follicle oocyte pools; 0=equal transcript abundance between follicle classifications; 5= 32 fold lower in small follicle oocyte pools). Y-axis denotes $\log_{\text{-}10}$(FDR P-Value) where 1.3 equals FDR=0.05 and 1 equals FDR=0.10. Each dot represents one transcript. Red dots denote transcripts significantly different between small and spontaneous follicle oocyte pools at a false discovery rate (FDR) of <0.10.

Table 3.5. Differentially abundant transcripts between oocyte pools derived from small and spontaneous pre-ovulatory follicles (Genome)[a].

Transcripts Higher in Small Follicle Oocyte Pools compared to Spontaneous Follicle Oocyte Pools:

Accession Number	Gene ID	Function or Protein Encoded	Log FC[b]	P Value[c]	FDR[d]
	COX1	mitochondrial gene; key enzyme in electron transport	-0.97	1.8e-07	0.002
	ND1	mitochondrial gene; enzyme in electron transport	-0.73	7.4e-06	0.026
XM_005203860.1	MTMR11	pseudophosphatase	-7.28	2.3e-05	0.060
NM_001193246.1	DAB2	mitogen activated phosphoprotein	-3.55	3.3e-05	0.060
	ATP6	subunit of ATP synthase; oxidative phosphorylation	-0.79	3.8e-05	0.060
XM_005222747.1	C22H3orf62	chromosome 3open reading frame	-5.97	8.2e-05	0.069
XM_005223722.1	ZNF391	zinc finger protein	-3.41	8.9e-05	0.069
XM_005218604.1	ATXN1L	repressor of notch signaling	-1.41	1.3e-04	0.069
	ND5	mitochondrial gene; enzyme in electron transport	-0.89	1.4e-04	0.069
XM_005219965.1	TBX4	T-box family transcription factor	-6.05	1.4e-04	0.069
NM_001081743.2	EDA	transmembrane protein	-1.43	1.4e-04	0.069
XM_005225444.1	ENTPD1	gene expression, protein synthesis, RNA modification	-7.57	1.4e-04	0.069
XM_005209229.1	ZNF496	zinc finger protein	-2.38	1.7e-04	0.078
XM_002684809.2	SEMA5B	encodes a semaphorin protein	-5.66	2.2e-04	0.086
	COX3	mitochondrial gene; key enzyme in electron transport	-0.69	2.9e-04	0.095

Transcripts Higher in Spontaneous Follicle Oocyte Pools compared to Small Follicle Oocyte Pools:

Accession Number	Gene ID	Function or Protein Encoded	Log FC[b]	P Value[c]	FDR[d]
NM_001103094.1	CBX6	transcriptional repressor	6.71	3.9e-10	0.000
NM_001034645.2	UNC119	expressed in photoreceptors of the retina	1.34	3.0e-05	0.060
XM_005203214.1	C1QA	C1Q coats materials to be endocytosed by fibronectin	7.12	3.7e-05	0.060
XM_002685338.2	IFIH1	DEAD box protein; RNA helicase	5.81	4.1e-05	0.061
NM_001102303.2	NSUN5	methyltransferase	3.27	5.2e-05	0.069
NM_174012.2	CD247	part of the T-cell receptor-CD3 complex	4.07	6.4e-05	0.069
NM_001034467.2	DCP1B	may remove 7-methyl guanine cap from RNA	6.22	7.7e-05	0.069
NM_001206962.1	DCXR	glycosaminoglycan metabolism; oxidoreductase	6.92	8.0e-05	0.069
NM_001038065.1	GPNMB	type I transmembrane glycoprotein	5.28	8.3e-05	0.069
XM_002695172.3	MYPOP	transcription factor, chromatin binding	3.08	8.3e-05	0.069

Transcripts Higher in Spontaneous Follicle Oocyte Pools compared to Small Follicle Oocyte Pools cont.:

Accession Number	Gene ID	Function or Protein Encoded	Log FC[b]	P Value[c]	FDR[d]
XM_005205788.1	PTN	heparin-binding mitogen or growth factor	3.39	9.5e-05	0.069
NM_001040606.1	OAS1Y	ATP, double-stranded RNA, nucleotide binding	4.38	1.0e-04	0.069
XM_005219515.1	LOC101906828	unknown	2.45	1.1e-04	0.069
NM_001077831.2	COX6A1	terminal enzyme of mitochondrial respiratory chain	1.95	1.2e-04	0.069
NM_001034388.2	PSMB9	essential subunit of 20S proteasome complex	6.44	1.2e-04	0.069
NM_001101100.2	CDC25A	part of maturation promoting factor; MII arrest	1.00	1.2e-04	0.069
XM_003587150.2	SRRM4	promotes alternative splicing in mRNAs	5.10	1.3e-04	0.069
XM_002696335.3	LOC530348	hyaluronan-binding proteoglycan	6.91	1.3e-04	0.069
NM_001015584.1	WDR77	interacts with protein arginine methyltansferases	3.67	1.4e-04	0.069
XM_005224057.1	CCDC178	unknown	5.37	1.5e-04	0.069
NM_001192377.1	ANKRD35	ankyrin repeat domain-containing protein 35	6.22	2.0e-04	0.083
NM_001075734.1	CBR3	carbonyl reductase	1.95	2.0e-04	0.085
XM_005221069.1	C19H17orf62	chromosome 19 open reading frame	6.49	2.1e-04	0.086
NM_001080246.1	PKN1	protein kinase C superfamily	6.23	2.5e-04	0.089
XM_005217036.1	GLTPD1	transfers C1P between intracellular membranes	2.51	2.8e-04	0.094
NM_001076122.1	HS3ST1	heparin sulfate biosynthesis	6.10	2.9e-04	0.095
XM_005208958.1	SIRT6	DNA repair; telomere maintenance	1.51	2.9e-04	0.095
XM_002694739.2	CMIP	T-cell signaling pathway	0.95	2.9e-04	0.095

[a] Data represent transcripts aligned to a bovine genome (Cow_3.1_btau_4.6.1_Y_ncbi)and found to be differentially abundant by the edgeR Robust GLM test (FDR <0.10). Only protein coding transcripts from annotated regions of the genome are included in Table 3.5.

[b] Log_2 of the ratio between the normalized edgeR read count values for small or spontaneous follicle oocyte pools (-5= 32 fold higher in small follicle oocyte pools; 0=equal transcript abundance between follicle classifications; 5= 32 fold higher in spontaneous follicle oocyte pools.)

[c] Unadjusted P-Value for the difference in transcript abundance between oocyte pools derived from small and spontaneous follicle classifications.

[d] False discovery rate (FDR) P-Value (adjusted for multiple comparisons) for the difference in transcript abundance between oocyte pools derived from small and spontaneous follicle classifications.

Oocyte pools from large versus spontaneous pre-ovulatory follicles

Following alignment to the Bos Taurus transcriptome, 19 transcripts were differentially abundant between oocyte pools derived from large and spontaneous follicle classifications (Figure 3.7), of which 4 transcripts were elevated in abundance in large follicle oocyte pools and 15 were elevated in spontaneous follicle oocyte pools (Table 3.6.)

When analysis was conducted after alignment to the bovine genome, 88 transcripts were differentially abundant between large and spontaneous follicle oocyte pools (Figure 3.8.) Thirty-seven of the differentially abundant transcripts originated from annotated regions of the genome, of which 12 were higher in abundance in large follicle oocyte pools and 25 were elevated in spontaneous follicle oocyte pools (Table 3.7.)

Again, relatively equal numbers of transcripts associated with cell cycle progression or transcriptional activity were observed to be elevated in large follicle oocytes (RALYL, ZNF391, ADORA1) and spontaneous follicle oocytes (CBX6, CDC25A). One transcript related to the ubiquitin/proteasome pathway (UBE3C) was higher in abundance in large follicle oocytes, and two genes (PSMB9, UBE2D4) were higher in spontaneous follicle

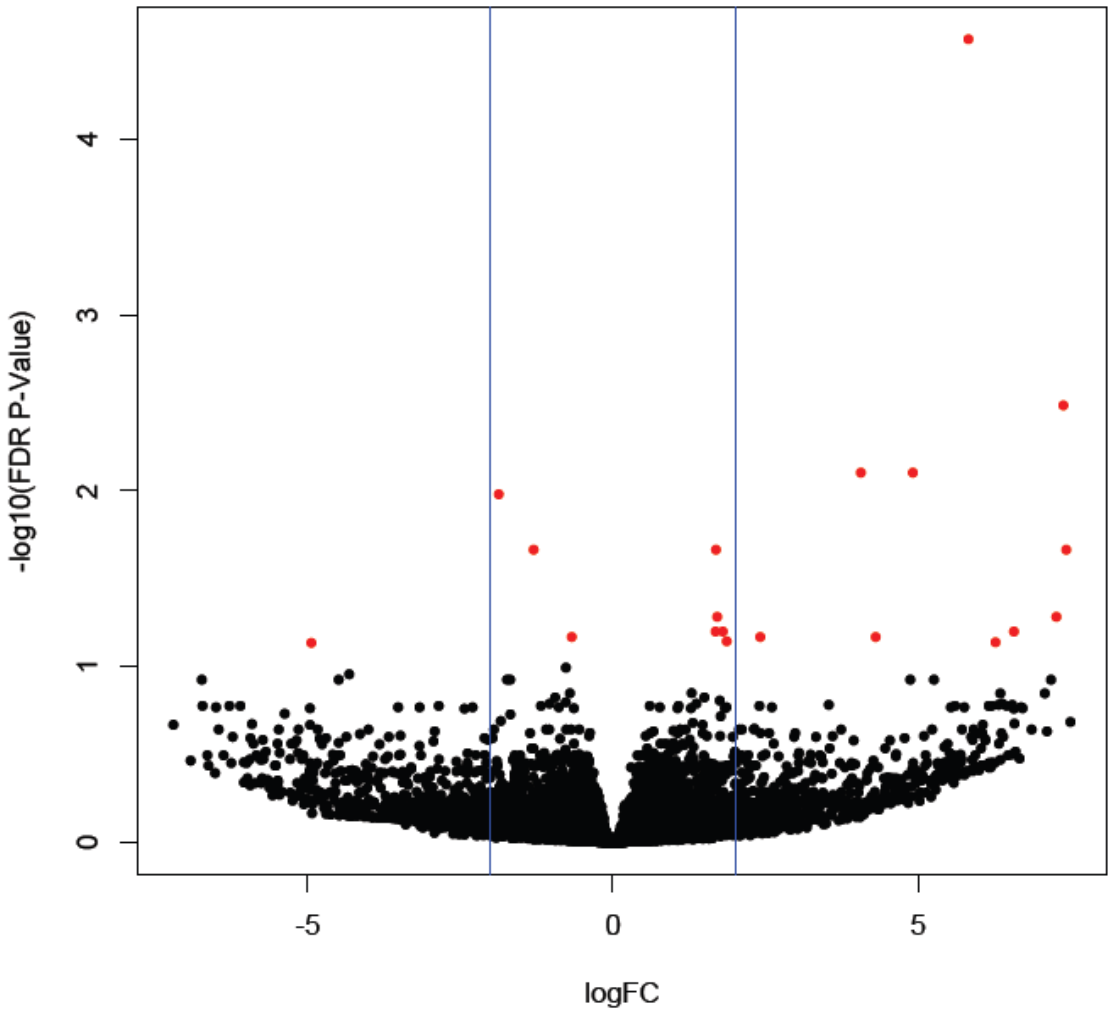

Figure 3.7. Volcano plot depicting differences in transcript abundance between large follicle oocyte pools and spontaneous follicle oocyte pools when mapped to a RefSeq Bos Taurus transcriptome from NCBI with additional annotations. X-axis denotes the $\log_2$ of the ratio between the normalized edgeR Robust read count values for large and spontaneous follicle oocyte pools (-5= 32 fold higher in large follicle oocyte pools; 0=equal transcript abundance between follicle classifications; 5= 32 fold lower in large follicle oocyte pools). Y-axis denotes $\log_{\text{-}10}$(FDR P-Value) where 1.3 equals FDR=0.05 and 1 equals FDR=0.10. Each dot represents one transcript. Red dots denote transcripts significantly different between large and spontaneous follicle oocyte pools at a false discovery rate (FDR) of <0.10.

Table 3.6. Differentially abundant transcripts between oocyte pools derived from large and spontaneous pre-ovulatory follicles (Transcriptome)[a].

Transcripts Higher in Large Follicle Oocyte Pools compared to Spontaneous Follicle Oocyte Pools:

Accession Number	Gene ID	Function or Annotated Protein	Log FC[b]	P Value[c]	FDR[d]
NM_001192188.1	UBE3C	substrate specific E3 ubiquitin-protein ligase	-1.87	3.5e-06	0.010
XM_002694841.1	ATXN1L	chromatin-binding factor; suppress Notch signaling	-1.30	9.0-06	0.022
XM_002690201.1	SYNCRIP	RNA binding protein	-0.67	7.1e-05	0.068
XM_001787429.1	KIF26B	transport organelles along microtubules	-4.94	9.4e-05	0.073

Transcripts Higher in Spontaneous Follicle Oocyte Pools compared to Large Follicle Oocyte Pools:

Accession Number	Gene ID	Function or Annotated Protein	Log FC[b]	P Value[c]	FDR[d]
NM_001103094.1	CBX6	transcriptional repressor	5.82	1.8e-09	0.000
NM_001034388.1	PSMB9	essential subunit of 20S proteasome complex	7.38	4.4e-07	0.003
XM_002686551.1	MAP7D1	microtubule cytoskeleton organization	4.91	1.8e-06	0.008
NM_001046402.1	ALKBH7	2-oxoglutarate- and Fe(II)-dependent oxygenase	4.06	2.1e-06	0.008
NM_001075806.1	TMEM136	transmembrane protein 136	7.43	1.2e-05	0.022
NM_001035307.1	EDF1	transcriptional coactivator	1.69	1.2e-05	0.022
NM_001102294.1	SHROOM1	microtubule/actin cytoskeleton assembly	7.27	3.3e-05	0.052
XM_001256663.3	IRF2BP1	transcriptional corepressor, possible E3 ligase	1.71	3.5e-05	0.052
NM_176672.2	NDUFA13	mitochondrial NADH:ubiquinone oxidoreductase	1.68	5.4e-05	0.063
NM_001075442.1	RASSF1	inhibition of G1/S-phase progression	6.57	5.5e-05	0.063
NM_001076235.1	MED18	activate transcription via RNA polymerase II	1.80	5.6e-05	0.063
NM_001083371.1	C7H19ORF43	chromosome 7 open reading frame	2.41	6.8e-05	0.068
NM_001102140.2	BRINP3	negative regulation of the cell cycle transition	4.31	7.3e-05	0.068
NM_001101177.1	LSM2	LSm family of RNA-binding proteins	1.86	8.2e-05	0.071
NM_001046176.1	SEPT10	cytoskeletal protein with GTPase activity	6.27	8.8e-05	0.072

[a] Data represent transcripts aligned to a RefSeq Bos Taurus transcriptome with additional annotations and found to be differentially abundant by the edgeR Robust GLM test (FDR <0.10).

[b] Log_2 of the ratio between the normalized edgeR read count values for large or spontaneous follicle oocyte pools (-5= 32 fold higher in large follicle oocyte pools; 0=equal transcript abundance between follicle classifications; 5= 32 fold higher in spontaneous follicle oocyte pools.)

[c] Unadjusted P-Value for the difference in transcript abundance between oocyte pools derived from large and spontaneous follicle classifications.

[d] False discovery rate (FDR) P-Value (adjusted for multiple comparisons) for the difference in transcript abundance between oocyte pools derived from large and spontaneous follicle classifications.

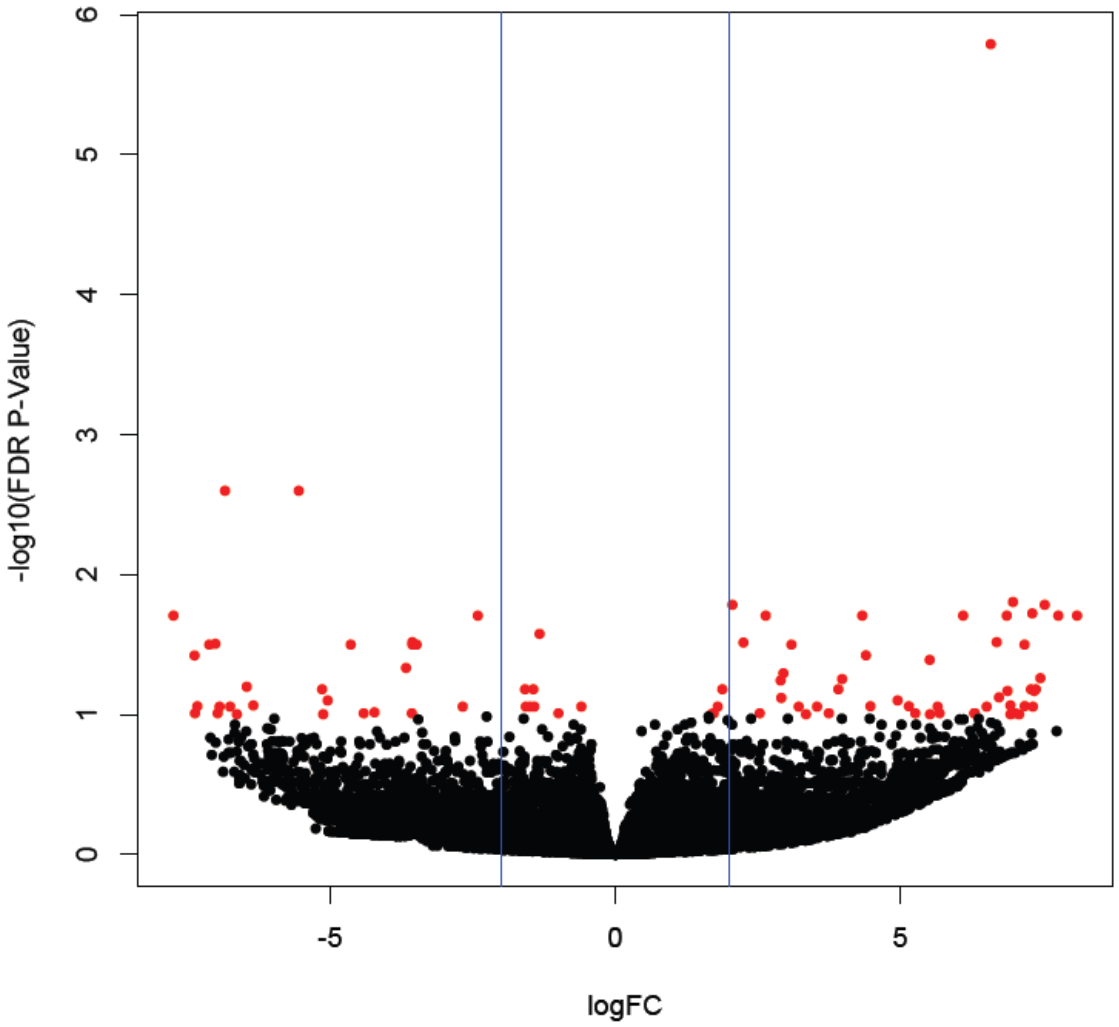

Figure 3.8. Volcano plot depicting differences in transcript abundance between large follicle oocyte pools and spontaneous follicle oocyte pools when mapped to the bovine genome (Cow_3.1_btau_4.6.1_Y_ncbi). X-axis denotes the $\log_2$ of the ratio between the normalized edgeR Robust read count values for large and spontaneous follicle oocyte pools (-5= 32 fold higher in large follicle oocyte pools; 0=equal transcript abundance between follicle classifications; 5= 32 fold lower in large follicle oocyte pools). Y-axis denotes $\log_{\text{-10}}$(FDR P-Value) where 1.3 equals P=0.05 and 1 equals P=0.10. Each dot represents one transcript. Red dots denote transcripts significantly different between large and spontaneous follicle oocyte pools at a false discovery rate (FDR) of <0.10.

Table 3.7. Differentially abundant transcripts between oocyte pools derived from large and spontaneous pre-ovulatory follicles (Genome)[a].

Transcripts Higher in Large Follicle Oocyte Pools compared to Spontaneous Follicle Oocyte Pools:

Accession Number	Gene ID	Function or Annotated Protein	Log FC[b]	P Value[c]	FDR[d]
XM_002684809.2	SEMA5B	semaphorin protein family; regulates axon growth	-6.84	2.2e-07	0.003
NM_001077932.1	RALYL	mRNA metabolism	-2.41	6.8e-06	0.020
XM_005218604.1	ATXN1L	chromatin binding factor; suppresses notch signaling	-1.33	1.5e-05	0.027
XM_005223722.1	ZNF391	zinc finger protein 391	-3.49	2.3e-05	0.032
NONE GIVEN	TMEM69	transmembrane Protein 69	-6.46	7.7e-05	0.063
NM_001081743.2	EDA	type II membrane protein; cell-cell signalling	-1.44	8.8e-05	0.066
NM_174622.3	TM7SF2	oxidoreductase activity	-1.58	9.7e-05	0.066
XM_002691231.3	CLEC4F	galactose/fucose receptor	-6.35	1.5e-04	0.086
XM_005210575.1	DFNB31	actin cystoskeletal assembly	-6.76	1.9e-04	0.088
XM_005216653.1	ADORA1	inhibits adenylate cyclase; decreases cAMP	-4.22	2.3e-04	0.097
XM_005224907.1	TGFB1I1	transforming growth factor β superfamily	-4.41	2.4e-04	0.098
XM_005203670.1	HAX1	suppress apoptosis	-1.00	2.6e-04	0.098

Transcripts Higher in Spontaneous Follicle Oocyte Pools compared to Large Follicle Oocyte Pools:

Accession Number	Gene ID	Function or Annotated Protein	Log FC[b]	P Value[c]	FDR[d]
NM_001103094.1	CBX6	transcriptional repressor	6.58	5.6-11	0.000
XM_005215962.1	TMEM136	transmembrane protein 136	7.53	3.2e-06	0.016
XM_005203228.1	MED18	activate transcription via RNA polymerase II	2.05	3.4e-06	0.016
XM_002687567.3	NXPH4	inhibits lipid peroxidation/subsequent cell degradation	6.87	8.3e-06	0.020
NM_001046402.2	ALKBH7	triggers collapse of mitochondrial membrane potential	4.33	9.65e-06	0.020
XM_005222348.1	UBE2D4	ubiquitin conjugating enzyme E2D4	2.64	1.0e-05	0.020
NM_001101177.1	LSM2	RNA binding protein	2.25	2.0e-05	0.031
XM_005209314.1	SHROOM1	microtubule/actin cytoskeleton assembly	7.18	2.4e-05	0.032
NM_001037586.2	TAF1D	component of nucleolar transcription factor	3.09	2.9e-05	0.032
XM_005213903.1	LOC521568	ATP binding cassette transporter	4.40	3.6e-05	0.038
XM_005202652.1	SPATS2L	protection from oxidative stress	3.99	6.4e-05	0.056
XM_005213514.1	EDF1	lipid metabolism	1.88	8.3e-05	0.066

Transcripts Higher in Spontaneous Follicle Oocyte Pools compared to Large Follicle Oocyte Pools cont.:

Accession Number	Gene ID	Function or Annotated Protein	Log FC[b]	P Value[c]	FDR[d]
XM_002686551.3	MAP7D1	structural molecule activity	3.91	8.5e-05	0.066
XM_002686915.2	TMEM229A	transmembrane protein 229A	7.38	9.6e-05	0.066
NM_001192956.1	HDDC3	pyrimidine metabolism	4.95	1.3e-04	0.079
XM_002697933.3	FLYWCH1	DNA binding	6.93	1.5e-04	0.086
NM_001192939.1	FGF11	member of fibroblast growth factor family	5.15	1.6e-04	0.087
NM_001206312.1	YIPF1[z]	RNA binding	4.48	1.6e-04	0.087
NM_001076023.1	C9H12orf49	chromosome 9 open reading frame	1.80	1.8e-04	0.088
NM_001206177.1	C8H9orf152	chromosome 8 open reading frame	6.51	2.0e-04	0.088
NM_001075825.2	MAP4K1	activates ERK and JNK kinase pathways	3.54	2.1e-04	0.088
XM_005203214.1	C1QA	binds fibronectin	6.30	2.7e-04	0.098
XM_005216773.3	BRINP3	negative regulation of cell cycle transition	2.53	2.7e-04	0.098
XM_005218513.1	MTHFSD	embryonic development	5.69	2.8e-04	0.098
NM_001046560.1	GSTM3	detoxification of electrophilic compounds	1.68	2.8e-04	0.100

[a] Data represent transcripts aligned to a bovine genome (Cow_3.1_btau_4.6.1_Y_ncbi)and found to be differentially abundant by the edgeR Robust GLM test (FDR<0.10). Only protein coding transcripts from annotated regions of the genome are included in Table 3.7.

[b] Log2 of the ratio between the normalized edgeR read count values for large or spontaneous follicle oocyte pools (-5= 32 fold higher in large follicle oocyte pools; 0=equal transcript abundance between follicle classifications; 5= 32 fold higher in spontaneous follicle oocyte pools.)

[c] Unadjusted P-Value for the difference in transcript abundance between oocyte pools derived from large and spontaneous follicle classifications.

[d] False discovery rate (FDR) P-Value (adjusted for multiple comparisons) for the difference in transcript abundance between oocyte pools derived from large and spontaneous follicle classifications.

[z] Transcript listed is an updated form of the transcript identified from the transcriptome to be differentially abundant (BLAST analysis of originally identified transcript matched this transcript with >99% accuracy.

oocytes. Additionally one transcript associated with mitochondria (NDUFA13) was more abundant in spontaneous follicle oocytes.

3.5 Discussion

In beef cattle, decreased pregnancy rates and increased late embryonic/fetal loss were observed following GnRH-induced ovulation of small compared to large dominant follicles (Perry et al., 2005). Further investigation determined that lowered pregnancy rates were the result of both an inadequate uterine environment and decreased oocyte competence (Atkins et al., 2013). Fertilization rates and embryo quality were lower in beef cows that were induced to ovulate small (<12.5mm) compared to large (≥12.5mm) dominant follicles (Atkins et al., 2013); however, a potential role of the maternal environment could not be eliminated, since embryo collection occurred on day 7 after GnRH-induced ovulation and insemination.

The follicular microenvironment has a role in acquisition of oocyte competence, which begins during the preantral stage and continues until the oocyte reaches MII (reviewed by Arlotto et al., 1996; Hendricksen et al., 2000; Eppig 2001). An important component of oocyte competence is acquisition of a complete transcriptome upon which the early bovine embryo must rely until the maternal zygotic transition (Sirard, 2001; Sirard et al., 2006). More specifically, rapid accumulation and storage of mRNA transcripts occurs during growth of the bovine oocyte (preantral follicle stage; Fair et al., 1997) and low levels of transcription continue until GVB and progression to MII (Fair et al., 1995; Mamo et al., 2011). In addition, the surrounding cumulus cells also contribute to the oocyte transcriptome by transferring mRNA directly to the oocyte via transzonal projections (Macaulay et al., 2014; Macaulay et al., 2015).

Numerous studies have tried to identify specific markers of oocyte competence in a variety of mammalian species (Nemcova et al., 2016; Angulo et al., 2015; Patel et al., 2007). Previous studies in cattle reported that increased expression of follistatin (FST) , inhibin βa (INHA), and inhibin βb (INHB) in oocytes collected from 3 to 7 mm follicles was associated with increased oocyte competence based on two experimental models (comparison of oocytes from prepubertal versus adult ovaries and comparison of early versus late cleaving embryos; Patel et al, 2007). However, Pohler (2011) reported that mRNA abundance of FST, INHA, and INHB in bovine oocytes decreased as dominant follicle size increased. In the current study, FST, INHA, and INHB transcript abundance was similar for the three follicle classifications. This is not entirely surprising, since oocytes in the present study were collected from follicles that were larger than those reported by Patel et al (2007) and they had all experienced expansion of the cumulus cells. In regards to the study by Pohler (2011), the oocytes were collected just before the preovulatory gonadotropin surge; whereas, the oocytes in the present study were collected after the preovulatory gonadotropin surge. To our knowledge, the effect of bovine follicle size and(or) the preovulatory gonadotropin surge on oocyte expression of FST, INHA, and INHB has not been investigated.

The current study compared the transcriptome of oocytes from small (<11.7 mm) and large (>12.5) pre-ovulatory follicles in cows that did not display estrus, but received a GnRH injection to induce a gonadotropin surge. The transcriptome of oocytes from cows in the spontaneous follicle classification (11.6-13.9mm; estrous expression; no GnRH injection) served as a control group, since we know that there is no negative effect of small dominant follicle size on the establishment of pregnancy when a cow

spontaneously expresses estrus and ovulates (Perry et al., 2005). A gonadotropin surge occurs within 90 minutes after GnRH injection (Atkins et al., 2008), and in cows that spontaneously express estrus and ovulate the preovulatory gonadotropin surge occurs before or at the onset of estrus (Swanson and Hafs, 1971). Therefore, it should be noted that the precise time of the preovulatory gonadotropin surge in the spontaneous group is not known and the interval from the gonadotropin surge to oocyte aspiration in the spontaneous group may be different then the interval from the GnRH-induced surge to oocyte aspiration in the small and large groups.

A number of studies have been conducted to examine the transcriptome of bovine oocytes that were matured in vivo versus in vitro (Lonergan et al., 2003; Mourot et al., 2006) or in which the transcriptome of GV versus MII oocytes was compared (Nemcova et al., 2016). In the preceding studies, a relatively large difference in transcript abundance was reported between treatments compared to the small difference in the transcriptomes of oocytes from different follicle classifications in the present study. The current study provided a comprehensive approach to characterize the transcriptome of oocytes that originated from dominant follicles from cows that experienced a pre-ovulatory gonadotropin surge (GnRH-induced or spontaneous surge). It was hypothesized that numerically small, but important, differences may exist in the transcriptomes of oocytes from small or large dominant follicles of cows that had not expressed estrus but had experienced a GnRH-induced gonadotropin surge. Oocytes were collected post-surge because it is known that transcription continues until germinal vesicle breakdown (Rodriguez and Farin, 2004), which is induced by the gonadotropin surge. Furthermore, transzonal processes, known to transport mRNA to the oocyte, are disrupted by the surge.

Analysis of the transcriptome of oocytes from small, large, and spontaneous pre-ovulatory follicles revealed relatively few differentially abundant transcripts, as expected, since the transcriptome of fully grown oocytes nearing the preovulatory gonadotropin surge should be mostly complete. However, further review of differentially abundant transcripts revealed possible differences in the functioning of specific pathways or organelles essential for oocyte competence. When differential transcript abundance was subjected to pathway analysis no distinct pathways were identified. However, there were several transcripts, which differed in abundance between follicle classifications, and were aligned with the following biological processes: ubiquitin/proteasome pathway, mitochondrial function, and cell signaling (i.e. protein kinase C, gamma). These are discussed further below.

Ubiquitin/Proteasome Pathway

The ubiquitin-proteasome system is responsible for proteolysis of around 75% of eukaryotic proteins. As reviewed by Sutovsky (2011), the ubiquitin-proteasome system is composed of three enzyme categories: 1) ubiquitin activating enzyme E1 (UBE1), 2) a ubiquitin conjugating enzyme (UBE2), and 3) an E3 ubiquitin ligase E3. These enzymes work together to allow for substrate specific ubiquitination of target proteins that are degraded by the 20S proteasome catalytic core of the 26S proteasome.

Specific enzymes in the UPP were differentially abundant in oocytes derived from the small, large, and spontaneous follicle classifications. Transcripts encoding for two forms of ubiquitin conjugating enzyme E2, UBE2B and UBE2D4, were higher in oocytes from large follicles compared to small follicles and oocytes from spontaneous follicles compared to large follicles, respectively. However, ubiquitin protein ligase E3C

(UBE3C) was higher in oocytes from large follicles compared to spontaneous follicles. A gene encoding for an essential subunit of the 20S proteasome (PSMB9) was higher in oocytes from spontaneous follicles compared to oocytes from both small and large follicles. In addition, ubiquitin specific peptidase 29 (USP29) was higher in oocytes from large follicles compared to small follicles. The preceding differences in transcript abundance reveal possible alterations in the UPP that may reflect a greater acquisition of competence in oocytes derived from larger follicles and in animals that experienced an endogenous gonadotropin surge compared to oocytes from small follicles. The role of the UPP in acquisition of oocyte competence is explained further below.

Ubiquitin dependent proteolysis was first shown to have a role in mitosis and later in meiosis (Peters, 2002). This pathway is essential to mitotic progression in somatic cells, as sister chromatid separation and the subsequent inactivation of cyclin dependent kinase 1 (CDK1), as well as entry into S phase, and the exit of mitosis (M phase) are regulated by the UPP. While most knowledge of ubiquitin's role in cyclin B destruction and chromatid separation during M phase exit was generated from mitotic cells, the same or similar mechanisms may be involved in segregation of the homologous chromosomes during meiosis I, or the separation of sister chromatids in meiosis II (Huo et al., 2004).

In starfish (Sawada et al., 1997) and toad (Takanashi, 1994) oocytes, inhibition of the proteasome prevented GVB, which suggests that meiotic progression is reliant on the production and ubiquitin specific substrate degradation of cell cycle regulators. Study of the UPP in the mouse oocyte revealed conjugation of ubiquitin around condensed chromosomes throughout oocyte maturation to MII. Though a slight increase in the

proportion of oocytes undergoing GVB was observed after inhibition of the proteasome, the ability to extrude a second polar body was decreased, depending on the proteasome inhibitor used (Hou et al., 2004). Further study in pigs revealed that meiotic progression was dependent on the UPP (Sun et al., 2004). More specifically, when porcine oocytes were cultured during maturation with two different proteasome inhibitors, MG132 and lactacystin, cumulus expansion and meiotic resumption were inhibited. After 26 and 44 hours of culture, GVB, chromosome condensation, and polar body extrusion were reduced when either inhibitor was utilized. Varying degrees of interruption of meiotic progression to MII were observed when differing amounts of proteasome inhibitors were added after GVB, suggesting a role of the UPP in cell cycle progression past GVB. Fertilization rates were also affected by inhibition of the UPP, as reduced sperm penetration was observed when oocytes were subjected to proteasome inhibition prior to in vitro fertilization.

You et al. (2012) studied the inhibition of the UPP in bovine oocytes during the first and last six hours of IVM. Inhibition of the UPP from 0 to 6 hr of maturation increased the proportion of oocytes remaining in MI and somewhat reduced meiotic progression to MII as well as reduced cleavage and blastocyst rates following IVF. However, the addition of 10μm of a proteasome inhibitor (MG132) to media following 16-22 hours of maturation increased cleavage and blastocyst rates. While proper functioning of the UPP is essential for the completion of the meiosis I, its continued function during the later stages of oocyte maturation may reduce oocyte competence through the proteasomal degradation of vital transcripts. Oocytes in the current study were collected an average of 23 hours post GnRH injection and had an expanded cumulus

mass. In the current study, oocytes in the follicle classification groups would have almost completed meiotic maturation, a time when the UPP could potentially have negative effects. However, the preceding data was collected during oocyte maturation in vitro; whereas, oocytes in the current study matured in vivo.

Our lab intends to further study whether the UPP could have a role in acquisition of oocyte competence in dominant follicles that differ in physiological maturity. Analysis of differential abundance of UPP proteins and enzyme activity are required to determine if the differences of transcript abundance reported herein are physiologically relevant Furthermore, localization of members of the UPP in pre-ovulatory bovine oocytes will allow a better understanding of the roles it plays in bovine oocyte competence.

Mitochondrial function

Adequate numbers of properly functioning mitochondria are essential for acquisition of oocyte competence (Bavister and Squirrell, 2000). More specifically, mitochondrial production of ATP via oxidative phosphorylation is required for fertilization, meiotic maturation, and preimplantation embryo development. The number of mitochondria in oocytes increases throughout oocyte maturation (reviewed by Ferrierra et al., 2009) and all mitochondria in embryos are derived from maternal mitochondria. Mitochondria present at the time of fertilization are divided among blastomeres during embryonic cleavage. In mice, no new mitochondria are produced until the time of implantation (Dumollard et al., 2009).

In the current study, several nuclear and mitochondrial derived transcripts, associated with the mitochondrial function and oxidative phosphorylation, were differentially abundant between oocytes derived from small, large, and spontaneous

follicular classifications. Two nuclear transcripts encoding for mitochondrial proteins, MRPL48 and AGXT2, were more abundant in large versus small follicle oocytes. Furthermore, COX61A and NDUFA13 were more abundant in oocytes from spontaneous follicles compared to small and large follicles, respectively. The above observations may indicate a higher level of mitochondrial function in oocytes from larger follicles or from cows that had an endogenous gonadotropin surge compared to mitochondria in oocytes of small follicles.

The mitochondria has its own double stranded, circular genome that is inherited from the maternal lineage (Chappel, 2013). Within our analysis of the oocyte transcriptome, 5 transcripts from the mitochondrial genome were higher in abundance in oocytes of small follicles compared to oocytes from spontaneous follicles. This discovery is particularly interesting, since a higher amount of mitochondrial transcripts could indicate an increased number of mitochondria in oocytes from small follicles (presumably less competent) or an increased rate of transcription of the mitochondrial genome. However, at the present time there is no way to resolve this question based on the current data, and one must also consider the possibility that mitochondrial transcripts in oocytes from the large and spontaneous follicle classifications may have been translated and subsequently degraded.

Evidence for the mitochondria's role in oocyte competence is compelling, as mitochondrial migration during oocyte maturation suggests a role in providing ATP for nuclear maturation events. As oocytes progress through maturation, the mitochondria increase in number and migrate centrally toward the nucleus (reviewed by Bavister and Squirrell, 2000). IVM conditions can alter mitochondrial migration, as proper migration

toward the nucleus was seen in mitochondria within MII oocytes matured in media primarily containing glucose and amino acid media, a culture system known to produce oocytes competent to develop to the blastocyst stage. However, when oocytes were matured in media containing glucose and lactate, poor blastocyst rates are observed. Mitochondria in oocytes cultured in glucose and lactate failed to migrate toward the nucleus, and remained distributed throughout the cytoplasm.

In addition, IVF success was decreased in women over the age of 35 because of lowered oocyte quality (Ramalho-Santos et al., 2009; Chappel, 2013). Functional ATP synthesis was decreased in aged oocytes due in part to increased damage of mitochondrial DNA and a higher frequency of mitochondrial membrane damage. Mitochondria have no mechanism for DNA repair, and therefore become less efficient.

Preventing oxidative damage is crucial within the oocyte. Coenzyme Q10 (CoQ10) is a component of the mitochondrial respiratory chain that is known to scavenge free radicals (Turi et al., 2012). Higher concentrations of CoQ10 have been associated with culture systems that increase bovine oocyte competence following thermal stress to the oocyte (Gendelman and Roth, 2012), and CoQ10 has been found within human follicular fluid (Turi et al., 2012). Unpublished data from the analysis of the transcriptome of cumulus cells surrounding the oocytes utilized in the current study revealed higher transcript abundance of ubiquinone (CoQ10) in cumulus cells surrounding the large compared to small follicle oocytes.

Further investigation is needed to verify possible differences in mitochondrial function in preovulatory oocytes encased in varied follicular microenvironments. Avenues for investigation include quantitation of the number of mitochondria,

localization of mitochondria, and ATP content of oocytes derived from small, large, and spontaneous follicle classifications.

Protein Kinase C, gamma

The protein kinase C (PKC) family of serine/threonine kinases is known to have an important role in oocyte maturation and fertilization (Fan et al., 2002). PKC modulates intracellular calcium oscillations, within the oocyte, following fertilization, leading to cortical granule release and a subsequent polyspermy block (Fan et al., 2002). Furthermore, PKC promotes meiotic resumption (Wu et al., 2006, Fan et al., 2002). In the current study, protein kinase C, gamma (PRKCG) was more abundant in oocytes from large follicles compared to small follicles. PRKCG is a member of the classical protein kinase C subclass (cPKC); which is the most studied category of PKC in the oocyte. In humans (Wu et al., 2006) and pigs (Fan et al., 2002), cPKCs were localized to the germinal vesicle but dispersed evenly throughout the cytoplasm upon progression to MII and subsequent oocyte activation by a fertilizing spermatozoa. Upon oocyte activation, cPKC was translocated to the periphery of the cytoplasm (Wu et al., 2006, Fan et al., 2002). In pigs, PKC interacts with inositol 1,4,5-triphosphate to signal calcium release and subsequent cortical granule exocytosis. When PKC activation was inhibited, neither cPKC migration nor cortical granule exocytosis was observed, indicating PKC may have a role in the block to polyspermy. Protein kinase C is a crucial signaling molecule in pathways essential to the oocyte. Therefore, its potential role in acquisition of oocyte competence as bovine preovulatory follicles acquire physiological maturity should be further investigated. Determination of protein levels and enzyme activity of PRKCG is essential for further study.

In summary, analysis of the transcriptome of bovine oocytes from dominant follicles that differ in size (small versus large) or physiological status (estrous expression versus no estrous expression) revealed a small list of differentially abundant transcripts that could regulate important pathways leading to the acquisition of oocyte competence.

APPENDIX A

Trans-vaginal follicle aspiration for the collection of cumulus-oocyte complexes

Rational

Inadequate oocyte competence is a potential explanation for reduced pregnancy rates and(or) embryonic/fetal mortality when small dominant follicles are induced to ovulate prematurely. The reciprocal embryo transfer study indicated that fertilization rate was decreased following GnRH-induced ovulation of small follicles. However, a potential confounding influence of the donor cow's oviductal/uterine environment from the time of fertilization (day 1) until embryo collection (day 7) cannot be ruled out. Therefore, this objective will test the hypothesis that the physiological status of an ovulatory follicle has a direct effect on competence of the oocyte. Numerous investigators have examined the relationship between oocyte competence and expression of specific genes in the oocyte and(or) cumulus cells; however, identification of a definitive marker of oocyte competence in oocytes, cumulus cells, and(or) follicular cells has not been identified. Therefore, studying the transcriptome of oocytes and cumulus cells from follicles that vary in physiological status could be helpful in identifying specific gene products that may have a role in the acquisition of oocyte competence as well as follicular maturity

Hypothesis

Expression of genes that serve as markers of oocyte competence will differ between the oocyte and cumulus cells collected from small or large dominant follicles.

Specific aim

Determine the effect of dominant follicle diameter 15 to 20 hours after a GnRH-induced gonadotropin surge (CO-Synch protocol; see below) on markers of oocyte competence (follistatin expression in oocytes, cathepsin expression in cumulus cells, and potential granulosa cell markers of oocyte competence [e.g. Sprouty homolog 2; see Table 1 below]), and to characterize steroidogenic capacity of the dominant follicle following the GnRH-induced ovulation.

Experimental Design

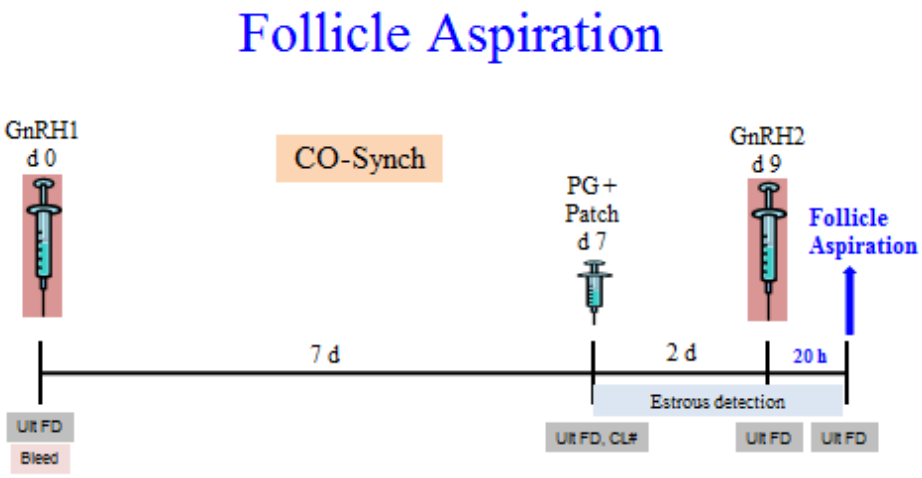

Endpoints to be measured

1) Ultrasound – ovarian scans (follicles > 8 mm and corpora lutea) of all cows at PGF (d 7), GnRH2, and aspiration. Cows that show estrus will be scanned at aspiration.

2) Hormone assays – Progesterone and estradiol at GnRH1, PGF, GnRH-2, aspiration, and 7 days after aspiration will be measured in serum. Estradiol/progesterone ratio in follicular fluid.
3) Estrous activity from GnRH1 until aspiration. We will apply Estrotech patches at GnRH1 and detect estrus every 6 hr beginning 24 hr before PGF, and determine the E/P ratio in follicular fluid to determine if cows show estrus by the time of aspiration.
4) Transcriptome analysis of oocytes and cumulus cells in each of the treatments. There will also be an opportunity to examine expression of granulosa cells markers of oocyte competence (e.g. Sprouty homolog 2) in the granulosa cells collected at aspiration. However, it should be noted that the granulosa cells collected at aspiration may not be physiologically representative of the mural granulosa cells that remain attached to the follicle wall.
5) A photograph of cumulus –oocyte complex may be taken if the photograph is of sufficient quality to be helpful.

Methodology

1.) Estrous detection

a. Heifers and cows will receive Estrotech patches at GnRH1and will be detected for estrus every six hours from 24 hr before PGF until aspiration. Cows detected in estrus will be aspirated as a separate group 15 to 22 hours after estrous detection.

2.) Ultrasonography

a. Ovaries will be scanned at PGF (d 7), GnRH2, and aspiration. Follicle diameter and the number and location of corpora lutea will be recorded at each scan.

3.) Blood sample collection

a. Blood samples will be collected at GnRH1 (d 0), PGF (d 7), GnRH2, and aspiration.

4.) Transvaginal aspiration of oocyte

a. Dominant follicle diameter will be measured before aspiration via transrectal ultrasonography.

b. Aspirate the dominant follicle and collect the first syringe of follicular fluid. Place a new syringe onto the aspiration tubing and flush the follicle as many times as feasible before finishing by using PVA-TL HEPES media. Once the aspiration is complete, we will begin searching the dish with only the follicular fluid without any other media added. If the oocyte is not located then we will proceed to searching the 2nd dish with the follicular flushes.

c. Collect cumulus-oocyte complex.

5.) COC processing

a) Collection of the cumulus cells: It is a good idea to frequently or spray your hands with 70 % ethanol. Once the COC is located place the COC into 500 ul of PVA-TL HEPES in an eppendorf tube. Vortex for 30 seconds to remove oocyte from cumulus mass. Place the contents of

the tube in a small petri dish and determine if the oocyte has separated from the cumulus mass. **DO NOT** discard tube until oocyte has been located! Pick up the cumulus mass, place into an Eppendorf tube, spin at 1500 x g for 3 minutes with the tail of tube out in order to locate pellet. Pipette out the media very carefully without disturbing the cumulus cells pellet (It could be difficult to see the cumulus cells pellet from a single oocyte). Retain ONLY 5-10 ul of media in the tube to avoid disturbing the cumulus cells pellet. Then add 90 ul of lysis buffer, and mix by pipetting, to lyse the cumulus cells. Immediately snap freeze the centrifuge tubes.

b) Denuding the cumulus cells surround the oocyte: Collect the oocyte in 150 ul of PVA-TL HEPES. Cumulus cells are denuded with repeated pipetting, with an RNAse free tip until the oocyte is completely free from cumulus cells. We may remove the remaining cumulus cells in PVA-TL HEPES containing 1000 units of hyaluronidase per ml.

c) Freezing the oocytes for RNA isolation: Add 9 ul of lysis buffer provided in the RNA aqueous micro kit (Ambion, Cat. No: 1931) to each sterile centrifuge tube (place the tubes containing lysis buffer on ice and the lysis buffer should be kept on ice). Dispense the oocyte into lysis buffer in tube (in less than 5 ul of medium) using Drummond micro dispenser. The tip of the dispenser should be dipped in the lysis buffer when the oocyte is dispensed. This is to avoid the oocyte sticking to the sides of the tube, rather than the lysis buffer. Pipette the

Drummond sterile tip in lysis buffer more than once, to make sure the oocyte is dispensed into lysis buffer. This step should be completed under a dissecting microscope to ensure that the oocyte has indeed been transferred in the lysis buffer. Once the oocyte is in the lysis buffer you will not be able to visualize so it is critical that the transfer into the tube is seen. Immediately snap freeze the tubes in liquid nitrogen [avoid tossing the tube into liquid nitrogen, because this may disperse the lysis buffer to the wall and the cap of the tube. Immerse the tube delicately with a forceps into the liquid nitrogen, until the lysis buffer freezes and remains at the bottom of the tube.] Store the tubes at -80^0 C.

6.) *Follicular Fluid Collection*

a) Turn dish sideways to drain all follicular fluid to side and collect with a pipette with a sterile pipette tip.
b) Place follicular fluid into an Eppendorf tube.
c) Briefly microfuge at low speed and remove follicular fluid from cells.
d) The pelleted granulosa cells can be snap frozen without adding lysis buffer. Collecting these cells may allow us to potentially examine granulosa cell markers of oocyte competence.
e) Split the follicular fluid in half into two separate 2 ml screw cap vials.
f) Label and freeze at -80

Table A.1. Genes associated with oocyte competence

Location	Abbreviation	Name	Relative Expression in Competent Oocytes or Follicular Cells	Species	Reference
Oocyte	FST	Follistatin	High	Cattle	Patel et al 2007
Oocyte	INHBA	Inhibin, beta A	High	Cattle	Patel et al 2007
Oocyte	INHBB	Inhibin, beta B	High	Cattle	Patel et al 2007
Cumulus Cells	INHBA	Inhibin, beta A	High	Cattle	Patel et al 2007, Assidi et al 2008
Cumulus cells	TNFAIP6	Tumor necrosis factor, alpha-induced protein 6	High	Mouse, Cattle, Pig	Fulop et al 2003, Assidi et al 2008, Nagyova et al 2009
Cumulus cells	CTSB	Cathepsins B	Low	Cattle	Bettegowda et al 2008, Balboula et al 2010
Cumulus cells	CTSZ	Cathepsins Z	Low	Cattle	Bettegowda et al 2008
Cumulus cells	CTSS	Cathepsins S	Low	Cattle	Bettegowda et al 2008
Cumulus cells	HAS2	Hyaluronic acid synthase 2	High	Humans, Cattle	McKenzie et al 2004, Cillo et al 2007, Assidi et al 2008
Cumulus cells	GREM1	Gremlin1	High	Humans, Cattle	McKenzie et al 2004, Cillo et al 2007, Assidi et al 2008
Cumulus cells	PTGS2	Prostaglandin-endoperoxide synthase 2	High	Humans, Cattle	McKenzie et al 2004, Assidi et al 2008

Granulosa cells	HSD3B1	3-beta-hydroxysteroid dehydrogenase 1	High	Humans	Hamel et al 2008
Granulosa cells	FDX1	Ferredoxin 1	High	Humans	Hamel et al 2008
Granulosa cells	SERPINE2	Serine proteinase inhibitor clade E member 2	High	Humans	Hamel et al 2008
Granulosa cells	CYP19A1	Cytochrome P450 aromatase	High	Humans	Hamel et al 2008
Granulosa cells	CDC42	Cell division cycle 42	High	Humans	Hamel et al 2008, Hamel et al 2010
Granulosa cells	SPRY 2	Sprouty homolog 2	High	Cattle, Human	Robert et al 2001, Hamel et al 2008
Granulosa cells	PGKI	Phophoglycerate kinase I	High	Human	Hamel et al 2010
Granulosa cells	RGS2	Regulator of G-protein signaling	High	Human	Hamel et al 2010

PVA-TL HEPES

pH 7.4 Osmolarity 275-280

	Component	1 Liter	2 Liter	6 Liter
1	NaCl	6.6633 g	13.326 g	39.980 g
2	KCl	0.2386 g	0.4772 g	1.4316 g
3	NaHCO3	0.1680 g	0.3360 g	1.0080 g
4	NaH2PO4	0.0408 g	0.0816 g	0.2448 g
5	Na Lactate	1.868 ml	3.736 ml	11.208 ml
6	MgCl2*6H2O	0.1017 g	0.2034 g	0.6102 g
7	HEPES	2.3830 g	4.7660 g	14.298 g
8	CaCl2*2H2O	0.2940 g	0.5880 g	1.7640 g
9	PVA	0.1 g	0.2 g	6 g
10	Sorbitol	2.1860 g	4.3720 g	13.116 g
11	Gentamicin	1 ml	2 ml	6 ml
12	Pyruvate	0.0220 g	0.0440 g	0.132 g

Mix all chemicals together in order using sterilized glassware and ddH2O. After reagents are added, Adjust the pH to 7.40 using HCl and NaOH stocks. Next check the osmolarity. Be certain that you standardize the pH meter and the osmometer before using. Filter media with 0.22-micron filter unit. Refrigerate until needed or place in refrigerator. Discard media after 2-2.5 weeks.

*Add PVA after mixing all other chemicals as PVA is difficult to dissolve at this concentration. Add to beaker slowly while it is mixing.

*Add PVA slowly and allow to sit. Mix very slowly as to not disturb PVA resting on top of solution. PVA dissolves best in cold water.

Cat #s:

1	NaCl	S-5886
2	KCl	P-4505
3	NaHCO3	S-5761
4	NaH2PO4	S-5011
5	Na Lactate	L-7900
6	MgCl2*6H2O	M-0250
7	HEPES	H-3784
8	CaCl2*2H2O	C-7902
9	PVA	P-8136
10	Sorbitol	S-1876
11	Gentamicin	
12	Pyruvate	P-4562

Table A.2. Summary of follicle aspiration results following synchronization of ovulation in postpartum beef cows.

Parameter:	Number:
Total Number of Cows Synchronized[a]	250
Successful Collection of Cumulus-Oocyte Complex	127
Small Follicle Oocytes[b]	30
Large Follicle Oocytes[c]	36
Spontaneous Follicle Oocytes[d]	21
Spontaneous + GnRH Oocytes[e]	28
Intact COCs[f]	12
Sample Not Successfully Collected	123
Follicle not aspirated[g]	15
Ovulation before aspiration[h]	9
Follicle ruptured during aspiration[i]	5
No COC located[j]	56
COC lost during processing[k]	8
COC deemed unacceptable[l]	15
Miscellaneous[m]	15

[a]Total number of cows in which ovulation was synchronized for follicle aspiration
[b]Number of oocytes frozen from the small follicle oocyte classification
[c]Number of oocytes frozen from the large follicle oocyte classification
[d]Number of oocytes frozen from the spontaneous follicle oocyte classification
[e]Number of oocytes frozen that originated from follicles of cows that expressed estrus (spontaneous) but received a GnRH2 injection before estrous expression; not analyzed in present study
[f]Number of intact COCs collected; not analyzed in present study
[g]Number of cows that did not receive follicle aspiration due to improper follicle sizes, regressed dominant follicle, etc.
[h]Number of cows that ovulated before follicle aspiration; as confirmed by the absence of the dominant follicle at aspiration
[i]Number of cows that the follicle ruptured during follicle aspiration and no COC was collected
[j]Number of aspirations in which no COC was located.
[k]Number of located COCs that were lost during processing
[l]Number of located COCs that were deemed unacceptable because of few cumulus cells, the cumulus complex that had not expanded, the COC appeared to be degenerated, grainy appearing oocyte cytoplasm, etc.
[m]Number of cows removed from the project or oocytes not frozen for varied reasons (e.g. aspirated two follicles, error during COC processing, etc).

APPENDIX B

RNA-sequencing project

Preliminary Instructions:

RNA extraction

RNA was extracted from pools of 4 oocytes. In an effort to increase the number of experimental replicates, pools of 4 oocytes were utilized, as this was the smallest number of oocytes that consistently yielded RNA from this means of extraction. The author's personal experience with this method of RNA extraction leads to the following suggestions:

1. Perform RNA extractions in small batches. Performing extractions of only 4 pools of oocytes at one time is suggested to allow for timely extraction and freezing of extracted material to minimize degradation.
2. Use 14 µl of RNAase free H_2O for elution of RNA. This provides a yield of approximately 12µl of eluded RNA. Efforts to increase concentration of RNA in elute by using smaller volumes of H_2O for elution led to reduced incidence of successful RNA extraction.

Reverse transcription and amplification

Use individual PCR-reaction tubes for the procedures in this protocol. Allot 7 hours for this protocol's completion. Ensure the PCR tubes are in adequate contact with the magnetic strip for all steps of the parts of this protocol that utilize magnetic beads. Inadequate contact of the PCR tubes with the magnetic strip will result in sub adequate

attraction of the magnetic beads to the sides of the tube, and will lead to less precision when pipetting media away from the beads.

Alignment of filtered reads to the transcriptome or genome

In the current study, alignment of reads to a refseq Bos Taurus transcriptome with additional annotations was performed with the following criteria for alignment: 1) reads must align to a specific region of the transcriptome with 95% accuracy, and 2) ambiguous mapping was allowed for all transcripts in which reads mapped with 95% accuracy. When alignment was performed to the Bos Taurus genome, the following criteria were established for mapping: 1) reads must align to a specific region of the transcriptome with 95% accuracy, and 2) ambiguous mapping was not allowed; only the first area of the genome in which a transcript mapped with 95% accuracy was recorded. The author suggests utilizing the same mapping criteria between the transcriptome and genome in future experiments. After alignment, it is essential to review the mapping percentages for all libraries before proceeding.

Table B.1. Summary of oocyte reads generated by deep sequencing (*Illumina HiSeq 2000*)[a]

Sample ID[b]	Tissue Type	Number of reads before trimming[c]	Number of reads after trimming[d]	Percentage of reads retained after trimming[e]
O1	Oocyte Pool	8,585,628	7,577,695	88.3%
O2	Oocyte Pool	9265058	8172555	88.2%
O3	Oocyte Pool	6785587	5919821	87.2%
O4	Oocyte Pool	8146641	7196583	88.3%
O5	Oocyte Pool	8838690	7802692	88.3%
O6	Oocyte Pool	7652036	6724529	87.9%
O7	Oocyte Pool	8619483	7626781	88.5%
O8	Oocyte Pool	9224112	8142706	88.3%
O9	Oocyte Pool	8139230	7199121	88.4%
O10	Oocyte Pool	8072268	7121650	88.2%
O11	Oocyte Pool	6862866	6034039	87.9%
O12	Oocyte Pool	8896120	7834764	88.1%
O14	Oocyte Pool	8428323	7438386	88.3%
O15	Oocyte Pool	8494126	7472610	88.0%
O16	Oocyte Pool	7880930	6897953	87.5%
O17	Oocyte Pool	9930075	8735968	88.0%

[a] Sequencing was performed on an Illumina HiSeq 2000. Oocyte pools were multiplexed, sequenced in a single lane, 100 base pairs per read, with adaptors removed at trimming.
[b]Identification (ID) for each sample (O=oocyte pool 1-17 *pool 13 was removed prior to sequencing due to low cDNA content).
[c] Total number of reads generated for each oocyte pool.
[d] Number of reads that met the minimum criteria for quality score and read length.
[e] Percentage of total reads (column 4) that met the minimum criteria for quality score and read length.

Table B.2. Summary of oocyte reads that mapped to the transcriptome and genome.

Sample ID[a]	Tissue Type	Number of reads after trimming[b]	Number of reads mapped Transcriptome[c]	Percentage of trimmed reads that mapped Transcriptome	Percentage of ambiguous mapping Transcriptome[d]	Number of reads mapped Genome[e]	Percentage of trimmed reads that mapped Genome	Percentage of ambiguous mapping Genome[f]
O1	Oocyte	7577695	4842813	63.9%	9.8%	4968871	65.6%	0%
O2	Oocyte	8172555	4971967	60.8%	9.4%	5455505	66.8%	0%
O3	Oocyte	5919821	2694261	45.5%	9.3%	4190111	70.8%	0%
O4	Oocyte	7196583	4536814	63.0%	9.5%	4755792	66.1%	0%
O5	Oocyte	7802692	4704018	60.3%	9.5%	5161798	66.2%	0%
O6	Oocyte	6724529	4181776	62.2%	9.4%	4384733	65.2%	0%
O7	Oocyte	7626781	4998612	65.5%	9.4%	4993829	65.5%	0%
O8	Oocyte	8142706	5168178	63.5%	9.6%	5363045	65.9%	0%
O9	Oocyte	7199121	4690261	65.2%	9.8%	4712782	65.5%	0%
O10	Oocyte	7121650	4417573	62.0%	9.0%	4732085	66.4%	0%
O11	Oocyte	6034039	3749663	62.1%	9.3%	3962780	65.7%	0%
O12	Oocyte	7834764	4310012	55.0%	9.5%	5233710	66.8%	0%
O14	Oocyte	7438386	4803207	64.6%	9.2%	4881685	65.6%	0%
O15	Oocyte	7472610	4514867	60.4%	9.5%	4783901	64.0%	0%
O16	Oocyte	6897953	4177132	60.6%	9.0%	4484904	65.0%	0%
O17	Oocyte	8735968	5620322	64.3%	9.5%	5779578	66.2%	0%

[a] Identification (ID) for each sample (O=oocyte pool 1-17*pool 13 was removed prior to sequencing due to low cDNA content).
[b] Number of reads that met the minimum criteria for quality score and called base number.
[c] Number of reads that mapped to a specific location on the bovine transcriptome (refseq Bos Taurus transcriptome from NCBI with additional annotations).
[d] Percentage of reads that mapped to greater than one specific location on the transcriptome.
[e] Number of reads that mapped to a specific location on the bovine genome (Cow_3.1_btau_4.6.1_Y_ncbi).
[f] Ambiguous mapping was not allowed in genome alignment. Only the first alignment for each read was recorded.

Table B.3. Most Abundant Transcripts in Pre-Ovulatory Oocyte Pools[a]

Accession Number	Transcript Name	Abundance Small Follicle Oocytes	Abundance Large Follicle Oocytes	Abundance Spontaneous Follicle Oocytes
XM_002706880.1	thymosin, beta 4	7908.31	9541.72	9784.61
XM_002692986.1	B-cell translocation gene 4-like	4311.76	4452.70	4376.78
XM_002695859.1	Os05g0242100-like	3923.72	3680.44	3781.02
XM_002686059.1	histone cluster 1, H2bd-like	3102.71	3529.72	3746.19
XM_002686811.1	regulator of G-protein signaling 2-like	2429.57	2298.44	2647.16
XM_002697530.1	histone cluster 1, H1a-like	2133.18	2575.37	2438.75
NM_001038028.1	aurora kinase A	2386.27	2385.77	2383.01
NM_001038687.1	oocyte-secreted protein 1	1849.02	2171.15	2204.63
NM_001098945.1	high-mobility group nucleosomal binding domain 2	1891.75	2039.53	2044.43
XM_001252596.2	tropomyosin 4	2082.43	1957.78	2023.46
NM_001034204.1	tubulin, alpha 1c	1823.95	1731.05	1998.47
NM_001113311.1	CDC28 protein kinase regulatory subunit 1B	1912.51	2075.62	1931.64
NM_001075135.1	similar to Putative ubiquitin-conjugating enzyme E2 D3-like protein	2004.20	1991.84	1920.53
NM_173973.2	zona pellucida glycoprotein 2	2034.17	1908.03	1831.99
NM_001034310.2	pituitary tumor-transforming 1	1944.13	1907.50	1809.60

[a]Transcripts ranked by average RPKM abundance in spontaneous follicle oocyte pools when aligned to a Bos Taurus transcriptome from NCBI with additional annotations.

Table B.4. Validation of Complementary DNA (cDNA) amplification[a].

Official Gene Symbol[b]	RPKM Literature	RPKM (Current Study)
PABPNIL	0.4	na
CPSF1	0.6	1.5
CPEB1	1.2	102
CPEB2	1.5	3.8
PABPC5	2.1	2.6
CPEB3	4.1	9.2
CPSF6	5.8	24.3
CPSF3	9.8	9.2
PABPN1	11.8	27.8
PUM2	21.1	65.6
CPSF2	23.4	37.5
PABPC1	38.2	232
PAPD4	38.8	102.1
CPEB4	39.4	31.3
PARN	60.1	32
TACC3	208.5	743

[a] Comparison of abundance (RPKM) of polyadenylated bovine oocyte transcripts published by Reyes et al. (2016) to the abundance of the same transcripts generated by deep sequencing in the current study. Correlation = 0.93.
[b]Gene name based on official gene symbol.

Table B.5. Correlation of transcript abundance (≥1 RPKM) within and among classification of oocyte pools[a,b,c]

	Small Follicle Oocytes						Large Follicle Oocytes						Spontaneous Follicle Oocytes			
	Pool 1	Pool 2	Pool 3	Pool 4	Pool 5	Pool 6	Pool 7	Pool 8	Pool 9	Pool 10	Pool 11	Pool 12	Pool 14	Pool 15	Pool 16	Pool 17
Pool 1	1.00	0.97	0.94	0.97	0.98	0.96	0.98	0.98	0.96	0.98	0.98	0.97	0.96	0.97	0.96	0.97
Pool 2	0.97	1.00	0.95	0.96	0.98	0.97	0.98	0.98	0.96	0.96	0.96	0.96	0.95	0.97	0.97	0.97
Pool 3	0.94	0.95	1.00	0.95	0.95	0.94	0.96	0.96	0.95	0.94	0.93	0.93	0.90	0.96	0.97	0.97
Pool 4	0.97	0.96	0.95	1.00	0.97	0.97	0.97	0.97	0.98	0.96	0.97	0.96	0.94	0.98	0.95	0.97
Pool 5	0.98	0.98	0.95	0.97	1.00	0.97	0.97	0.99	0.97	0.98	0.98	0.98	0.96	0.97	0.97	0.97
Pool 6	0.96	0.97	0.94	0.97	0.97	1.00	0.97	0.97	0.97	0.94	0.94	0.95	0.92	0.97	0.94	0.96
Pool 7	0.98	0.98	0.96	0.97	0.97	0.97	1.00	0.98	0.96	0.95	0.95	0.95	0.93	0.97	0.96	0.98
Pool 8	0.98	0.98	0.96	0.97	0.99	0.97	0.98	1.00	0.97	0.97	0.97	0.97	0.96	0.97	0.97	0.98
Pool 9	0.96	0.96	0.95	0.98	0.97	0.97	0.96	0.97	1.00	0.96	0.96	0.96	0.93	0.98	0.95	0.97
Pool 10	0.98	0.96	0.94	0.96	0.98	0.94	0.95	0.97	0.96	1.00	0.99	0.98	0.98	0.96	0.97	0.96
Pool 11	0.98	0.96	0.93	0.97	0.98	0.94	0.95	0.97	0.96	0.99	1.00	0.98	0.98	0.96	0.97	0.96
Pool 12	0.97	0.96	0.93	0.96	0.98	0.95	0.95	0.97	0.96	0.98	0.98	1.00	0.98	0.96	0.96	0.96
Pool 14	0.96	0.95	0.90	0.94	0.96	0.92	0.93	0.96	0.93	0.98	0.98	0.98	1.00	0.93	0.95	0.94
Pool 15	0.97	0.97	0.96	0.98	0.97	0.97	0.97	0.97	0.98	0.96	0.96	0.96	0.93	1.00	0.96	0.97
Pool 16	0.96	0.97	0.97	0.95	0.97	0.94	0.96	0.97	0.95	0.97	0.97	0.96	0.95	0.96	1.00	0.97
Pool 17	0.97	0.97	0.97	0.97	0.97	0.96	0.98	0.98	0.97	0.96	0.96	0.96	0.94	0.97	0.97	1.00

[a] Classification = Small follicle oocytes(pools 1-6), large follicle oocytes(pools 7-12), and spontaneous follicle oocytes (pools 14-17)

[b] Transcript abundance (reported in RPKM) for each gene mapped to the oocyte transcriptome (ReSeq transcriptome from NCBI with additional annotations)

[c] Simple correlation coefficients within and among classification of oocyte pools when all transcripts with average abundance >1 RPKM are considered.

Table B.6. Correlation of transcript abundance (≥ 1 and ≤100 RPKM) within and among classification of oocyte pools[a,b,c]

	Small Follicle Oocytes						Large Follicle Oocytes						Spontaneous Follicle Oocytes			
	Pool 1	Pool 2	Pool 3	Pool 4	Pool 5	Pool 6	Pool 7	Pool 8	Pool 9	Pool 10	Pool 11	Pool 12	Pool 14	Pool 15	Pool 16	Pool 17
Pool 1	1.00	0.80	0.78	0.80	0.83	0.79	0.84	0.83	0.86	0.84	0.83	0.78	0.82	0.82	0.82	0.82
Pool 2	0.80	1.00	0.83	0.79	0.83	0.79	0.83	0.86	0.83	0.82	0.84	0.80	0.83	0.80	0.79	0.80
Pool 3	0.78	0.83	1.00	0.77	0.81	0.75	0.81	0.84	0.80	0.83	0.83	0.81	0.81	0.80	0.85	0.85
Pool 4	0.80	0.79	0.77	1.00	0.82	0.80	0.81	0.83	0.85	0.80	0.82	0.77	0.80	0.79	0.72	0.77
Pool 5	0.83	0.83	0.81	0.82	1.00	0.82	0.84	0.86	0.88	0.85	0.86	0.81	0.84	0.82	0.76	0.79
Pool 6	0.79	0.79	0.75	0.80	0.82	1.00	0.81	0.82	0.84	0.80	0.81	0.78	0.80	0.78	0.71	0.75
Pool 7	0.84	0.83	0.81	0.81	0.84	0.81	1.00	0.86	0.86	0.83	0.84	0.79	0.85	0.82	0.79	0.84
Pool 8	0.83	0.86	0.84	0.83	0.86	0.82	0.86	1.00	0.87	0.85	0.87	0.81	0.87	0.82	0.80	0.83
Pool 9	0.86	0.83	0.80	0.85	0.88	0.84	0.86	0.87	1.00	0.86	0.87	0.82	0.84	0.84	0.75	0.80
Pool 10	0.84	0.82	0.83	0.80	0.85	0.80	0.83	0.85	0.86	1.00	0.85	0.81	0.83	0.81	0.79	0.80
Pool 11	0.83	0.84	0.83	0.82	0.86	0.81	0.84	0.87	0.87	0.85	1.00	0.82	0.85	0.82	0.78	0.80
Pool 12	0.78	0.80	0.81	0.77	0.81	0.78	0.79	0.81	0.82	0.81	0.82	1.00	0.80	0.78	0.76	0.76
Pool 14	0.82	0.83	0.81	0.80	0.84	0.80	0.85	0.87	0.84	0.83	0.85	0.80	1.00	0.80	0.79	0.80
Pool 15	0.80	0.80	0.80	0.79	0.82	0.78	0.82	0.82	0.84	0.81	0.82	0.78	0.80	1.00	0.75	0.77
Pool 16	0.74	0.79	0.85	0.72	0.76	0.71	0.79	0.80	0.75	0.79	0.78	0.76	0.79	0.75	1.00	0.82
Pool 17	0.78	0.80	0.85	0.77	0.79	0.75	0.84	0.83	0.80	0.80	0.80	0.76	0.80	0.77	0.82	1.00

[a] Classification = Small follicle oocytes(pools 1-6), large follicle oocytes(pools 7-12), and spontaneous follicle oocytes(pools 14-17)

[b]Transcript abundance (reported in RPKM) for each gene mapped to the oocyte transcriptome (ReSeq transcriptome from NCBI with additional annotations)

[c] Simple correlation coefficients within and among classification of oocyte pools when only transcripts with average abundance of 1-100 RPKM are considered.

Table B.7. Correlation of transcript abundance (≥ 1 and ≤50 RPKM) within and among classification of oocyte pools[a,b,c]

	Small Follicle Oocytes						Large Follicle Oocytes						Spontaneous Follicle Oocytes			
	Pool 1	Pool 2	Pool 3	Pool 4	Pool 5	Pool 6	Pool 7	Pool 8	Pool 9	Pool 10	Pool 11	Pool 12	Pool 14	Pool 15	Pool 16	Pool 17
Pool 1	1.00	0.67	0.69	0.68	0.72	0.66	0.72	0.73	0.76	0.72	0.72	0.66	0.71	0.71	0.71	0.71
Pool 2	0.67	1.00	0.73	0.65	0.70	0.65	0.70	0.74	0.72	0.70	0.71	0.65	0.72	0.66	0.65	0.71
Pool 3	0.69	0.73	1.00	0.66	0.72	0.66	0.70	0.76	0.72	0.74	0.74	0.71	0.72	0.69	0.74	0.75
Pool 4	0.68	0.65	0.66	1.00	0.69	0.66	0.69	0.71	0.75	0.68	0.69	0.61	0.67	0.65	0.57	0.68
Pool 5	0.72	0.70	0.72	0.69	1.00	0.69	0.72	0.76	0.78	0.75	0.74	0.67	0.73	0.69	0.64	0.69
Pool 6	0.66	0.65	0.66	0.66	0.69	1.00	0.68	0.71	0.73	0.67	0.69	0.63	0.68	0.64	0.56	0.65
Pool 7	0.72	0.70	0.70	0.69	0.72	0.68	1.00	0.76	0.75	0.70	0.72	0.63	0.74	0.69	0.65	0.74
Pool 8	0.73	0.74	0.76	0.71	0.76	0.71	0.76	1.00	0.79	0.75	0.76	0.68	0.77	0.71	0.68	0.76
Pool 9	0.76	0.72	0.72	0.75	0.78	0.73	0.75	0.79	1.00	0.77	0.78	0.70	0.74	0.73	0.62	0.72
Pool 10	0.72	0.70	0.74	0.68	0.75	0.67	0.70	0.75	0.77	1.00	0.74	0.69	0.72	0.70	0.66	0.70
Pool 11	0.72	0.71	0.74	0.69	0.74	0.69	0.72	0.76	0.78	0.74	1.00	0.68	0.74	0.70	0.64	0.70
Pool 12	0.66	0.65	0.71	0.61	0.67	0.63	0.63	0.68	0.70	0.69	0.68	1.00	0.65	0.64	0.61	0.63
Pool 14	0.71	0.72	0.72	0.67	0.73	0.68	0.74	0.77	0.74	0.72	0.74	0.65	1.00	0.68	0.67	0.71
Pool 15	0.69	0.66	0.69	0.65	0.69	0.64	0.69	0.71	0.73	0.70	0.70	0.64	0.68	1.00	0.62	0.67
Pool 16	0.61	0.65	0.74	0.57	0.64	0.56	0.65	0.68	0.62	0.66	0.64	0.61	0.67	0.62	1.00	0.69
Pool 17	0.68	0.71	0.75	0.68	0.69	0.65	0.74	0.76	0.72	0.70	0.70	0.63	0.71	0.67	0.69	1.00

[a] Classification = Small follicle oocytes(pools 1-6),large follicle oocytes(pools 7-12),and spontaneous follicle oocytes(pools 14-17)

[b]Transcript abundance (reported in RPKM) for each gene mapped to the oocyte transcriptome (ReSeq transcriptome from NCBI with additional annotations)

[c] Simple correlation coefficients within and among classification of oocyte pools when only transcripts with average abundance of 1-50 RPKM are considered.

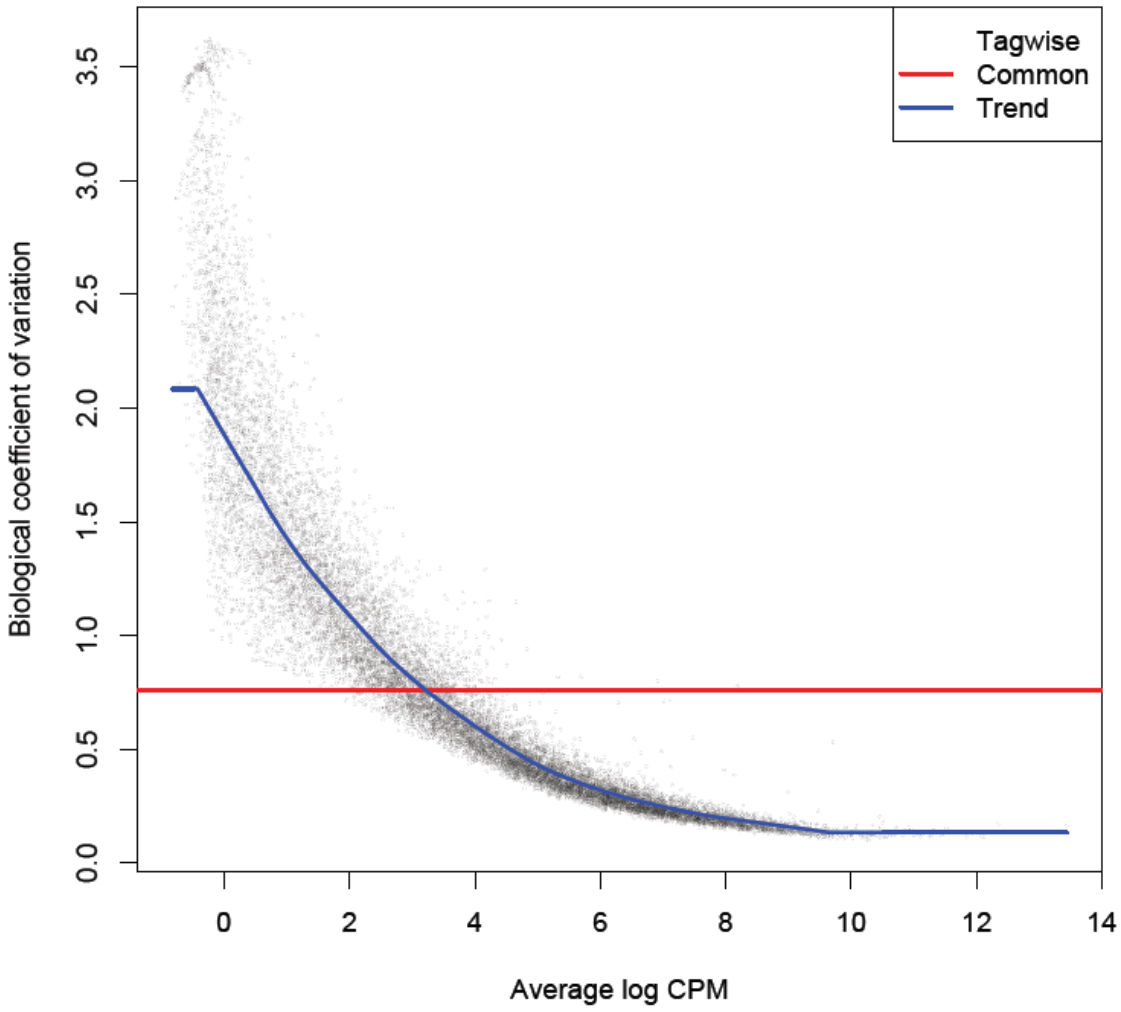

Figure B.1. Graphical representation of the biological coefficient of variation (BCV) for replicates of small and large follicle oocyte pools when alignment was performed to a RefSeq Bos Taurus transcriptome from NCBI with additional annotations. The BCV is the coefficient of variation measuring the (unknown) true amount of variation of a gene between replicates if sequencing depth was increased indefinitely. The X-axis denotes average $\log_2$ counts per million for transcript abundance, and the Y-axis denotes the BCV. The red line signifies the overall BCV (0.76), black dots represent the BCV for each transcript, and the blue line is a fitted curve for BCV according to transcript abundance.

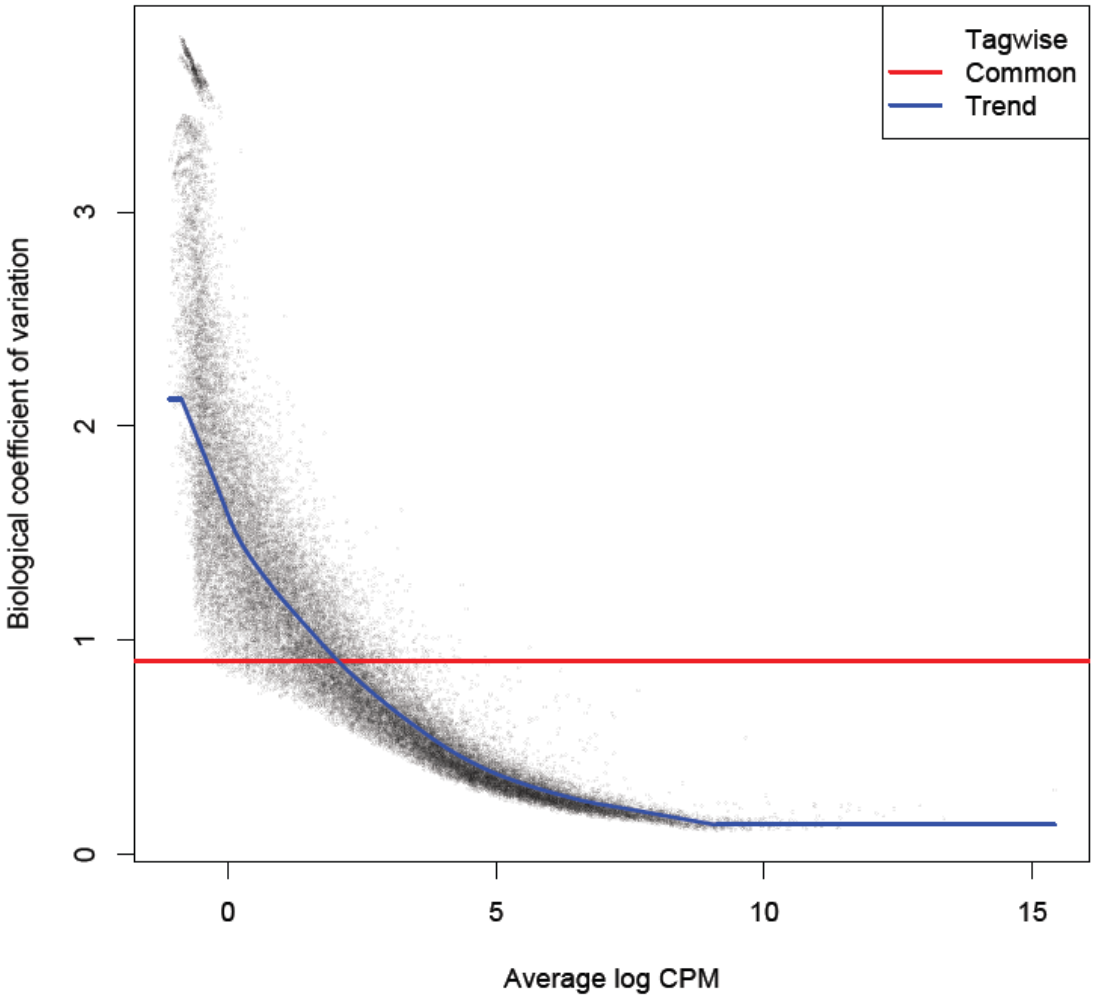

Figure B.2. Graphical representation of the biological coefficient of variation (BCV) for replicates of small and large follicle oocyte pools when alignment was performed to the bovine genome (Cow_3.1_btau_4.6.1_Y_ncbi). The BCV is the coefficient of variation measuring the (unknown) true amount of variation of a gene between replicates if sequencing depth was increased indefinitely. The X-axis denotes average $\log_2$ counts per million for transcript abundance, and the Y-axis denotes the BCV. The red line signifies the overall BCV (0.90), black dots represent the BCV for each transcript, and the blue line is a fitted curve for BCV according to transcript abundance.

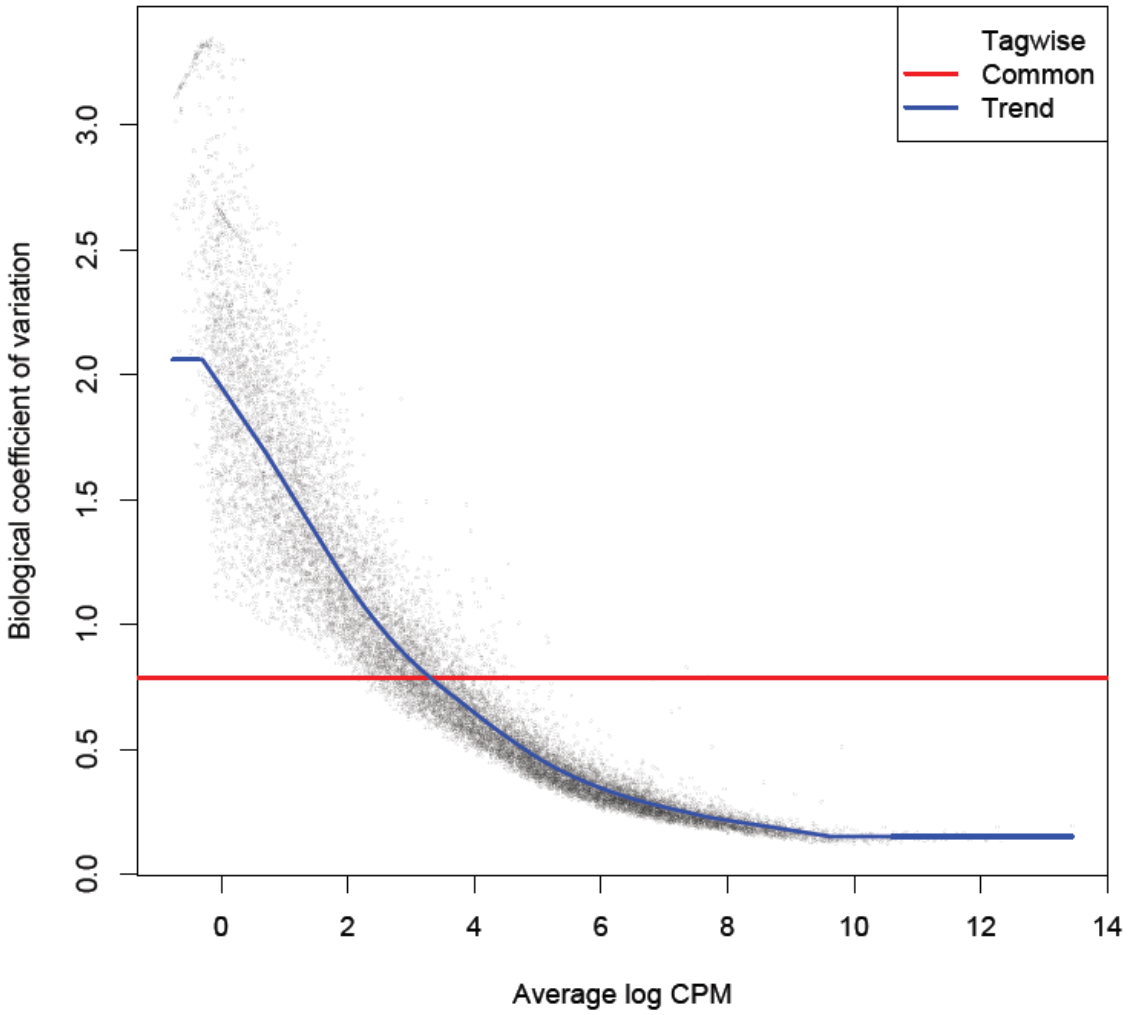

Figure B.3. Graphical representation of the biological coefficient of variation (BCV) for replicates of small and spontaneous follicle oocyte pools when alignment was performed to a RefSeq Bos Taurus transcriptome from NCBI with additional annotations. The BCV is the coefficient of variation measuring the (unknown) true amount of variation of a gene between replicates if sequencing depth was increased indefinitely. The X-axis denotes average $\log_2$ counts per million for transcript abundance, and the Y-axis denotes the BCV. The red line signifies the overall BCV (0.79), black dots represent the BCV for each transcript, and the blue line is a fitted curve for BCV according to transcript abundance.

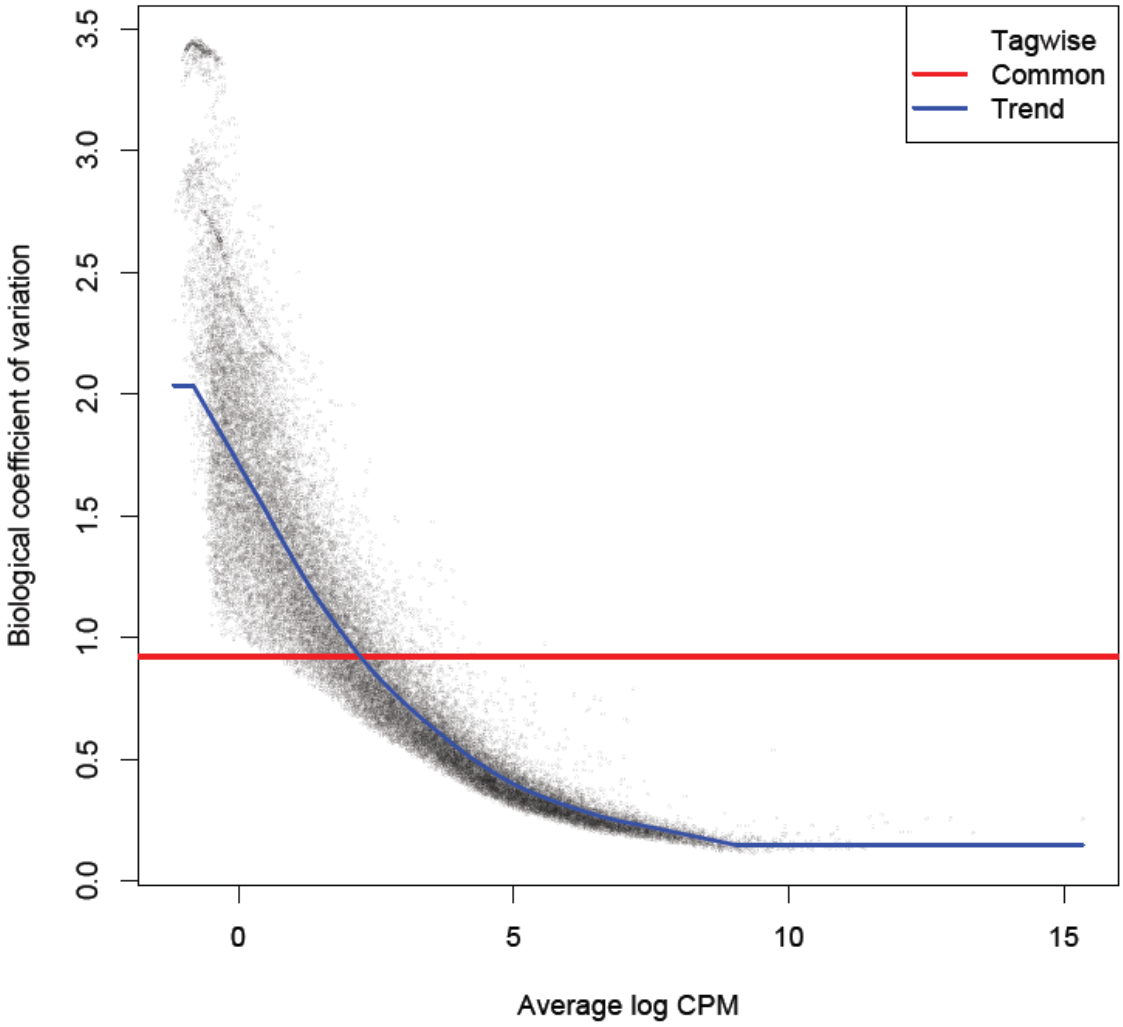

Figure B.4. Graphical representation of the biological coefficient of variation (BCV) for replicates of small and spontaneous follicle oocyte pools when alignment was performed to the bovine genome (Cow_3.1_btau_4.6.1_Y_ncbi). The BCV is the coefficient of variation measuring the (unknown) true amount of variation of a gene between replicates if sequencing depth was increased indefinitely. The X-axis denotes average $\log_2$ counts per million for transcript abundance, and the Y-axis denotes the BCV. The red line signifies the overall BCV (0.92), black dots represent the BCV for each transcript, and the blue line is a fitted curve for BCV according to transcript abundance.

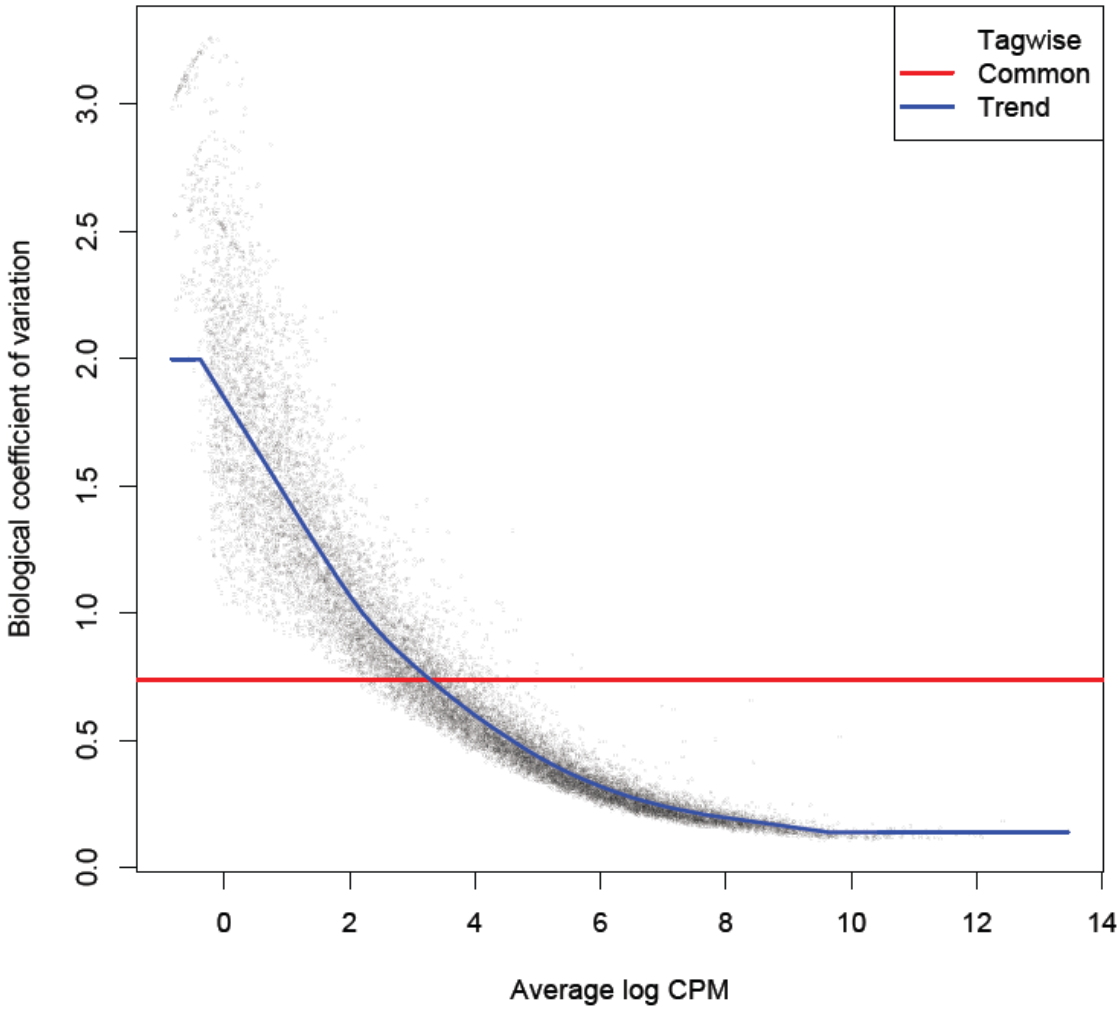

Figure B.5. Graphical representation of the biological coefficient of variation (BCV) for replicates of large and spontaneous follicle oocyte pools when alignment was performed to a RefSeq Bos Taurus transcriptome from NCBI with additional annotations. The BCV is the coefficient of variation measuring the (unknown) true amount of variation of a gene between replicates if sequencing depth was increased indefinitely. The X-axis denotes average $\log_2$ counts per million for transcript abundance, and the Y-axis denotes the BCV. The red line signifies the overall BCV (0.74), black dots represent the BCV for each transcript, and the blue line is a fitted curve for BCV according to transcript abundance.

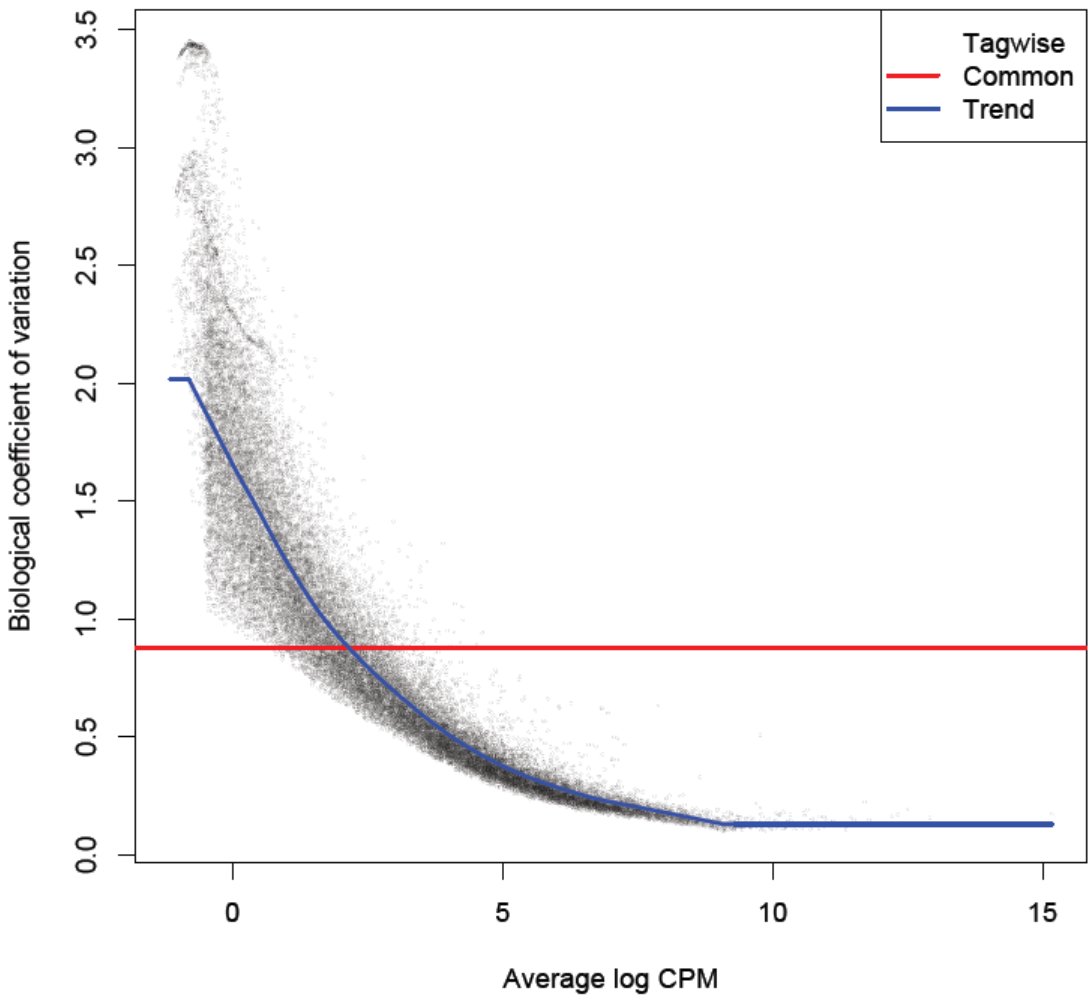

Figure B.6. Graphical representation of the biological coefficient of variation (BCV) for replicates of large and spontaneous follicle oocyte pools when alignment was performed to the bovine genome (Cow_3.1_btau_4.6.1_Y_ncbi). The BCV is the coefficient of variation measuring the (unknown) true amount of variation of a gene between replicates if sequencing depth was increased indefinitely. The X-axis denotes average $\log_2$ counts per million for transcript abundance, and the Y-axis denotes the BCV. The red line signifies the overall BCV (0.89), black dots represent the BCV for each transcript, and the blue line is a fitted curve for BCV according to transcript abundance.

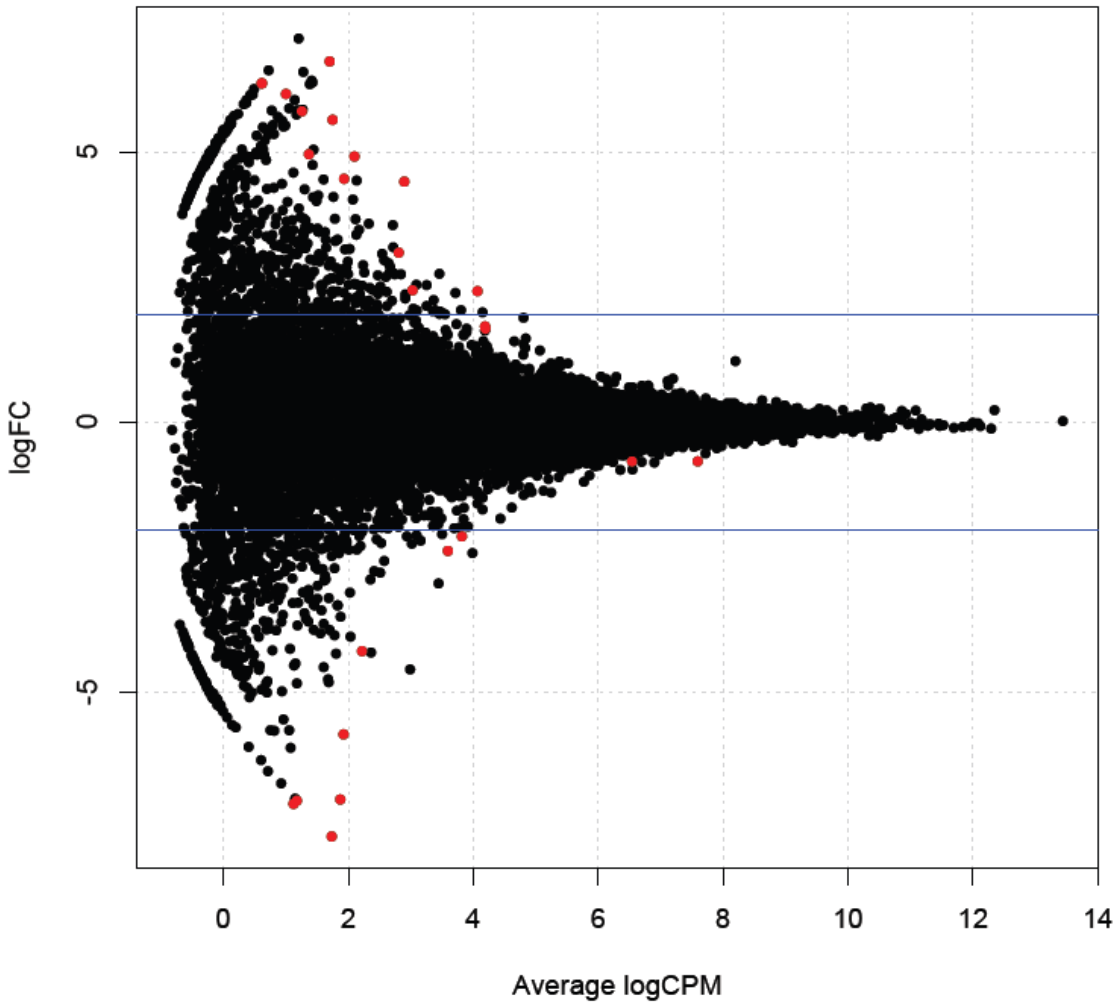

Figure B.7. Smear plot depicting differences in fold change for transcript abundance between small follicle oocyte pools and large follicle oocyte pools as average transcript counts per million (CPM) increases. Transcripts were mapped to a RefSeq Bos Taurus transcriptome from NCBI with additional annotations. The X-axis denotes average $\log_2$ counts per million for transcripts and the Y-axis denotes the $\log_2$ of the ratio between the normalized edgeR robust read count values for small and large follicle oocyte pools (-5= 32 fold higher in small follicle oocyte pools; 0=equal transcript abundance between follicle classifications; 5= 32 fold lower in small follicle oocyte pools). Each dot represents one transcript. Red dots denote transcripts significantly different between small and large follicle oocyte pools at a false discovery rate (FDR) of <0.10.

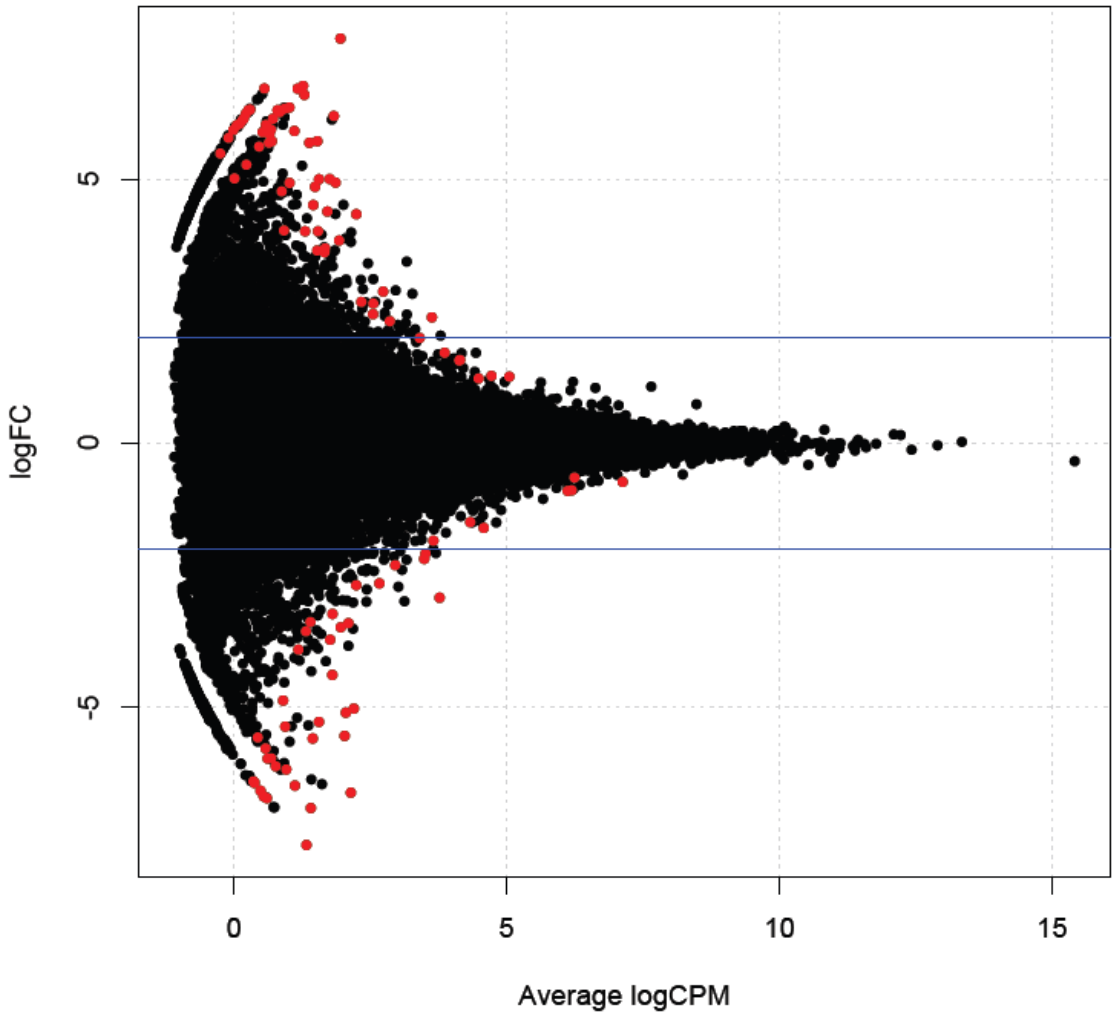

Figure B.8. Smear plot depicting differences in fold change for transcript abundance between small follicle oocyte pools and large follicle oocyte pools as average transcript counts per million (CPM) increases. Transcripts were mapped to the bovine genome (Cow_3.1_btau_4.6.1_Y_ncbi). X-axis denotes average $\log_2$ counts per million for transcripts and the Y-axis denotes the $\log_2$ of the ratio between the normalized edgeR robust read count values for small and large follicle oocyte pools (-5= 32 fold higher in small follicle oocyte pools; 0=equal transcript abundance between follicle classifications; 5= 32 fold lower in small follicle oocyte pools). Each dot represents one transcript. Red dots denote transcripts significantly different between small and large follicle oocyte pools at a false discovery rate (FDR) of <0.10.

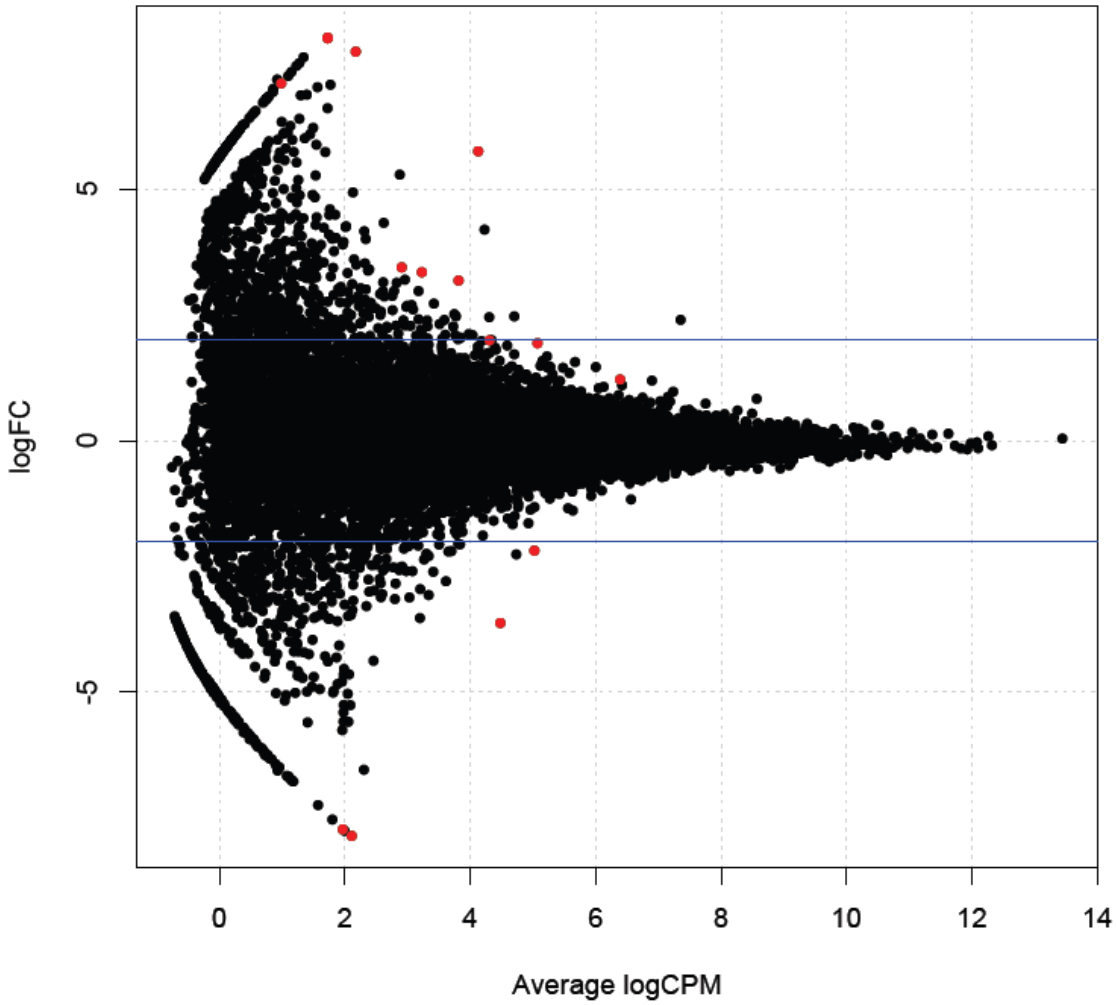

Figure B.9. Smear plot depicting differences in fold change for transcript abundance between small follicle oocyte pools and spontaneous follicle oocyte pools as average transcript counts per million (CPM) increases. Transcripts were mapped to a RefSeq Bos Taurus transcriptome from NCBI with additional annotations. X-axis denotes average $\log_2$ counts per million for transcripts and the Y-axis denotes the $\log_2$ of the ratio between the normalized edgeR robust read count values for small and spontaneous follicle oocyte pools (-5= 32 fold higher in small follicle oocyte pools; 0=equal transcript abundance between follicle classifications; 5= 32 fold lower in small follicle oocyte pools). Each dot represents one transcript. Red dots denote transcripts significantly different between small and spontaneous follicle oocyte pools at a false discovery rate (FDR) of <0.10.

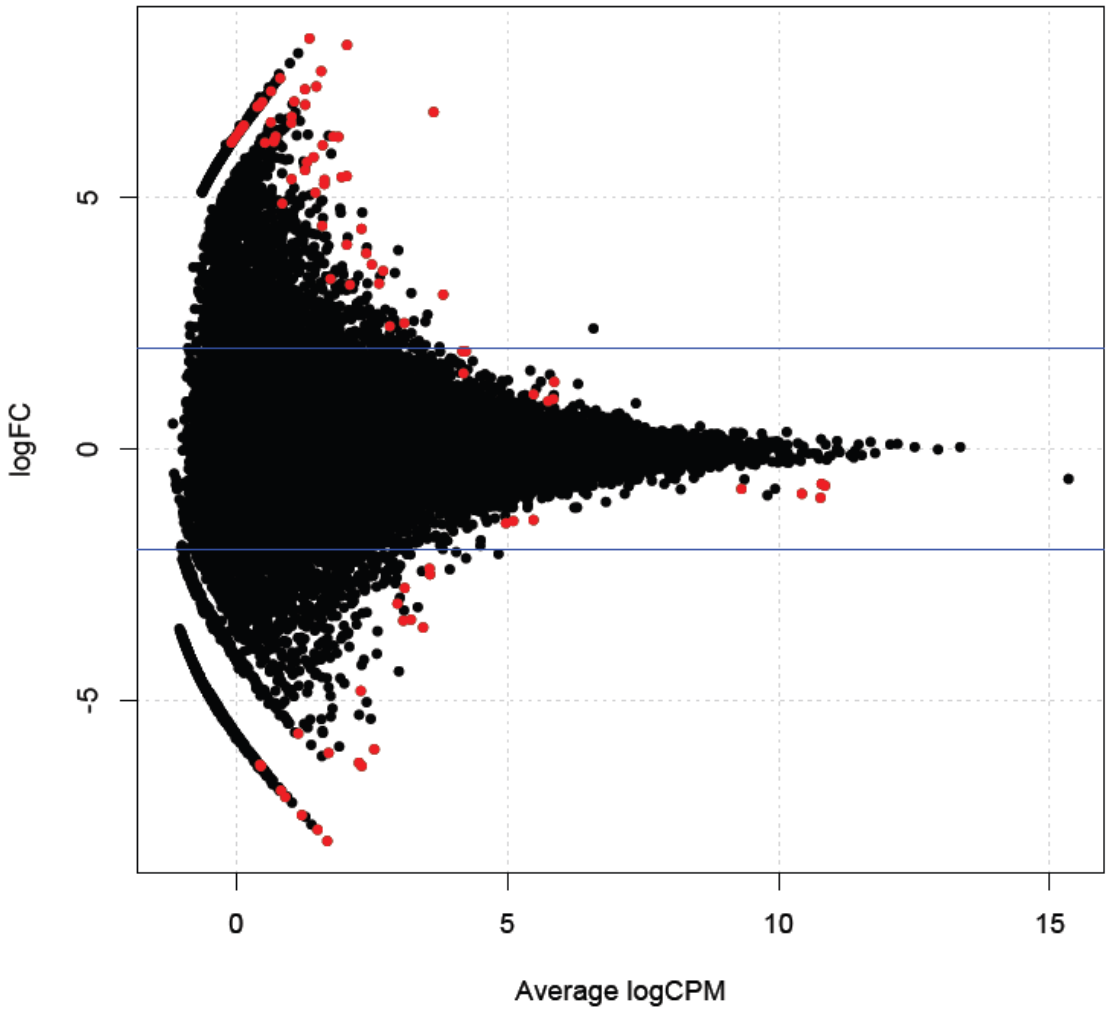

Figure B.10. Smear plot depicting differences in fold change for transcript abundance between small follicle oocyte pools and spontaneous follicle oocyte pools as average transcript counts per million (CPM) increases. Transcripts were mapped to bovine genome (Cow_3.1_btau_4.6.1_Y_ncbi). X-axis denotes average $\log_2$ counts per million for transcripts and the Y-axis denotes the $\log_2$ of the ratio between the normalized edgeR robust read count values for small and spontaneous follicle oocyte pools (-5= 32 fold higher in small follicle oocyte pools; 0=equal transcript abundance between follicle classifications; 5= 32 fold lower in small follicle oocyte pools). Each dot represents one transcript. Red dots denote transcripts significantly different between small and spontaneous follicle oocyte pools at a false discovery rate (FDR) of <0.10.

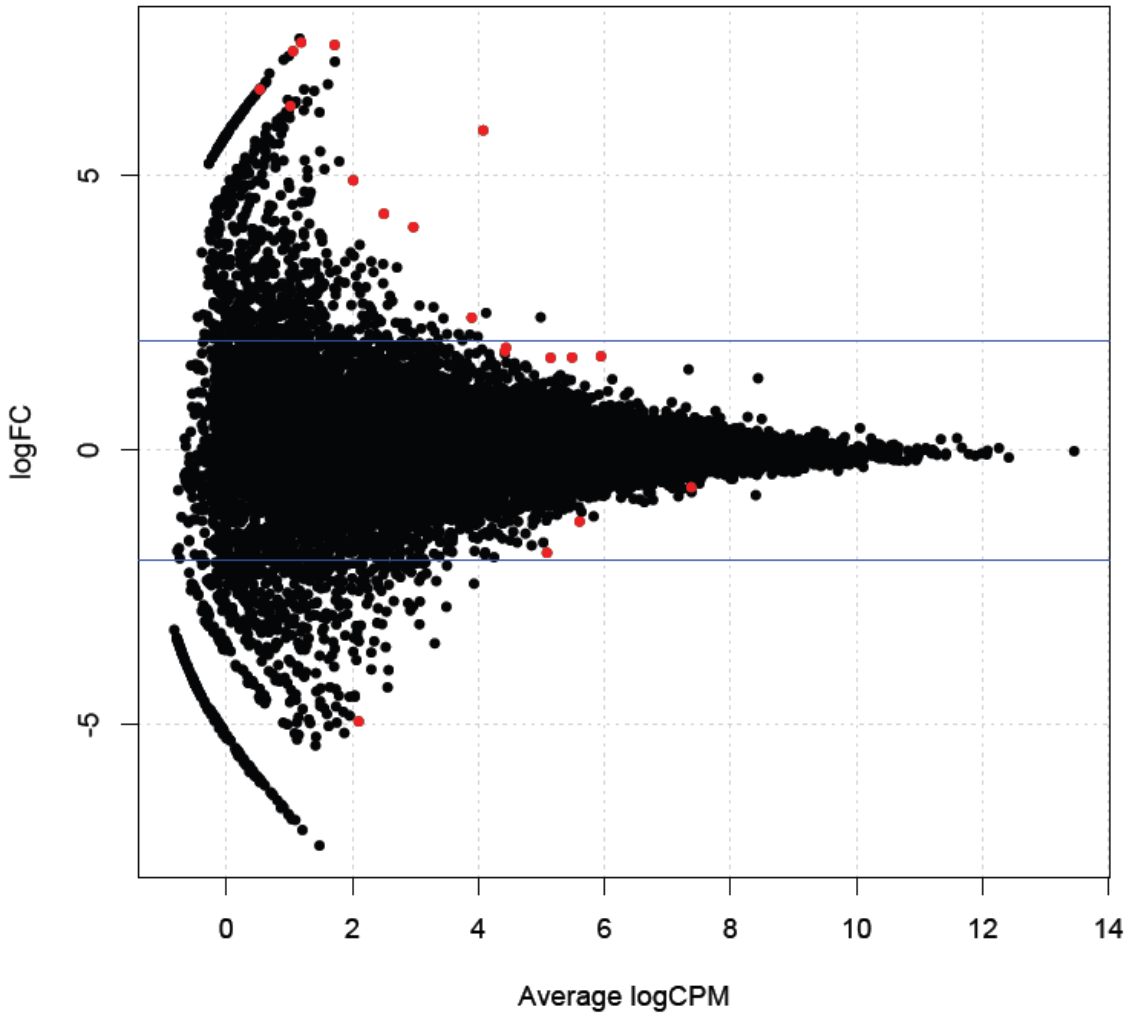

Figure B.11. Smear plot depicting differences in fold change for transcript abundance between large follicle oocyte pools and spontaneous follicle oocyte pools as average transcript counts per million (CPM) increases. Transcripts were mapped to a RefSeq Bos Taurus transcriptome from NCBI with additional annotations. X-axis denotes average $\log_2$ counts per million for transcripts and the Y-axis denotes the $\log_2$ of the ratio between the normalized edgeR robust read count values for large and spontaneous follicle oocyte pools (-5= 32 fold higher in large follicle oocyte pools; 0=equal transcript abundance between follicle classifications; 5= 32 fold lower in large follicle oocyte pools). Each dot represents one transcript. Red dots denote transcripts significantly different between large and spontaneous follicle oocyte pools at a false discovery rate (FDR) of <0.10.

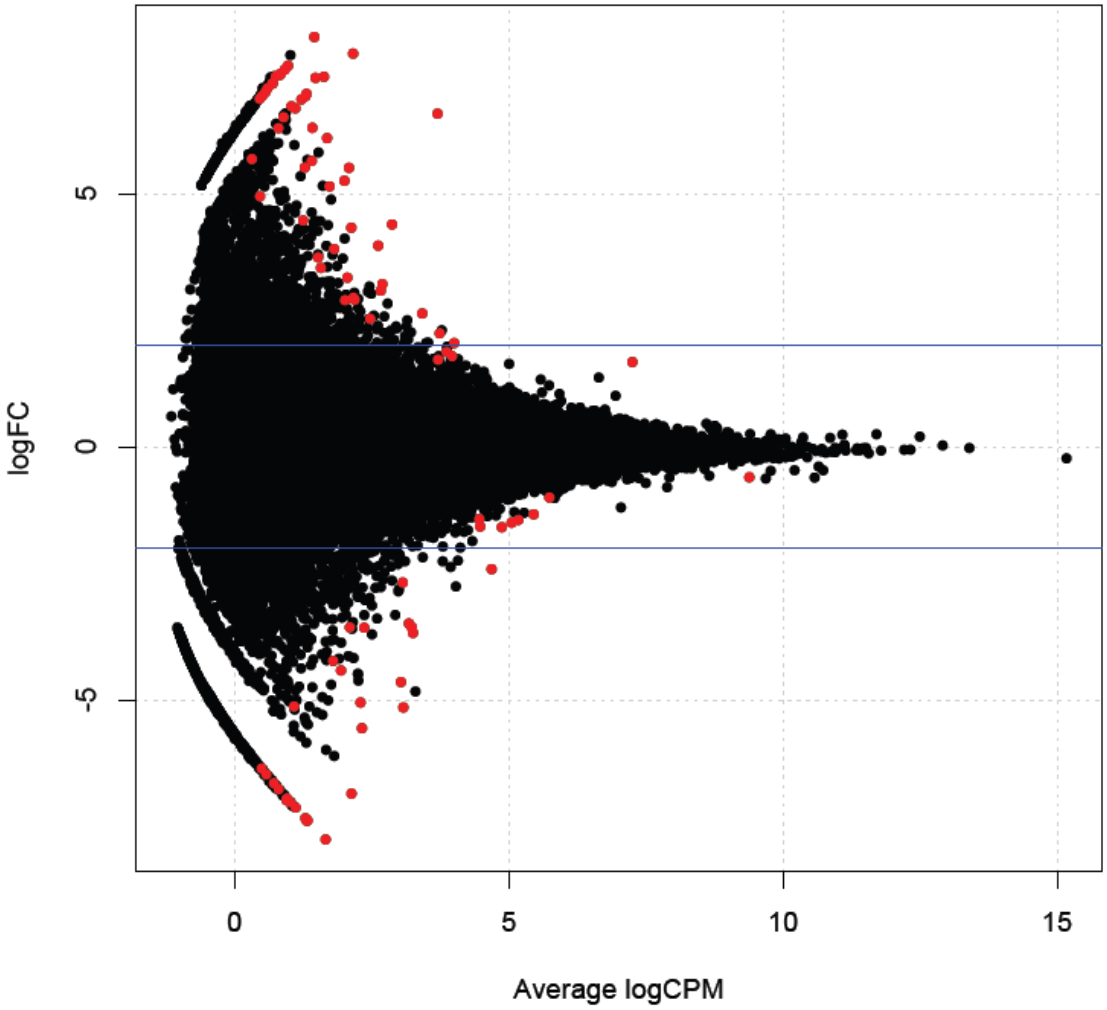

Figure B.12. Smear plot depicting differences in fold change for transcript abundance between large follicle oocyte pools and spontaneous follicle oocyte pools as average transcript counts per million (CPM) increases. Transcripts were mapped to the bovine genome (Cow_3.1_btau_4.6.1_Y_ncbi). X-axis denotes average $\log_2$ counts per million for transcripts and the Y-axis denotes the $\log_2$ of the ratio between the normalized edgeR robust read count values for large and spontaneous follicle oocyte pools (-5= 32 fold higher in large follicle oocyte pools; 0=equal transcript abundance between follicle classifications; 5= 32 fold lower in large follicle oocyte pools). Each dot represents one transcript. Red dots denote transcripts significantly different between large and spontaneous follicle oocyte pools at a false discovery rate (FDR) of <0.10.

LITERATURE CITED

Angulo, L., C.Guyader-Joly, S. Auclair, C. Hennequet-Antier, P. Papillier, M. Boussaha, S. Fritz, K. Hugot, F.ois Moreews, C. Ponsart, P. Humblot, and R. Dalbies-Tran. 2015. An integrated approach to bovine oocyte quality: from phenotype to genes. Reprod Fertil Dev.

Arlotto, T., J.-L. Schwartz, N. L. First, and M. L. Leibfried-Rutledge. 1996. Aspects of follicle and oocyte stage that affect in vitro maturation and development of bovine oocytes. Theriogenology 45: 943-956.

Atkins, J. A., D.C. Busch, J.F. Badger, D.H. Keisler, D.J. Patterson, M.C. Lucy, and M.F. Smith. 2008. Gonadotropin-releasing hormone-induced ovulation and luteinizing hormone release in beef heifers: effect of day of the cycle. J Anim Sci 86: 83-93.

Atkins, J. A., M. F. Smith, M. D. MacNeil, E. M. Jinks, F. M. Abreu, L. J. Alexander and T.W. Geary. 2013. Pregnancy establishment and maintenance in cattle. J Anim Sci 91: 722-733.

Bavister, B. D., and J. M. Squirrell. 2000. Mitochondrial distribution and function in oocytes and early embryos. Human Reproduction 15: 190-198.

Bettegowda, A., O.V. Patel, K.B. Lee, K.E. Park, M. Salem, J. Yao, J.J. Ireland, and G.W. Smith. 2008. Identification of novel bovine cumulus cell molecular markers predictive of oocyte competence: functional and diagnostic implications. Biol Reprod 79: 301-309.

Bhak, J. S., S.L. Lee, S.A. Ock, B. Mohana kumar, S.Y. Choe, G.J. Rho. 2006. Developmental rate and ploidy of embryos produced by nuclear transfer with different activation treatments in cattle. Anim Reprod Sci 92: 37-49.

Blondin, P., D. Bousquet, H. Twagiramungu, F. Barnes, and M. A. Sirard. 2002. Manipulation of follicular development to produce developmentally competent bovine oocytes. Biol Reprod 66: 38-43.

Blondin, P., L. A. Guilbault, and M. A. Sirard. 1997. The time interval between FSH-P administration and slaughter can influence the developmental competence of beef heifer oocytes. Theriogenology 48: 803-813.

Brevini-Gandolfi, T. A. L., L.A. Favetta, L. Mauri, A.M. Luciano, F. Cillo, and F. Gandolfi. 1999. Changes in poly(A) tail length of maternal transcripts during in vitro maturation of bovine oocytes and their relation with developmental competence. molecular reproduction and development 52: 427-433.

Chappel, S. 2013. The role of mitochondria from mature oocyte to viable blastocyst. Obstet Gynecol Int 2013: 1-10.

Day, M. L. 2004. Hormonal induction of estrous cycles in anestrous Bos taurus beef cows. Anim Reprod Sci 82-83: 487-494.

Dennis, G. J. et al. 2003. DAVID: database for annotation, visualization, and integrated discovery. Genome Biol 4: 3.

Dumollard, R., J. Carroll, M. R. Duchen, K. Campbell, and K. Swann. 2009. Mitochondrial function and redox state in mammalian embryos. Seminars in Cell & Developmental Biology 20: 346-353.

Eppig, J. J. 2001. Oocyte control of ovarian follicular development and function in mammals. Biol Reprod 1: 829-838.

Erickson, G. F., and S. Shimasaki. 2000. The role of the oocyte in folliculogenesis. TEM 11: 193-198.

Fair, T. 2003. Follicular oocyte growth and acquisition of developmental competence. Animal Reproduction Science 78: 203-216.

Fair, T., S. C. J. Hulschof, P. Hyttel, T. Greve, and M. Boland. 1997. Nucleus ultrastructure and transcriptional activity of bovine oocytes in preantral and early antral follicles. Mol Reprod Dev 1: 208-215.

Fair, T., P. Hyttel, and T. Greve. 1995. Bovine oocyte diameter in relation to maturational competence and transcriptional activity. Mol Reprod Dev 42: 437-442.

Fan, H.-Y., C. Tong, M.Y. Li, L. Lian, D.Y. Chen, H. Schatten, and Q.Y. Sun. 2002. Translocation of the Classic Protein Kinase C Isoforms in Porcine Oocytes: Implications of Protein Kinase C Involvement in the Regulation of Nuclear Activity and Cortical Granule Exocytosis. Experimental Cell Research 277: 183-191.

Ferreira, E. M., A.A. Vireque, P.R. Adona, F.V. Meirelles, R.A. Ferriani, and P.A.A.S. Navarro. 2009. Cytoplasmic maturation of bovine oocytes: structural and biochemical modifications and acquisition of developmental competence. Theriogenology 71: 836-848.

Geary, T. W., E. R. Downing, J. E. Bruemmer, and J. C. Whittier. 2000. Ovarian and estrous response of suckled beef cows to the select synch estrous synchronization protocol. Professional Animal Scientist 16: 1-5.

Gendelman, M., and Z. Roth. 2012. Incorporation of coenzyme Q10 into bovine oocytes improves mitochondrial features and alleviates the effects of summer thermal stress on developmental competence. Biol Reprod 87: 1-12.

Gilchrist, R. B., L. J. Ritter, and D. T. Armstrong. 2004. Oocyte-somatic cell interactions during follicle development in mammals. Anim Reprod Sci 82-83: 431-446.

Hendricksen, P. J. M., P. L. A. M. Vos, W. N. M. Steenweg, M. M. Bevers, and S. J. Dieleman. 2000. Bovine follicular development and its effect on the in vitro competence of oocytes. Theriogenology 53: 11-20.

Huo, L. J., H.Y. Fan, Z.S. Zhong, D.Y. Chen, H. Schatten, and Q.Y. Suna. 2004. Ubiquitin-proteasome pathway modulates mouse oocyte meiotic maturation and fertilization via regulation of MAPK cascade and cyclin B1 degradation. Mech Dev 121: 1275-1287.

Hyttel, P., T. Fair, H. Callesen, and T. Greve. 1997. Oocyte growth, capacitation, and final maturation in cattle. Theriogenology 47: 23-32.

Jinks, E. M., M. F. Smith, J. A. Atkins, K. G. Pohler, G. A. Perry, M. D. MacNeil, A. J. Roberts, R. C. Waterman, L. J. Alexander, and T. W. Geary. 2013. Preovulatory estradiol and the establishment and maintenance of pregnancy in suckled beef cows. J Anim Sci 91: 1176-1185.

Juengel, J. L., H.R. Sawyer, P.R. Smith, L.D. Quirke, D.A. Heath, S. Lun, S.J. Wakefield, and K.P. McNatty. 2002. Origins of follicular cells and ontogeny of steroidogenesis in ovine fetal ovaries. Mol Endocrinol 191: 1-10.

Juengel, J. L., and P. Smith. 2014. Formation of ovarian follicles in ruminants. In: J. L. Juengel et al. (eds.) Reproduction in domestic ruminants VIII. p 277-293. Context Products Ltd, Packington.

Lamb, G. C., J. S. Stevenson, D. J. Kesler, H. A. Garverick, D. R. Brown, and B. E. Salfen. 2001. Inclusion of an intravaginal progesterone insert plus GnRH and Prostaglandin F2a for ovulation control in postpartum suckled beef cows. J Anim Sci 79: 2253-2259.

Larson, D. M., and R. N. Funston. 2009. Estrous synchronization increases early calving frequency, which enhances steer progeny value. In: Western Section, American Society of Animal Science, Fort Collins, CO

Larson, J. E., G. C. Lamb, J. S. Stevenson, S. K. Johnson, M. L. Day, T. W. Geary, D. J. Kesler, J. M. DeJarnette, F. N. Schrick, A. DiCostanzo and J. D. Arseneau. 2006. Synchronization of estrus in suckled beef cows for detected estrus and artificial insemination and timed artificial insemination using gonadotropin-releasing hormone, prostaglandin F2a, and progesterone. J Anim Sci 84: 332-342.

Lodde, V., S.Modina, P. Maddox-Hyttel, F. Franciosi, A. Lauria, and A.M. Luciano. 2008. Oocyte morphology and transcriptional silencing in relation to chromatin remodeling during the final phases of bovine oocyte growth. Mol Reprod Dev 75: 915-924.

Lonergan, P., A. Gutierrez-Adan, D. Rizos, B. Pintado, J. De La Fuente, and M.P. Boland. 2003. Relative messenger RNA abundance in bovine oocytes collected in vitro or in vivo before and 20 hr after the preovulatory luteinizing hormone surge. Mol Reprod Dev 66: 297-305.

Lucy, M. C. 2007. The bovine dominant ovarian follicle. J Anim Sci. 85 (E. Suppl.):E89-E99.

Macaulay, A. D., I. Gilbert, J. Caballero, R. Barreto, E. Fournier, P. Tossou, M.A. Sirard, H.J. Clarke, É.W. Khandjian, F.J. Richard, P. Hyttel, and C. Robert et al. 2014. The gametic synapse: RNA transfer to the bovine oocyte. Biol Reprod 91: 1-12.

Macaulay, A. D., I.Gilbert, S. Scantland, E. Fournier, F. Ashkar, A. Bastien, H.A. Shojaei Saadi, D.Gagne´, M.A. Sirard, E.W. Khandjian, F.J. Richard, P. Hyttel, and C. Robert. 2016. Cumulus Cell Transcripts Transit to the Bovine Oocyte in Preparation for Maturation. Biol Reprod 94: 1-11.

Machatkova, M., E. Jokesova, F. Horky, and A. Krepelova. 2000. Utilization of the growth phase of the first follicular wave for bovine oocyte collection improves blastocyst production. Theriogenology 54: 543-550.

Mamo, S., F. Carter, P. Lonergan, C.L.V. Leal, A.A. Naib, P. McGettigan, J.P. Mehta, A.C.O. Evans, and T. Fair. 2011. Sequential analysis of global gene expression profiles in immature and in vitro matured bovine oocytes: potential molecular markers of oocyte maturation. BMC Genomics 12: 151.

Marteil, G., L. Richard-Parpaillon, and J. Z. Kubiak. 2009. Role of oocyte quality in meiotic maturation and embryonic development. Reproductive Biology 9: 203-224.

McCarthy, D. J., Y. Chen, and G. K. Smyth. 2012. Differential expression analysis of multifactor RNA-Seq experiments with respect to biological variation. Nucleic Acids Res 40: 4288-4297.

Mourot, M., I. Dufort, C. Gravel, O. Algriany, S. Dieleman, and M.A. Sirard. 2006. The influence of follicle size, FSH-enriched maturation medium, and early cleavage on bovine oocyte maternal mRNA levels. Mol Reprod Dev 73: 1367-1379.

Nemcova, L., D. Jansova, K. Vodickova-Kepkova, P. Vodicka, M. Jeseta, M. Machatkova, and J. Kanka. 2016. Detection of genes associated with developmental competence of bovine oocytes. Anim Reprod Sci 166: 58-71.

Otoi, T., K. Yamamotol, N. Koyamal, S. Tachikawal, and T. Suzuki. 1997. Bovine oocyte diameter in relation to developmental competence. Theriogenology 48: 769-774.

Patel, O. V., A. Bettegowda, J.J. Ireland, P.M. Coussens, P. Lonergan, and G.W Smith. 2007. Functional genomics studies of oocyte competence: evidence that reduced transcript abundance for follistatin is associated with poor developmental competence of bovine oocytes. Reproduction 133: 95-106.

Patterson, D. J., F. N. Kojima, and M. F. Smith. 2003. A review of methods to synchronize estrus in replacement beef heifers and postpartum cows. J Anim Sci 81: E166-E177.

Perry, G. A., M.F. Smith, M.C. Lucy, J.A. Green, T.E. Parks, M.D. MacNeil, A.J. Roberts, and T.W. Geary. 2005. Relationship between follicle size at insemination and pregnancy success. Proc Natl Acad Sci USA 102: 5268-5273.

Peters, J. M. 2002. The anaphase-promoting complex: proteolysis in mitosis and beyond. Molecular Cell 9: 931-943.

Peterson, A. J., and R. S. Lee. 2003. Improving successful pregnancies after embryo transfer. Theriogenology: 59 687-697.

Picton, H., D. Briggs, and R. Gosden. 1998. The molecular basis of oocyte growth and development. Mol Endocrinol 1: 27-37.

Pohler, K.G. 2011. Effect of ovulatory follicle size on steroidogenic capacity, molecular markers of oocyte competence and bovine pregnancy associated glycoproteins. Master's Thesis. University of Missouri-Columbia.

Ramalho-Santos, J., S. Varum, S. Amaral, P.C. Mota, A.P. Sousa, and A. Amaral. 2009. Mitochondrial functionality in reproduction: from gonads and gametes to embryos and embryonic stem cells. Hum Reprod Update 15: 553-572.

Reyes, J.M. and P.J. Ross. 2016. Cytoplasmic polyadenylation in mammalian oocyte maturation. WIREs RNA 2016, 7:71–89.

Robinson, M. D., D. J. McCarthy, and G. K. Smyth. 2010. edgeR: a Bioconductor package for differential expression analysis of digital gene expression data. Bioinformatics 26: 139-140.

Rodriguez, K.F., C.E. Farin. 2004. Gene transcription and regulation of oocyte maturation. Reprod.Fertil.Dev. 16:55-67.

Sawada, M.T., K. Kyozuka, C. Morinaga, K. Izumi, and H. Sawada. 1997. The proteasome is an essential mediator of the activation of pre-MPF during starfish oocyte maturation. Biochem Biophys Res Commun. 236: 40-43.

Senger, P. L., and R. G. Saacke. 1970. Unusual mitochondria of the bovine oocyte. The Journal of Cell Biology 46: 405-408.

Sirard, M. A. 2001. Resumption of meiosis: mechanism involved in meiotic progression and its relation with developmental competence. Theriogenology 1: 1241-1254.

Sirard, M. A. 2012. Factors affecting oocyte and embryo transcriptomes. Reprod Domest Anim 47 Suppl 4: 148-155.

Sirard, M. A., F. Richard, P. Blondin, and C. Robert. 2006. Contribution of the oocyte to embryo quality. Theriogenology 65: 126-136.

Sun, Q. Y., D. Fuchimoto, and T. Nagai. 2004. Regulatory roles of ubiquitin-proteasome pathway in pig oocyte meiotic maturation and fertilization. Theriogenology 62: 245-255.

Sutovsky, P. 2011. Sperm proteasome and fertilization. Reproduction 142: 1-14.

Swanson, L. V., and H. D. Hafs. 1971. LH and prolactin in blood serum from estrus to ovulation in holstein heifers. J Anim Sci 33: 1038-1041.

Takahashi, M., T. Tokumoto, and K. Ishikawa. 1994. DFP-sensitive multicatalytic protease complexes (proteasomes) involved in the control of oocyte maturation in the toad, Bufo japonicas. Mol Repro Dev 38: 310-317.

Turi, A., S.R. Giannubilo, F. Brugè, F. Principi, S. Battistoni, F. Santoni, A.L. Tranquilli, G.P. Littarru, and L. Tiano. 2012. Coenzyme Q10 content in follicular fluid and its relationship with oocyte fertilization and embryo grading. Arch Gynecol Obstet 285: 1173-1176.

van den Hurk, R., and J. Zhao. 2005. Formation of mammalian oocytes and their growth, differentiation and maturation within ovarian follicles. Theriogenology 63: 1717-1751.

Vansconcelos, J. L. M., R. Sartori, H. N. Oliveira, J. G. Guenther, and M. C. Wiltbank. 2001. Reduction in size of the ovulatory follicle reduces subsequent luteal size and pregnancy rate. Theriogenology 56: 307-314.

Wassarman, P. M., and F. Albertini. 1994. The mammalian ovum. In: E. Knobil and J. D. Neill (eds.) The physiology of reproduction No. 1. p 79-115. Raven Press, Ltd., New York, NY.

Wrobel, K. H., and F. Süß. 1998. Identification and temporospatial distribution of bovine primordial germ cells prior to gonadal sexual differentiation. Anat Embryol 197: 451–467.

Wu, X. Q., X. Zhang, X.H. Li, H.H. Cheng, Y.R.R. Kua, S. Wang, and Y.L. Guo. 2006. Translocation of classical PKC and cortical granule exocytosis of human oocyte in germinal vesicle and metaphase II stage. Acta Pharmacol Sin 27: 1353-1358.

You, J., E. Lee, L. Bonilla, J. Francis, J. Koh, J. Block, S. Chen, and P.J. Hansen. 2012. Treatment with the proteasome inhibitor MG132 during the end of oocyte maturation improves oocyte competence for development after fertilization in cattle. PLoS One 7: e48613.

VITA

Sarah Elizabeth Dickinson was born on October 26, 1991 to Bryan and Christine Dickinson of Citronelle, Alabama. She was raised on her family's beef cattle farm and currently owns a small herd of Simmental and Simmental influenced females. Dickinson earned her B.S. in Animal Science from Auburn University in May of 2014. After graduation with her M.S. in Animal Science from the University of Missouri in May 2016, she will return to Alabama as a Regional Extension Agent in Animal Sciences and Forage, serving Auburn, Alabama and surrounding counties.